# Modeling Flight Characteristics of a Ba-349 "Natter" Aircraft using Modern Software and Analytical Methods to Determine Feasibility as a Bomber Interceptor

a project presented to
The Faculty of the Department of Aerospace Engineering
San Jose State University

in partial fulfillment of the requirements for the degree
***Master of Science in Aerospace Engineering***

by

**Benjamin S. Hopkins**

December 2022

approved by

Mr. Sean Montgomery
Faculty Advisor

ABSTRACT

**Modeling Flight Characteristics of a Ba-349 "Natter" Aircraft using Modern Software and Analytical Methods to Determine Feasibility as a Bomber Interceptor**

Benjamin S. Hopkins

The Ba 349 "Natter" was a wooden-framed, rocket-propelled bomber interceptor developed in the latter years of WWII. It used non-strategic resources in its design such as wood and steel and was considered a "last ditch" effort by the Germans to stop the relentless waves of allied bombing. It never saw combat service and the only manned test flight resulted in the pilot's death. Other than basic flight specifications like its engine's thrust and theoretical top speed, there is scant information, analysis or documentation of its flight characteristics. Modern software such as Solidworks and AVL enable engineers to determine a design's flight performance without physically verifying them. The purpose of this project is to fully model the aircraft flight surfaces, specifications, mass and material properties, subject it to aerodynamic and stability/control analyses and determine if it was suitable for its intended purpose. The Smithsonian and Deutsches Museum have the only two remaining original aircraft. Aviation/military historians, engineers and safety/accident investigators could benefit from information from these analyses. Numerical and analytical analyses indicate that the Natter could have met many of the altitude, speed and combat requirements set by the RLM. The Natter had a maximum possible altitude of 13711 meters (44984 feet) with a maximum speed of Mach 0.9. Maximum combat radius was 14.4 kilometers (8.94 miles). The aircraft was longitudinally stable but its questionable if the pilot would be able to control the aircraft at transonic speeds. Additionally the g-forces on the aircraft during maneuvers could cause the wooden airframe to fail.

Acknowledgments

I would like to thank my wife, Hannah, for her support, love and encouragement through my graduate school journey.

# Table of Contents

# List of Figures

# Abbreviations & Symbols

| Symbol | Definition | Units |
|---|---|---|
| $C_L$ | Coefficient of Lift | ----- |
| $C_D$ | Coefficient of Drag | ----- |
| $C_M$ | Coefficient of Moment | ----- |
| $C_f$ | Coefficient of Friction | ----- |
| S | Surface Area | $m^2$ ($ft^2$) |
| R | Reynolds Number | ----- |
| $R_{cutoff}$ | Cutoff Reynolds Number | ----- |
| M | Mach Number | ----- |
| L | Length / Lift Force | $m$ (ft)/ N (lbf) |
| k | Skin Roughness Value | ----- |
| u | External Flow Speed | $m/s$ ($ft/s$) |
| c | Speed of Sound / Chord Length | $m/s$ ($ft/s$) / $m$ ($ft$) |
| T | Air Temperature / Thrust Force | $^o$K ($^o$F) / N (lbf) |
| FF | Form Factor | ----- |
| f | Interference Factor | ----- |
| K | Drag Due to Lift Factor / Pitching Moment Factor | ----- |
| e | Oswald Efficiency Factor | ----- |
| $a_0$ | 2D Wing Lift Coefficient with Respect to α | ----- |
| $a$ | 3D Wing Lift Coefficient with Respect to α | ----- |
| Mdd | Drag-Divergent Mach Number | ----- |
| F / T | Thrust | N (lbf) |
| V | Aircraft Velocity | $m/s$ ($ft/s$) |
| W | Weight / Width / Frequency | N (lbf) / $m$ ($ft$) / rad/sec |

| Symbol | Definition | Units |
|---|---|---|
| D | Drag | N (lbf) |
| g | Gravitational Constant | $m/s^2$ $(ft/s^2)$ |
| $m_n$ | Aircraft Mass | kg (lbm) |
| $l_n$/ X | Aircraft Moment Arm | $m$ $(ft)$ |
| $\overline{V_t}$ | Tail to Wing Area Ratio | ----- |
| $h_0$ /$X_W$ | Wing Aerodynamic Center | % MAC / $m$ $(ft)$ |
| $h_n$ | Neutral Point Location | % MAC |
| q | Dynamic Pressure | $N/m^2$ $(lbf/ft^2)$ |
| $I_{yy}$ | Longitudinal Moment of Inertia | $kg \cdot m^2$ $(lbm \cdot ft^2)$ |
| n | Load Factor | $g\left(9.81 m/s^2\right)$ / $\left(32.1 ft/s^2\right)$ |
| PS | Specific Excess Power | m/s $(ft/s)$ |
| | | |
| Greek Symbols | | |
| γ | Adiabatic Constant / Trajectory Angle | - / degrees |
| α | Angle of Attack | degrees |
| θ | Pitch Angle | degrees |
| ρ | Air Density | $kg/m^3$ $(lbm/ft^3)$ |
| ε | Downwash Angle | degrees |
| η | Horizontal Stabilizer Efficiency | ----- |
| ζ | Damping Ratio | ----- |
| | | |
| Subscripts | | |
| $()_f$ | Friction / Fuselage | ----- |
| $()_X$ | X-Direction | ----- |
| $()_Z$ | Z-Direction | ----- |
| $()_{wet}$ | Wetted Surface Area | ---- |
| $()_W$ / $()_{ref}$ | Wing | ----- |
| $()_T$ / $()_{tail}$ | Tail | ----- |

| Symbol | Definition | Units |
|---|---|---|
| $()_{\delta e}$ | Elevator Deflection | ----- |
| $()_n$ | Aircraft Component | ----- |
| $()_u$ | Speed | ----- |
| $()_\alpha$ | Angle of Attack | ----- |
| $()_{\dot{\alpha}}$ | Angle of Attack Rate | ----- |
| $()_q$ | Pitch Rate | ----- |
| | | |
| Acronyms | | |
| WWII | World War Two | ----- |
| Me | Messerschmidt | ----- |
| Ba | Bachem | ----- |
| RLM | Reichsluftfahrtministerium (Reich Air Ministry) | ----- |
| SS | Schutzstaffel (Protection Squadron) | ----- |
| JATO | Jet Assisted Takeoff | ----- |
| Mig | Mikoyan-Gurevich | ----- |
| DFS | Deutsche Forschungsinstitut (German Research Institute for Sailplanes) | ----- |
| VTO | Vertical Takeoff | ----- |
| HWK | Hellmuth Walter Kommanditgesellschaft | ----- |
| CFD | Computational Fluid Dynamics | ----- |
| RANS | Reynolds Average Navier Stokes | ----- |
| NACA | National Advisory Committee for Aeronautics | ----- |
| NASM | National Air and Space Museum | ----- |
| FW | Focke-Wulf | ----- |

| Symbol | Definition | Units |
|---|---|---|
| WBL5 | Wing-Body Linear Longitudinal-Lateral Lifting Line | ----- |
| AVL | Athena Vortex Line | ----- |
| VLM | Vortex Lattice Method | ----- |
| Ho | Horten | ----- |
| BV | Blohm and Voss | ----- |
| SAE | Society of Automotive Engineers | ----- |
| RDS | Raymer Design Software | ----- |
| UF | Urea-Formaldehyde | ----- |
| DVL | Deutsche Versuchsanstalt für Luftfahrt (German Research Institute for Aviation) | ----- |
| L/D | Lift-To-Drag | ----- |
| STP | Standard Temperature and Pressure | ----- |
| CG | Center of Gravity | ----- |
| NP | Neutral Point | ----- |
| MAC | Mean Aerodynamic Chord | ----- |
| EM | Energy Maneuverability | ----- |

# 1. Introduction

## 1.1 Background

During the latter days of WWII, Germany was desperate to stop the nearly daily assault by allied bombers. After initial successes in Europe, Germany declared war on the USA, an industrial powerhouse across the Atlantic Ocean. Over time the allies were able to produce materiel faster than the axis could destroy them. This prompted the Germans to take more risk and invest in military projects that could turn the war back in their favor. Examples include the well known V-2 rocket designed by Wernher Von Braun. The Me-262 and Me-163 are well known examples of aircraft that were at built to counter the aerial threat.

The Ba-349 “Natter” was built to impede allied bombers but it was not on the leading edge of technical development. It utilized a laminated wood frame, simple cable-pulley control system and rudimentary instruments. Its innovation was using a bi-propellant liquid rocket engine to quickly accelerate the aircraft to 12,000 meters (39370 feet) in order to engage allied bombers. Unlike the previously mentioned aircraft, documentation on the validity of the Natter’s ability other than first hand accounts are either lost or destroyed. The ability to intercept bombers in its planned configuration was never tested. This project aims to validate technical specifications and abilities of the Natter using numerical and analytical models, stability analysis and energy-maneuverability diagrams. Results from these analyses will determine if the Natter was suitable for its intended purpose and met the initial requirements set by the Reich Air Ministry (RLM).

## 1.2 Literature Review

Resources for this project are split into four sections; historical sources, comparative aircraft, analytical techniques and contemporary performance limitations. These sections will detail what is already known about the Natter, examining analogous aircraft such as the Me-163 and detailing methods for determining the validity of the aircraft for its intended use.

### 1.2.1 Historical Sources

The first step in analyzing the Natter is to determine what is already known about the aircraft. There are three books, two in English and one in German, detailing the history of the aircraft, its development, testing regime and final days. The authors of these books, Forsyth [1], Myrha [2], and Dressel [3] reference private documents of Erich Bachem, RLM and the Schutzstaffel (SS) stored at archives such as the Library of Congress and Bundesarchiv. Access to these original records require an in-person appointment. All three books detail extensive technical data on the aircraft including its top speed, weight, range and ceiling. They also detail how prototypes of the Natter were

tested in wind tunnels or towed gliding tests. For the majority of its development, the Natter was known by its creators as the BP-20 and was given the "Ba-349" designation by the RLM only until spring of 1945. There were a total of 52 built and tested with most test results undocumented, destroyed or lost [1].

In 1944, a scale model of the aircraft was tested in a high-speed wind tunnel but no records of its performance other than Erich Bachem's first hand account exist. The Natter's glide characteristics were tested by towing the aircraft behind a He-111 and releasing it. The pilot would test the aircraft's controls and performance in gliding flight and would then either land or bail out at the conclusion of the test. There are only rough figures and first/second hand accounts by the pilot and observers from these flights. According to Myhra, a series of manned towed flights determined the aircraft was stable and able to glide though the pilot claimed that the Natter "sunk like a rock" [2]. These test revealed the aircraft had a maximum dive speed of 700 km/h (377 knots) and stall speed of 200 km/h (107 knots) [2]. The only piloted rocket powered test resulted in the pilots death where shortly after takeoff, the aircraft's canopy blew open and the pilot was knocked unconscious [4].

Both Myhra and Dressel detail the weight of each of the aircraft's components but where Myhra simply states the weight of a component (i.e crew and equipment), Dressel further resolves this figure into subcomponents (i.e instrument panel, controls, etc). These weights can be used to perform an in depth stability analysis of the aircraft and validate other technical specifications.

There is one major difference between the final version of the Natter and the prototypes used in previous tests. All test aircraft had a plexiglass nose cone that covered the internal cavity which held rockets intended to be fired into an allied bomber formation. This plexiglass cover created a smooth surface that reduced drag and increased speed. Though never tested, the aircraft was supposed to jettison this nose cone, allowing the rockets to be fired. None of the technical data derived from the test describe the aerodynamics of the aircraft without this cover in place. This exposed cavity would significantly increase drag and possibly make it unflyable. This project aims to determine the flight characteristics of the Natter in this configuration.

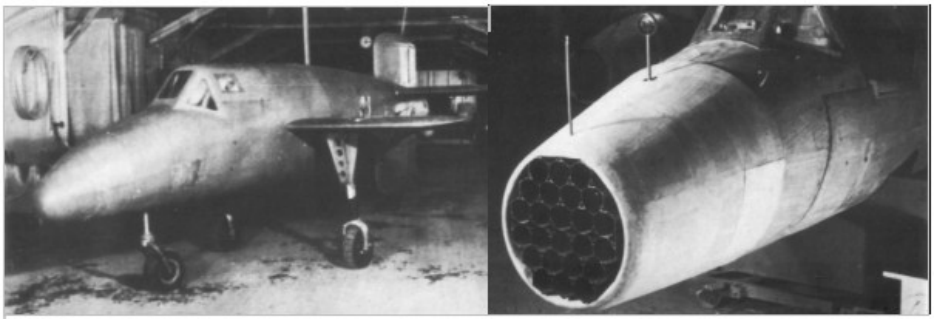

Figure 1.1 Natter prototype with tricycle gear and rocket assembly [1]

### 1.2.2 Comparative Aircraft

There are two other German rocket powered aircraft that existed prior to the Natter: the He-176 and Me-163. The Germans had advanced significantly in the field of rocket science and engineering during the interwar period. A period of “rocket-mania” existed within Germany in the 1920s and 30s. Amateur societies with varying degrees of funding were formed to pursue to budding discipline. A famous example is the Society for Spaceship travel in Breslau (Wroclaw) where a young Wernher Von Braun developed his interest in rockets [1]. Riding on the accomplishments in rocket science before the war, German engineers developed rocket powered aircraft to meet defensive requirements during the war. These requirements would be further developed in the latter half of WWII. Where the Germans focused on vertical takeoff, the Americans focused mostly on offensive rockets meant to barrage large swaths of ground. Both the allies and axis developed jet assisted takeoff (JATO) systems meant to greatly reduce the takeoff distance of a conventionally powered aircraft [5]. The Soviets had a later but brief foray into rocket powered interceptors as well. In 1945, development began on the Mig-270. A rocket powered interceptor initially meant for combat in WWII, it saw increasing interest to counter any potential western attack in the coming cold war. Only two examples were built and tested, both being destroyed during their test [6]. Turbojet powered fighters such as the P-80 and Mig-15 eventually met and exceeded the ally’s requirements for a point defense interceptor and interest was lost in rocket powered aircraft.

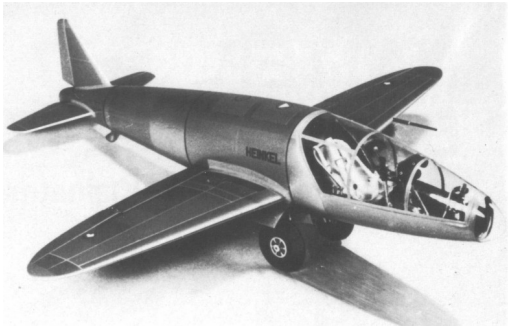

Figure 1.2 Model of He-176 [3]

Figure 1.3 MIG-270 soviet rocket fighter [6]

The He-176 was the brainchild of Werhner Von Braun's concept for a manned rocket powered interceptor. Johnson [7] details development and flight characteristics of the He-176. It was tested in 1939 but its performance was found unsatisfactory by the RLM. The concept was later given to the Deutsche Forschungsinstitut (DFS) and Fiesler for further development. Alexander Lippisch and Erich Bachem worked at DFS and Fiesler respectively. Lippisch took his experience with delta-wing aircraft and started development on the Me-163. Erich Bachem was Fiesler's technical director and left to form his own company to make wood components for aircraft. When emergent calls for a low-cost rocket powered interceptor was issued by the RLM, Bachem designed and developed his own aircraft from his experience at Fiesler. Technical specifications from Johnson [7], Piccirillo [8] are listed in Table 1.1

Table 1.1 - Comparative rocket powered aircraft technical specifications

| | He-176 [8] | Me-163B "Komet" [8] | Ba-349A "Natter" [1] |
|---|---|---|---|
| Max Speed | Mach 0.64 | Mach 0.84 | Mach 0.89 |
| Stall Speed (km/h / knots) | Unknown | 185 / 100 | ~ 200 / 108 |
| Landing Speed (km/h / knots) | 135 / 73 | 220 / 119 | N/A |
| Propulsion Plant Thrust (kg / lbm) | 600 / 1322 | 1750 / 3858 | 1700 / 3747 (2900 / 6393 w/ VTO Boosters) |
| Max Takeoff Weight (kg / lbm) | 1620 / 3571 | 4110 / 9722 | 1810 / 3990 (2270 / 5004 w/ VTO Boosters) |
| Time to 12,000 m (minutes) | N/A | 3.35 | 1.06 |
| Powered Flight Time (minutes) | 1 | 6 | 2 |
| Range/Combat Radius (km / miles) | 110 / 68.4 (Estimated) | 80 / 49.7 | 20 / 12.4 |

Both the Me-163 and Ba-349 used the same engine, a Hellmuth-Walter-Kommanditgesellschaft (HWK) 109-509 that used a combination of hydrazine, methanol and water for fuel and a hydrogen peroxide/water mixture for an oxidizer. Information about this engine comes from Piccirillo [8] and Forsyth [1]. Accidents with refueling and handling were plentiful and deadly. Safety was not an expectation, especially since the project was owned by the SS. HWK would make modifications to the 109-509 to allow it

to start in a vertical position [1]. Despite this difference, the engines used in the Me-163 and the Natter were identical.

Piccirillo [8] details the faults in the Me-163's operational history. The Me-163 was more successful than the Natter though in its entire operational history, it only scored 10 kills with 14 combat losses. To put this in perspective, a formation of 1047 aircraft bombed Cologne on May 30th, 1942 [9]. All the kills scored by all the Me-163's represent less than 1% of that formation on that single day. The ally's ability to replace those losses were substantial. At the peak of its production in 1944, the Willow Run Plant in Ypsilanti, MI was producing one B-24 Liberator every 63 minutes [10]. The time, investment and manpower over three years of development by the Germans could be undone in a matter of 10 hours by a single allied factory. Even if the Natter could achieve its intended purpose, it's hard to believe that the Germans could have scaled up production enough to put a dent in allied bombing.

### 1.2.3 Analytical Techniques

Two methods for analysis are investigated for this project; analytical and numerical. Both methods will be used for validating the specifications of the Natter. They can also be used to cross validate each other and build confidence in the results.

Analytical methods are methods for determining how an aircraft will perform by deriving equations based on the performance of similar aircraft. Raymer [11] is a widely available textbook that describes methods for designing, sizing and analyzing an aircraft. While this project will not be designing anything new, the same methods for determining weight distribution, wing size and drag are used to ascertain a good approximation of the aircraft's specifications. These methods are developed from best practices and experience from hundreds of aircraft developed over the past 100 years. These methods are quick to employ but can not exactly predict how an aircraft will perform. For instance, empirically estimating drag is quick but can only approximate an aircraft made out of ideally shaped bodies. Many analytical techniques can indirectly estimate the increase in drag due to a protuberance like an antenna or gun sight but are limited in estimating the exact value.

Computational fluid dynamics (CFD) allows a near exact prediction of how an aircraft would behave given a set of factors such as speed and angle of attack. Solidworks and Ansys Fluent are two software packages that can perform CFD for both 2D and 3D bodies. These software packages uses an algorithm called the Reynolds Averaged Navier-Stokes (RANS) that can solve large problems with high Reynolds numbers. They offer a more accurate approximation but require extensive setup and computational power that usually exceeds the capability of a single home computer. A large CFD problem may also require some physical verification (i.e wind tunnel test) of the result in order to ensure the model is accurate. CFD wise, there is extensive literature on the characteristics of the National Advisory Committee for Aeronautics (NACA) 0012 airfoil, the airfoil used by the Natter. Essuri [12] provides a study on the effect of different mesh sizes for analyzing a NACA 0012 airfoil.

Fernando and Mudunkotuwa [13] used Ansys Fluent to determine friction drag and lift of a NACA 0012 airfoil with bio-inspired modifications. The purpose of this analysis is to see if a biological wing (such as one seen on a bird) could provide any improvements in regards to drag or weight. They detail their methods for determining Cl and Cd using Fluent and provide an analysis of the results. Even though their analysis determined that their modifications would have little impact on the drag or weight, their analysis process is clear and data from the NACA 0012 can be used to help analyze the Natter.

Computational analyses of the NACA 0012 airfoil are further validations of wind tunnel tests performed by NACA in the 1950s [14]. These results give lift, drag and moment coefficients for high angles of attack with large amounts flow separation, something that's needed for modeling a rocket powered aircraft capable of vertical flight. This study is one of the few tests of this airfoil for post-stall angles of attack.

Previous studies of WWII era aircraft have used both computational and analytical techniques for analysis. Lednicer [15] uses a program called VSAERO to calculate pressure distribution along the entire wetted surface area of a P-51 Mustang, British Supermarine Spitfire and FW-190. Lednicer creates his models from drawings obtained from the National Air and Space Museum (NASM), aviation historical institutions and even the P-51's chief aerodynamicist, Ed Horkey. Based on pressure results, he was able to validate known issues with the P-51's longitudinal stability and low pressure areas behind the canopy bubble. Lednicer was also able to propose better designs for cooling ducts and windshields in order to increase aircraft performance, something that designers in the 1940s could not have done without modern software.

Barnes [16] uses the semi-empirical wing-body linear longitudinal-lateral lifting line (WBL5) method to calculate lift/drag profiles of experimental or planned German turbojet aircraft such as the Ho-229 and B&V-P209. This method shows the shape of the lift and drag profile over the entire wing span and body of the aircraft. Barnes determines which aircraft would have potential issues when it came to stabilization, specifically yaw. For instance, the Ho-229 was designed as a flying wing with no empennage. The designers believed this would reduce drag and increase speed but the lack of a rudder meant that drag rudders needed to be installed on the outside edges of the wing. Based on the WBL5 method, Barnes determines that the Ho-229 lacked the intended "bell-shaped" lift profile and thus would have suffered from a nearly neutral or unstable yaw moment. This would have meant the pilot would need near constant use of drag rudders, increasing drag and negating the designers intent for removing the empennage in the first place. Much of the same can be said for the BV-P209.


Figure 1.4 B&V-P209 [16]


Figure 1.5 Ho-229 [16]

Creating and solving the equations of motion will determine the forces, final velocity and altitude of the Natter. Cook [17] is a textbook that gives generic state space models for aircraft in two dimensions. These can be solved with Matlab using ODE45 or by making a Simulink model. Cook also provides methods for analyzing stability such as determining an aircraft's neutral point (NP) and equations to approximate stability derivatives. Stability analysis can also be done using a numerical program called Athena Vortex Line (AVL). This program is able to approximate flow over slender bodies and allows users to create complex wing geometries and control surfaces. The use can set a variety of flight conditions to analyze performance. This program uses the vortex lattice method (VLM) in order to approximate 3D flow over a lifting surface.

### 1.2.4 Performance Limitations

Though this project will not be performing an in depth analysis on the strength of the wood fuselage and aeroelastic properties of wood, the limits of contemporary wood construction should be known in order to set realistic limitations on the aircraft's performance. Issues with wood construction were well known during WWII. A Society of Automotive Engineering (SAE) journal paper from 1943 [18] lists the issues with wood air frames, most importantly wood's relative weakness when subjected to shear stresses and issues with adhesive bonding. Forsyth claims that, "the fuselage was designed to take accelerations of 6g at a velocity of 1100 km/h (594 knots) at 3000 m (9843 ft) with a safety factor of 1.5" [1]. The Natter was an entirely wood construction aircraft. It's fuselage, skin and wings were made with a combination of heat treated plywood and spars held together by nails and a commonly used urea-formaldehyde (UF) adhesive named Kaurit W [1]. Kaurit W was a common adhesive used in gliders from the 1930s up until the 1960s.

A glider pilot and glider enthusiast, Bachem originally started Bachem-Werke to make wood components for Fiesler and Dornier. By virtue of his work, he was well versed in issues with all wood construction and as any engineer should have taken these effects into account when determining an aircraft's strength. As the war dragged on,

Bachem's concept of a wooden rocket powered interceptor was put under the auspices of the SS and production and testing of the Natter became a matter of rushed necessity. It's plausible to think that production quality suffered. The SS supplied unemployed furniture carpenters, not professionally trained technicians, to work at Bachem's workshop. Peterson notes the difficulty in bonding two wooden surfaces that are not smooth enough as a limitation in wood construction aircraft. Based on the rushed production, inexperience and the reusability requirements of the Natter, claims on the fuselage's strength should be taken with caution. Modern day tests of Kaurit W bonded structures determined that many vintage gliders have Kaurit W bonds that have significant reductions in strength. Konnerth [19] performed tensile/shear stress test on a 1958 wooden glider built with Kaurit W. Results found that bond strength was reduced by 50%, enough to prompt Konnerth to warn against flying in any vintage wooden glider built with the adhesive. Over the years, Kaurit W has been found to become brittle when exposed to moisture. Most notably, Müller [20] states UF adhesives will severely weaken when subjected to abrupt and large changes in temperature and humidity regardless of age, something the Natter would have experienced on a regular basis if it saw combat.

## 1.3 Mission Overview

Forsyth, Myrha and Dressel are the main sources that describe the concept of operations for the Natter. The aircraft was designed to meet a specific set of requirements. Unlike previous German aircraft that could perform multiple roles such as a fighter, ground attack, etc. The Natter was required to be low cost, able to shoot down bombers, and be semi-reusable. In Fall of 1944, the RLM issued a call for proposals for an aircraft that could meet these requirements. Erich Bachem's design was initially passed up and in turn he pursued an appointment with SS officials to see if they would support the project. At this time the SS was taking on more and more aerospace related projects due to RLM's commander-and-chief Hermann Göring's failure to effectively manage the Luftwaffe in the face of allied bombing. The SS is better known for their abuses in perpetrating the holocaust, massacring prisoners of war, and carrying out terror in occupied territories. They eventually pursued specialty "war deciding" projects such as the V-2 for two reasons: failure of the Luftwaffe to defend Germany and their ability to call upon thousands of forced laborers.

The Natter had the following concept of operations. The aircraft would be armed with 24 unguided air-to-air rockets in its nose and then lifted into a vertical position on a launch stand. When an allied bomber stream was to pass nearby, a pilot would enter the aircraft and be launched using a combination of four vertical takeoff assist solid fuel rockets as well as its own liquid fueled rocket. The aircraft would quickly ascend to the bomber's altitude, passing and firing its rockets into the underside of the bomber formation. All rockets would be fired with one pull of the trigger meaning that the pilot would only have one chance to aim and fire. After firing the pilot would then pitch down and through a combination of gliding and diving, descend to 3000 m (9843 ft) and deploy the aircraft's parachute, the force from which would cause the nose and canopy to

separate from the rest of the aircraft whereby the pilot could eject and deploy their own parachute. If the pilot's rockets missed, the pilot was supposed aim the aircraft at a bomber and ram it. This would have resulted in the pilot's death. A combination of fanatical loyalty, coercion and SS control meant this was an acceptable option at the time.

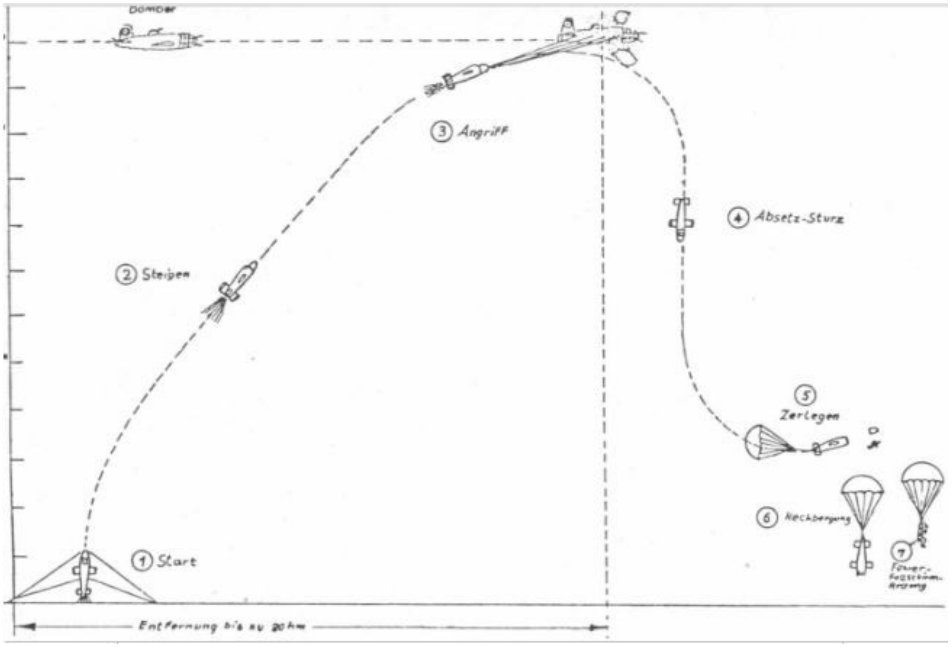

Figure 1.6 Natter concept of operations [1]

# 2. Drag Determination

## 2.1 Fuselage Drag

Three stages of flight: takeoff, attack and gliding will be modeled using analytical methods from Raymer. Each phase of flight has a specific set of properties that need to be calculated. This includes the drag of the aircraft, its mass and other atmospheric properties such as density and temperature. The aircraft's drag coefficient is calculated using the "component buildup" method. A component refers to the aircraft's constituent parts such as its fuselage and nacelles. The largest component of the aircraft is its fuselage and Raymer provides Equation 2.1 and 2.2 to estimate fuselage drag. This equation is able to take into account a fuselage's form and interference with other aircraft components. This method only calculates the parasitic drag of the aircraft and does not include induced drag or wave drag from transonic/supersonic flow.

$$C_{Df} = \frac{C_f \cdot FF \cdot Q \cdot S_{wet}}{S_{ref}} \tag{2.1}$$

$$C_f = \frac{0.455}{(\log_{10} R)^{2.58}(1+0.144\,M^2)^{0.65}} \tag{2.2}$$

$C_f$ is determined by first finding the $R_{cutoff}$ of the flow surrounding the aircraft. This number is used in place of the actual Reynolds Number in order to better estimate $C_f$ at lower speeds. The Reynolds number is usually determined using Equation 2.3 but since this problem involves an aircraft initially starting at rest and the change in $C_f$ is relatively low for high Reynolds numbers, it's simpler to use a constant value throughout the aircraft's flight. There are two equations for $R_{cutoff}$ : subsonic and transonic. Each requires three terms: characteristic length of the aircraft, skin roughness value, and Mach number. Skin roughness varies based on the smoothness of the aircraft skin, namely if its a smooth metal, composite or painted finish. The Natter had a sanded wood skin with camouflage paint. Raymer does not provide a k value for wood but he does provide one for an aluminum skin with camouflage paint $(1.015\,x10^{-5})$. This will be the value for k.

$$R = \frac{\rho V l}{\mu} \tag{2.3}$$

$$R_{cutoff} = 38.21\,(L/k)^{1.053} \tag{2.4}$$

$$R_{cutoff} = 44.62\,(L/k)^{1.053}\,M^{1.16} \tag{2.5}$$

The Mach number is found by dividing the speed of the aircraft by the speed of sound as seen in Equation 2.6. The Speed of sound (c) is determined using Equation 2.7 where T is air temperature. The decrease in temperature and air density with altitude can be estimated using references [21] and [22]. At each timestep, the aircraft rises in altitude and temperature, density, and the speed of sound need to be re-calculated for determining the next $C_f$ and hence the next $C_d$. Figure 2.1 represents the change in temperature, density and speed of sound from 0 to 15,000 m (49212 ft). Calculations are located in Appendix B.1.

$$M = \frac{u}{c} \tag{2.6}$$

$$c = \sqrt{\frac{\gamma R T}{M}} \tag{2.7}$$

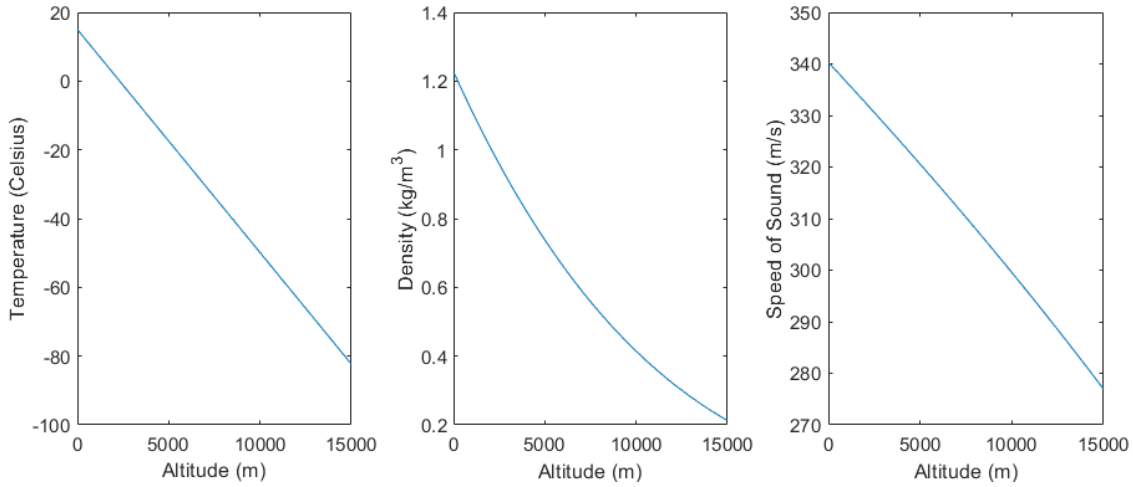

Figure 2.1 Atmospheric properties from sea level to 15,000 m (49212 ft)

Form Factor (Equation 2.8) is the term that estimates the increase in drag based on two parameters: the length of the fuselage and its maximum cross sectional area. Both of these terms are derived from Figure 2.2. An interference factor of 1.0 is chosen since the aircraft has no attached nacelles or stores.

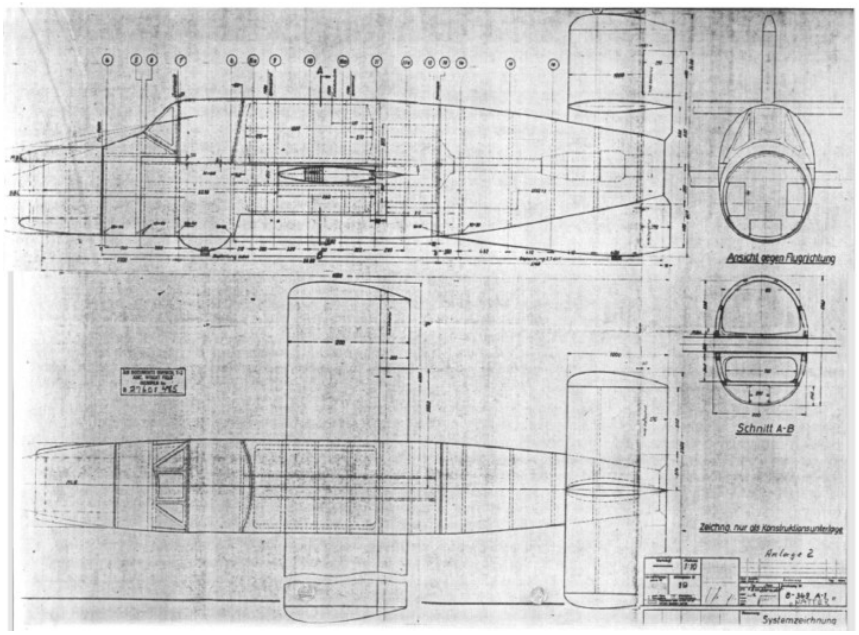

Figure 2.2 Ba-349A-1 "Natter" Plans [3]

$$f = \frac{l}{\sqrt{4/\pi \, A_{max}}} \tag{2.8}$$

$$FF = \left(1 + \frac{60}{f^3} + \frac{f}{400}\right) \tag{2.9}$$

$$(C_d)_{fus} = \Sigma (C_f \, FF \, Q \, S_{wet}) / S_{ref} \tag{2.10}$$

$S_{wet}$ is the total area of the fuselage that's in contact with air. This value is derived from a Solidworks model of the fuselage. Figure 2.3 provides a near perfect value. $S_{ref}$ is the wing reference area and is 3.6 square meters (38.75 square feet). The wingspan is 3.6 meters (11.8 feet) and chord of 1 meter (3.28 feet). In accordance with convention, this area includes both the top-down area of the wing external and internal to the aircraft. This value is used in all subsequent calculations with $S_{ref}$.

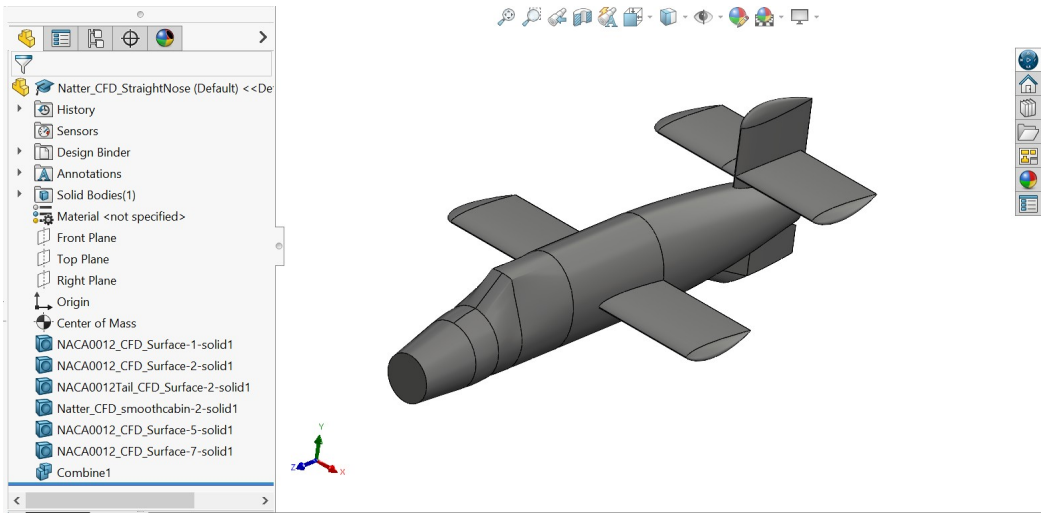


Figure 2.3 Ba-349 "Natter" solidworks isometric model

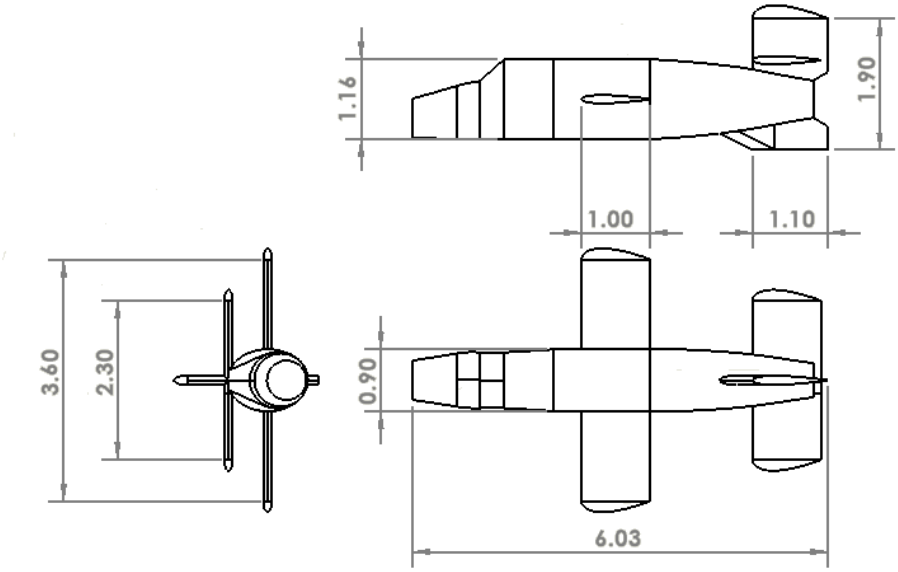


Figure 2.4 Natter standard three view model (m)

The fuselage drag that Raymer's method estimates only works for a typical fuselage body with sloping aft-facing surfaces, curves and a rounded nose. The fuselage changes shape as the Natter prepares to and expend its rockets. This alters the drag coefficient of the fuselage. For example, once the Natter's rockets are fired from the nose, there is a forward facing open area that acts as a rigid parachute, analogous to an open forward facing sphere. Raymer does not provide a method to calculate these changes in

fuselage shape. The increase in $(C_d)_f$ is proportional to the increase in Cd of an analogous geometric shape.

For the first stage of flight, the fuselage roughly resembles a bullet as shown in Figure 2.5. When the nose cap is ejected prior to firing its rockets, the nose becomes a flat/blunt surface, analogous to a bullet losing its rounded front and becoming a flying cylinder. Once the rockets are fired, the nose is an empty chamber similar to a forward facing open sphere. Starting with reference [11]'s estimation of $(C_d)_f$, the change in $C_d$ for each phase is proportional to the change in $C_d$ for the simplified geometries [23]. $C_d$ for each geometry and phase of flight is given in Table 2.1. These values vary slightly throughout the course of flight due to changes in $C_f$.

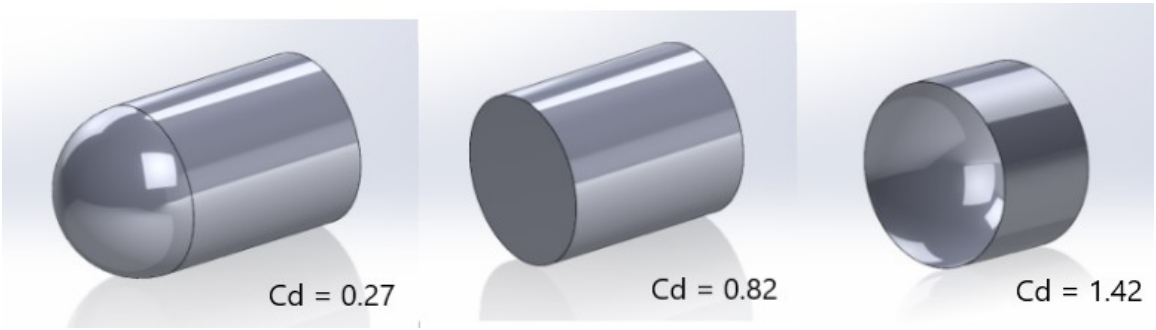

Figure 2.5 Bullet, long cylinder and forward facing sphere geometries

Table 2.1 - $C_d$ for analogous fuselage shapes

| Fuselage Shape (Analogous Shape) | Fuselage $C_d$ |
|---|---|
| Covered Nose (Bullet) | 0.0217 |
| Flat/Blunt Nose (Long Cylinder) | 0.0659 |
| Empty Nose (Forward Facing Open Sphere) | 0.1141 |

## 2.2 Induced and Wing Drag

Induced drag is drag caused by the redirection of air as it passes over a three dimensional finite airfoil. Vortices form on the end of the wing due to the differences in pressure between the top and bottom surfaces. Induced drag for an uncambered wing is

calculated using Equations 2.11-2.13 where e is the Oswald efficiency factor and A is the aspect ratio. Equation 2.11 also takes into account induced drag from the horizontal stabilizer.

$$C_D = C_{Do} + K_{wing} C_L^2 + K_{tail} \frac{S_{tail}}{S_{ref}} C_L^2 \tag{2.11}$$

$$K = \frac{1}{\pi A R e} \tag{2.12}$$

$$e = 1.78(1 - 0.045(AR)^{0.68}) - 0.64 \tag{2.13}$$

$C_L$ is derived from Reference [14]. In order to obtain usable $C_L$ data for all angles of attack, Figure 2.6 from reference [14] was imported into Solidworks and traced using a spline curve function. X/Y points from that curve were imported into Matlab and the same spline function was used to recreate the original curve shown in Figure 2.7. The same was done to derive $C_d$ for the wing at varying angles of attack. This enabled accurate use of data displayed in reference [14].

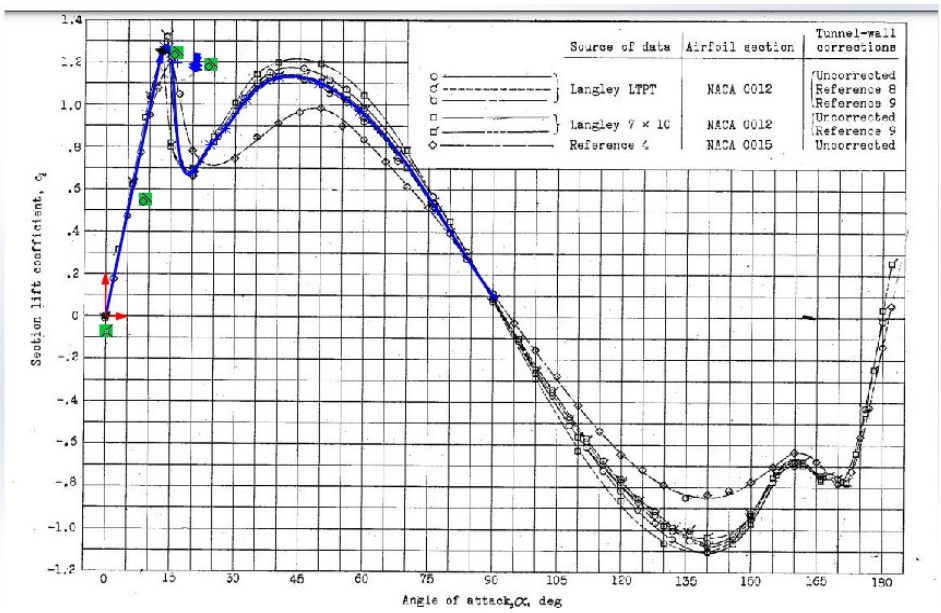

Figure 2.6 NACA 0012 solidworks spline trace [14]

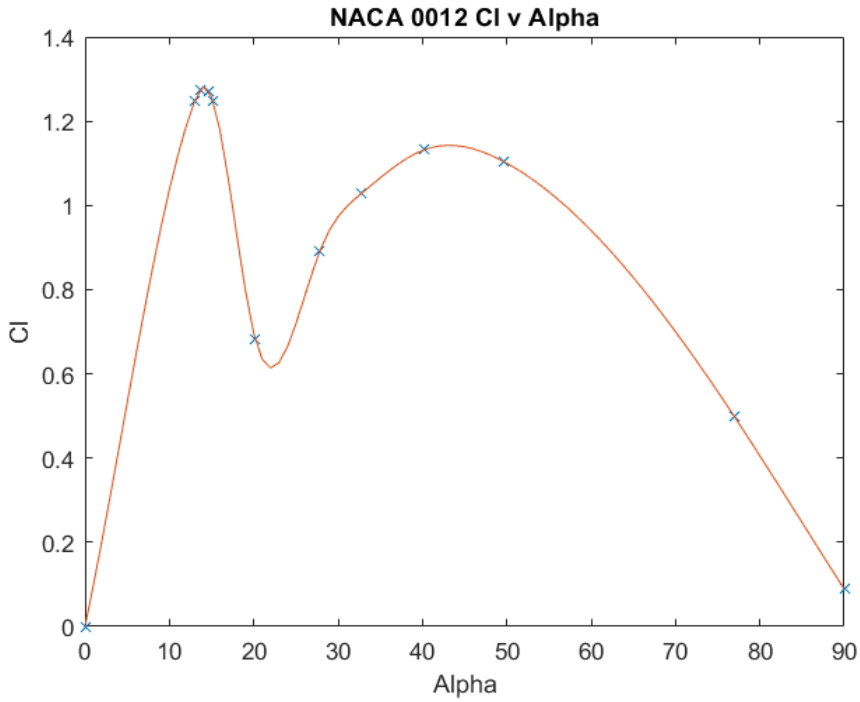

Figure 2.7 NACA 0012 matlab spline curve

This estimation is for a two dimensional wing. Equation 2.14 is used to obtain an accurate $C_L$ for a three dimensional finite wing. This accounts for losses due to wing tip vortices. A wing with a smaller aspect ratio has reduced lift compared to a larger or infinite wing.

$$C_{L\alpha w} = \frac{a_0}{1 + \frac{a_0}{\pi\, eAR}} \tag{2.14}$$

Zero angle of attack parasitic wing and tail drag is calculated using the same method as the fuselage (Equation 2.10) and is 0.0193.

## 2.3 Transonic Drag

All estimations of drag so far have been for subsonic flight. As an aircraft nears the speed of sound, air flowing over the aircraft can become supersonic. The speed between subsonic and supersonic flight is known as the transonic region. Drag increases greatly in this region due to the formation of shocks. Mdd needs to be determined to estimate the increase in drag. This is the speed at which drag starts to significantly increase. Mdd is approximated using the "Boeing" method described in Raymer. For an uncambered wing with a t/c of 12%, Mdd is 0.75 [11]. The increase is usually an S-

shaped curve as seen in Figure 2.8 and 2.9. According to transonic test data from NASA [24] and Raymer [11], the average $C_d$ at Mach 1.0 is approximately 3 times that of $C_d$ at Mdd. The spline curve method used in the previous section is used to estimate the rise in drag when the aircraft is in the transonic region.

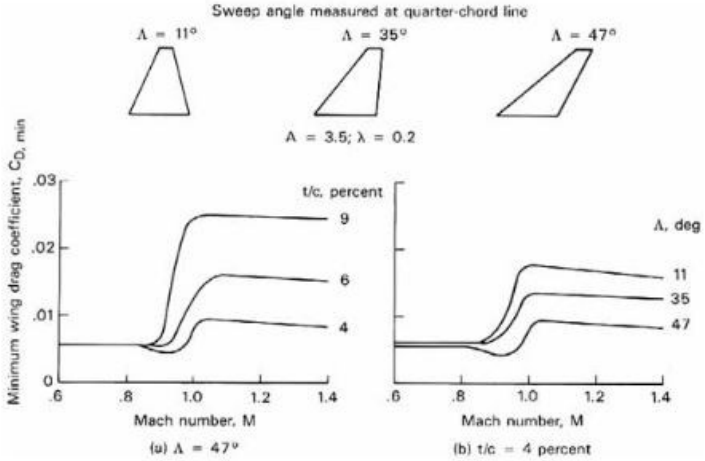


Figure 2.8 NASA transonic drag curve [24]

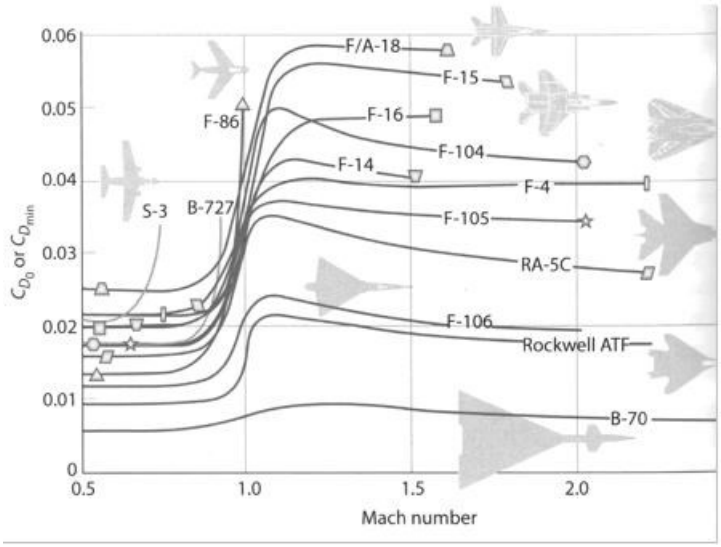


Figure 2.9 Raymer transonic drag curve [11]

## 2.4 Miscellaneous Drag

Table 2.2 lists the remaining aircraft drag components [11]. Leaks and Protuberance (L&P) drag is drag from air entering and exiting the aircraft such as vents

or small openings between movable panels. Protuberances are small geometries such as gun sights that extend from the aircraft and add a small amount of drag. According to Raymer, a 5% increase in the cumulative drag coefficient is enough to account for this increase [11]. [14]. Both the wings and tail are NACA 0012 airfoils.

Table 2.2 - Component drags

| Component | $C_d$ |
|---|---|
| Canopy (Sharp Edged) | 0.0076 |
| Vertical Takeoff (VTO) Boosters | 0.0228 |

Table 2.3 displays the summation of the fuselage, miscellaneous and L&P drag components for each stage of flight. These are the base drag values that will be used for calculating the aircraft's speed and altitude.

Table 2.3 - Total parasitic drag

| Stage of Flight | Total $C_{d0}$ |
|---|---|
| Vertical Takeoff | 0.0750 |
| Climb | 0.0510 |
| Attack | 0.0974 |
| Glide Phase | 0.1481 |

# 3. Mass Determination

## 3.1 Mass of Fuel

The mass of the Natter decreases as it burns fuel. Cstoff and Tstoff are Natter's fuel and oxidizer respectively. There is some disagreement between sources about the total mass of fuel. Assuming the final production version of the Natter needed to have 120 seconds worth of fuel, the model will use the largest figure from Myhra [2]. The mass of fuel was calculated using their percent volumes and densities at standard temperature and pressure (STP) shown in Table 3.1. The final mass of the fuel is 833 kg (1836 lbm). The aircraft burned 6.94 kg/sec (15.3 lbm/sec) of fuel assuming it had two minutes worth of fuel at full throttle. One VTO booster expends 5 kg/sec (11.02 lbm/sec) of solid fuel for a total of 8 seconds. The VTO boosters are shed from the aircraft's fuselage after 8 seconds for a total mass reduction of 460 kg (1014 lbm) [3].

Table 3.1 - Natter fuel mass/volumes from different sources

| Reference | Tstoff (kg / lbm) | Cstoff (kg / lbm) | Fuel/Oxidizer Ratio |
|---|---|---|---|
| Forsyth [1] | 496 / 1093 | 145 / 320 | 0.29 |
| Myhra [2] | 450 liters<br>(612 / 1349) | 250 liters<br>(221 / 487) | 0.36 |
| Dressel [3] | 520 / 1146 | 120 / 265 | 0.23 |

Table 3.2 - Tstoff/Cstoff mass determination

| Fuel | Volume (liters / US Gallons) | Constituent Components | Density ($kg/m^3$ / $lbm/ft^3$) [25] | Percent Volume (%) [25] | Total Mass (kg / lbm) |
|---|---|---|---|---|---|
| Tstoff | 450 / 119 | $H_2O_2$<br>$H_2O$ | 1.45 / 0.091<br>1.0 / 0.062 | 80<br>20 | 612 / 1349 |
| Cstoff | 250 / 66 | $CH_3OH$<br>$N_2H_4H_20$<br>$H_2O$ | 0.79 / 0.05<br>1.01 / 0.063<br>1.0 / 0.062 | 57<br>30<br>13 | 221 / 487 |

## 3.2 Total Mass

Dressel and Myhra each give breakdowns of the aircraft's mass. There is variation between the mass figures and the components included between the two sources. For example, Myhra simply lists the mass of the "nose section" as 30 kg (66 lbm). It does not specify if that includes the controls, instruments or other equipment. Dressel's breakdown is more specific. It includes the mass of individual instruments, controls and even the pilot's seat. For determining the total mass and center of gravity (CG) of the Natter, Dressel's breakdown is used. The mass of fuel is assumed to be 833 kg (1836 lbm) based on the most conservative estimate calculated in Table 3.2. The sum of Dressel's components and fuel results in a total mass of 2293 kg (5055 lbm).

Table 3.3 - Natter mass component breakdown

| Item | Mass (kg / lbm) |
|---|---|
| Wooden Frame | 206 / 454.2 |
| Control Parts | 25 / 55.1 |
| Course Control | 35 / 77.2 |
| Crew & Equipment | 100 / 220.5 |
| Pilot's Seat | 4 / 8.8 |
| Weapons & Ammunition | 185 / 407.9 |
| Bulletproof Glass | 25 / 55.1 |
| Instruments | 6 / 13.2 |
| Armor Plating | 139 / 306.5 |
| Accumulator | 25 / 55.1 |
| Tanks and Fuel | 833 /1836.7 |
| Engine | 170 / 374.9 |
| Fuselage Rescue Parachute | 80 / 176.4 |
| VTO Boosters | 460 / 1014.3 |
| Total Mass | 2293 / 5055.0 |

## 3.3 Center of Gravity

An aircraft's CG is important since its location will dictate the stability and controlability of the aircraft. The CG is calculated for all commercial aircraft prior to every flight to ensure the safety of the crew and passengers. It's assumed that the CG is located on the aircraft's longitudinal axis as is the thrust. Forsyth, Myhra, and Dressel all

include pictures of the aircraft's construction (Figures 3.1-3.2). By analyzing these pictures and comparing them with a Solidworks mockup (Figure 2.3) of the Natter, the location of certain equipment can be surmised within a few centimeters.

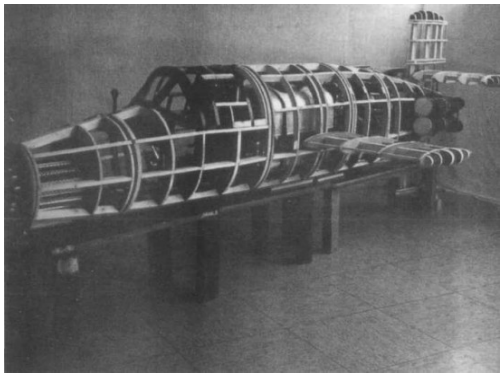

Figure 3.1 Ba-349 "Natter" with no skin [3]

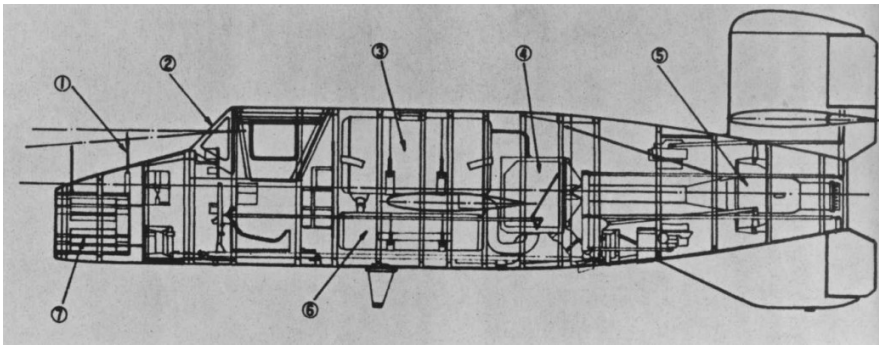


Figure 3.2 Ba-349 "Natter" side view and internals [3]

With the locations of each individual component known, the CG is found by summing the moments of each of the aircraft's components and dividing by the aircraft's total mass (M) as shown in Equation 3.1 where n is the number of individual components to be considered, m is the component mass, l is the moment arm from the nose of the aircraft.

$$CG = \frac{1}{M} \sum_{1}^{n} m_n l_n \tag{3.1}$$

The moment arm is measured from the nose of the aircraft in the "flat nose" configuration. This configuration is chosen since changes in stability and the pilot's ability to control it will be most consequential when the Natter is lining up its shot and expending its rockets.

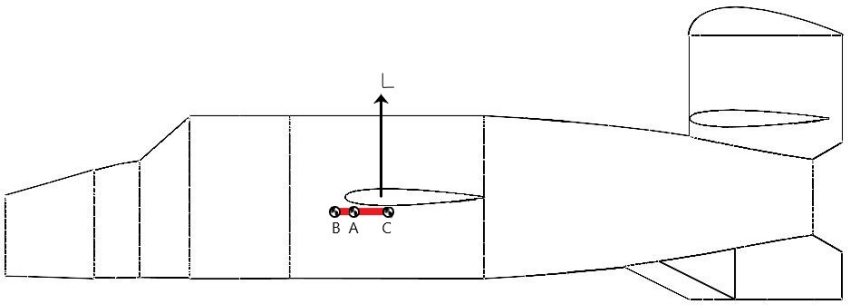


Figure 3.3 Natter with different CG locations

Figure 3.3 shows three CG locations. These are the most extreme scenarios during the extent of the flight. The aerodynamic center for a symmetric/non-cambered airfoil is the quarter chord of the wing. Table 3.4 lists the CG chord location for three scenarios in percent length of the mean aerodynamic chord (% MAC). A table of component locations, masses and moments for the Natter after it has fired its rockets 104 seconds into flight and for the scenarios listed in Table 3.4 are located in Appendix A.

Table 3.4 - CG locations for different mass distributions

| CG Position | Configuration | Chord Position (% MAC) |
|---|---|---|
| A | Full Fuel, Rockets Not Fired | 7.0 |
| B | Empty Fuel, Rockets Not Fired | -11.0 |
| C | Empty Fuel, Rockets Fired | 33.0 |

# 4. Flight Trajectory Modeling

## 4.1 Analytical Models

The flight trajectory of the Natter is modeled using two methods. The first method finds the maximum speed, altitude and range of the flight if the Natter's pitch is fixed throughout its climb. The second method continually varies the Natter's pitch to achieve the most force in the z direction. Both methods rely on equations of motion derived from [17]. The equations of motion are solved using Matlab's ODE45 function.

### 4.1.1 Fixed Pitch Model

For the first method, the takeoff and climb problem is broken into two parts: a vertical climb and then instantaneous turn to the desired pitch. Pitch is the angle between the longitudinal reference line of the aircraft and the horizon. After 8 seconds of vertical lift, the aircraft transitions to the desired pitch and is held constant. It's important to note that pitch is not the same as its actual trajectory or the aircraft's angle of attack. Figure 4.1 is a free body diagram that represents the Natter in flight. The flight path is solved in two dimensions. For simplicity, it's assumed the aircraft is launched in the direction of its target and does not turn during flight.

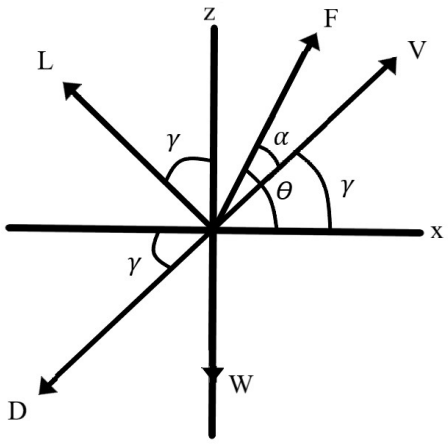


Figure 4.1 Natter two dimensional free body diagram [17]

### 4.1.2 Variable Pitch Model

The second method uses an algorithm to vary the pitch so the aircraft maintains the maximum possible force in the z-direction. The purpose is to find the maximum altitude the Natter could achieve by finding the most efficient pitch angle. As the Natter

takes off vertically, its initial pitch is 90 degrees with no movement in the horizontal direction. The algorithm finds the pitch with the largest combination of thrust and lift in the z-direction. Since the Natter starts in the vertical position, the algorithm would maintain 90 degrees pitch since any nose-down pitch would decrease vertical thrust. To mitigate this, the aircraft's pitch is set to a predetermined value for a specified amount of time. The Natter gains speed in the horizontal direction and once the specified amount of time has passed, the algorithm takes effect and selects the best pitch angle. The best pitch angle is calculated for each time step for the remaining time the rocket has fuel (120 seconds).

The goal of this analysis is to find the most realistic and plausible maximum altitude. The fixed pitch model could be easier to maintain for the pilot but result in a longer time to altitude. The variable pitch model could climb faster but would require more dexterity from the pilot. The pilot only had three instruments that displayed the aerodynamic state of the aircraft: an altimeter, air speed indicator, and a gyroscopic position indicator. The gyroscope only indicates pitch. Angle of attack could not be measured with the instruments provided. Pilots can usually base their desired climb rate based on their airspeed but the large change in airspeed throughout the entire climb would have made this exceedingly difficult. It would have been easier to simply pick a fixed pitch angle and use a gyroscope and the elevator to keep the Natter's nose in that position.

## 4.2 Equations of Motion

Equations 4.1 and 4.2 describe the Natter's motion. This is an initial value problem where the initial position and velocity are zero. The problem is two dimensional assuming the aircraft does not turn. ODE45 is used to solve these equations.

$$\frac{d^2x}{dt^2} = \frac{F\cos(\theta) - \frac{C_L S_{ref} \rho V^2}{2}\sin(\gamma) - \frac{C_D S_{ref} \rho V^2}{2}\cos(\gamma)}{m} \tag{4.1}$$

$$\frac{d^2z}{dt^2} = \frac{F\sin(\theta) + \frac{C_L S_{ref} \rho V^2}{2}\cos(\gamma) - \frac{C_D S_{ref} \rho V^2}{2}\sin(\gamma)}{m} - g \tag{4.2}$$

### 4.2.1 ODE45 Algorithm

ODE45 is an algorithm developed by Dormand and Prince that is based on the 4th and 5th order Runge-Kutta method. The method is explicit and best used for solving non-

stiff and non-linear differential equations. First used over 40 years ago, it has become the predominant method for solving ODEs among computer codes such as Matlab and Python [26]. ODE45 returns the horizontal and vertical positions and velocity. These values are used to calculate atmospheric and aerodynamic quantities such as air density and drag. This process is repeated until the Natter runs out of fuel.

# 5. Analytical Methods

## 5.1 Fixed and Variable Pitch Trajectories

The solutions to these two methods are used to answer four questions: what was the maximum achievable altitude, what was the minimum time to climb to 9700 meters (31824 feet), what was its maximum speed and what was its combat radius. Both methods are compared to find the best result.

To find the maximum altitude for the constant pitch method, a range of pitches that the pilot could have maintained while climbing are tested. Figure 5.1 shows the resulting two-dimensional solution for pitches ranging from 30 to 90 degrees. Angles from 30 to 40 degrees show that the aircraft would have lost altitude on the initial climb after transitioning from its vertical launch phase. This would have presented a safety issue for the pilot since the aircraft could hit trees or structures. This would have presented a serious control issue as well since there would have been little flow over the control surfaces.

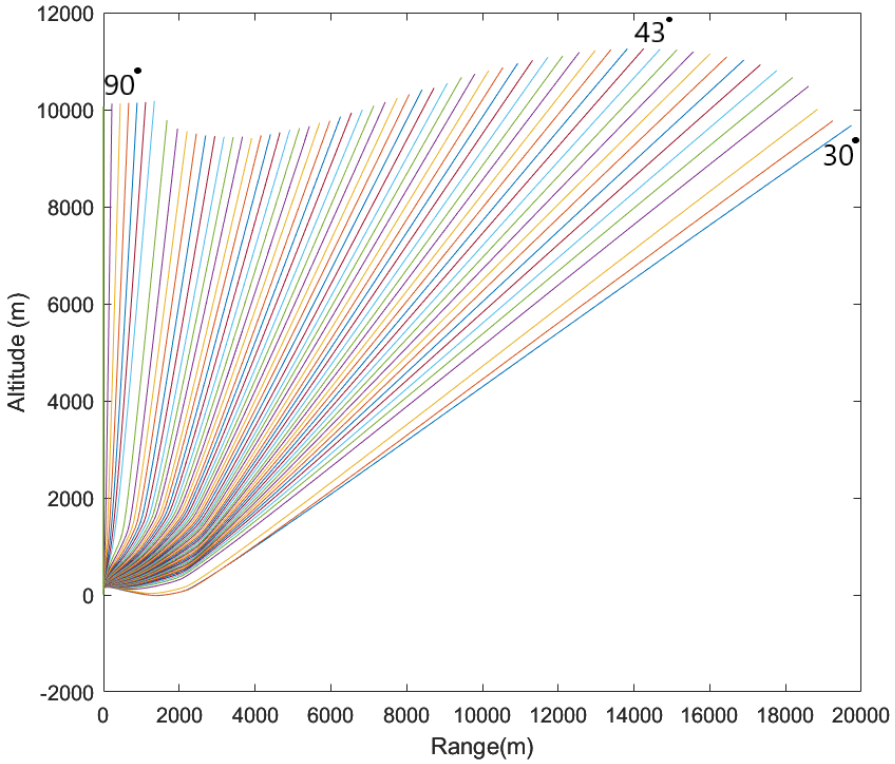


Figure 5.1 Fixed pitch flight trajectory for Natter (30°-90°)

For pitch angles that are nearly vertical, there is a slight increase in the Natter's maximum achievable altitude. This is due to a reduction in lift from the wings and thus a

reduction in induced drag. The aircraft almost exclusively rises due to the force of the engine at these large angles. This critical pitch angle starts at 80 degrees.

Where the fixed pitch model has one input that needs to be set, the variable pitch model has two: the initial pitch and time until the variable pitch algorithm takes effect. This is to allow the aircraft to gain more speed in the horizontal direction in order to generate more lift. The best combination of values was determined by trial and error. The values started at four extremes:

- High Pitch, Short Transition Time
- High Pitch, Long Transition Time
- Low Pitch, Short Transition Time
- Low Pitch, Long Transition Time

The trajectory at each of these extremes results is in an under performing climb. If pitch is too low, the aircraft may gain more speed in the x-direction but not have enough time to climb. If pitch is too high then the aircraft may struggle to gain vertical speed while also making minimal distance downrange. The same applies to the length of time before the variable pitch algorithm take effect. The fixed and variable flights reach a maximum altitude of 11255 (36925) and 13711 (44984) meters (feet) respectively.

Figure 5.2 is the flight trajectory of the variable pitch model compared with the fixed pitch model. Where the fixed pitch model is set to 43 degrees, the variable pitch model has an initial pitch to 40 degrees for the first 75 seconds of flight. Calculations are located in Appendix B.2 and B.3.

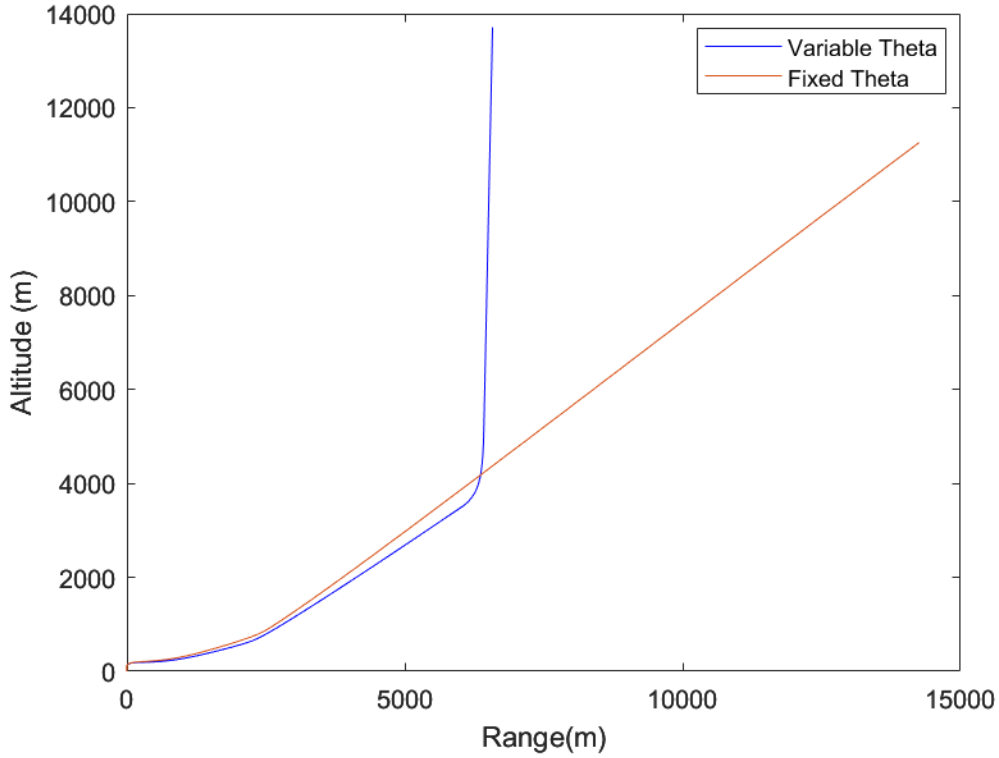

Figure 5.2 Range vs. altitude, fixed/variable pitch models

For the fixed pitch model, the Natter can nearly reach an altitude of 12,000 meters (39370 feet) with the design amount of fuel and thrust. The ability to reach this altitude was an RLM requirement. It was a conservative requirement due to the lack of information about the B-29's ceiling. The B-29's ceiling was actually 9700 meters (31824 feet), well within the Natter's climb radius. An inspection of the fixed pitch solution indicates that the Natter would have reached 9700 meters (31824 feet) in 111 seconds leaving 9 seconds left of fuel. Assuming it could hold level flight at ~280 m/s (918 ft/s) at this altitude for that remaining time, the Natter could extend its combat radius by 2.8 km (1.74 miles) for a total of 14.4 km (8.94 miles). RLM requirements dictated it have a 20 km (12.42 mile) range. The variable pitch model would reach 9700 m (31824 ft) in 104 seconds. At this altitude it would be 6.8 km (4.23 miles) downrange with a maximum combat radius of 12.4 km (7.71 miles). Results are summarized in Table 5.1.

Table 5.1 - Trajectory model results summary

| Trajectory Model | Time to 9700 m (31824 ft) (seconds) | Maximum Altitude (m / ft) | Combat Radius (km / miles) |
|---|---|---|---|
| Fixed Pitch | 111 | 11255 / 36925 | 14.4 / 8.94 |
| Variable Pitch | 104 | 13711 / 44984 | 12.4 / 7.71 |

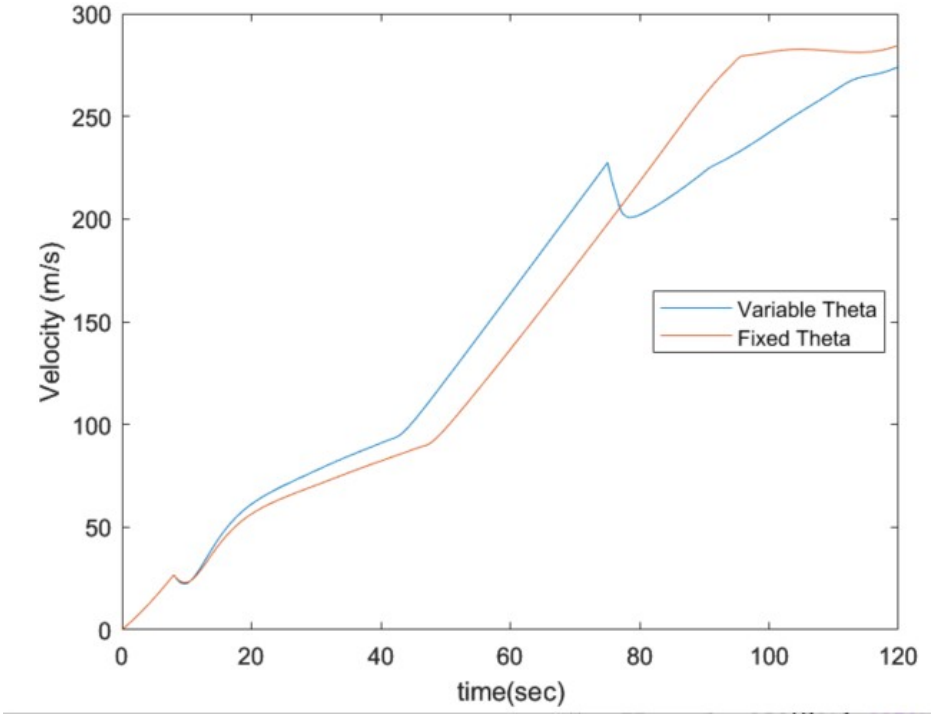


Figure 5.3 Natter velocity throughout flight

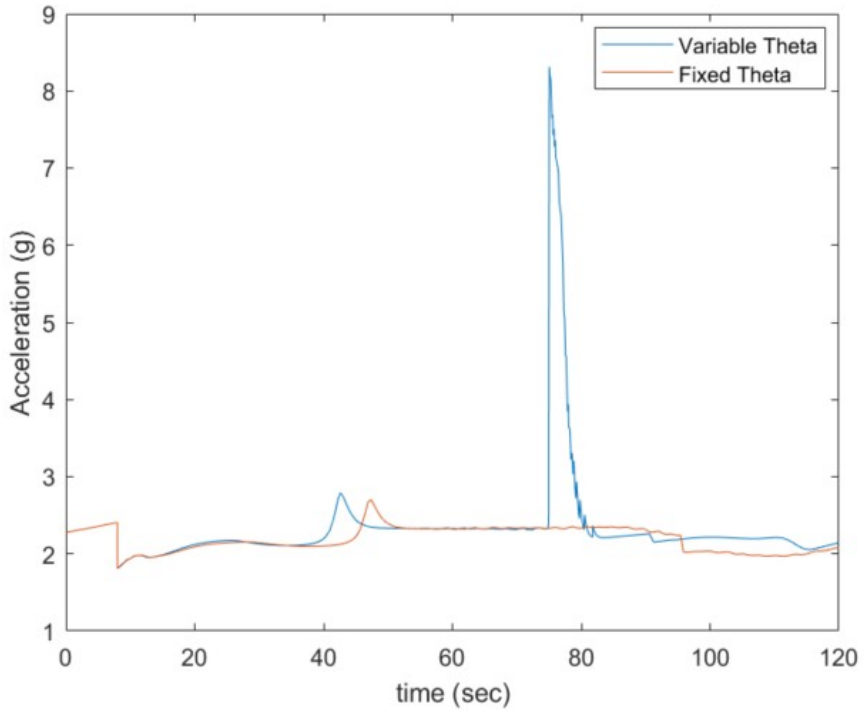

Figure 5.5 Natter total acceleration throughout flight

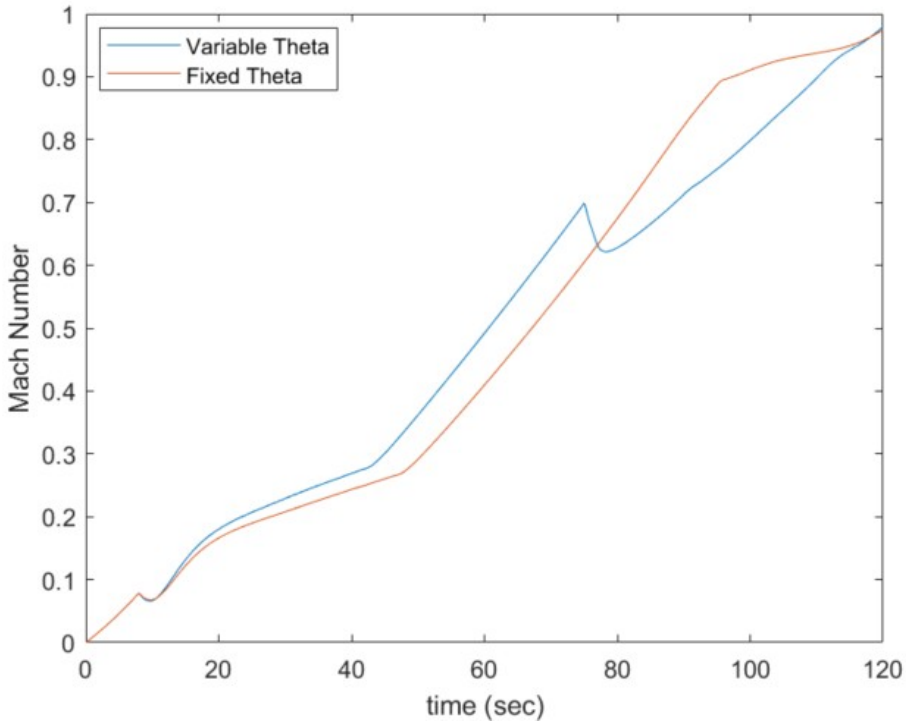

Figure 5.4 Natter mach number throughout flight

## 5.2 Natter Flight Characteristics

### 5.2.1 Natter Velocity Profile

Figures 5.3-5.5 show the total velocity, Mach number and acceleration of the aircraft during its climb. The Natter maintains 1700 kg (3747 lbm) of thrust during its flight while burning 833 kg (1836 lbm) of fuel, which is 46% of its total mass. The total velocity of the aircraft after its 8 second vertical rise is only 26 m/s (85.3 ft/s). Unless the pilot maintained a vertical pitch angle as it did in its unmanned gyro controlled test [1], it's unlikely that the control surface would have enough power to maintain a set pitch angle early in its flight. The velocity near the end of its flight tops out at roughly 280 m/s (918 ft/s) or 1008 km/h (544 knots). The aircraft continues to climb in altitude and nearly reaches the speed of sound.

Though this may have been physically possible given the high thrust to weight ratio and low density atmosphere, it's doubtful that the pilot would be able to control the aircraft in the transonic region. The horizontal stabilizer has a relatively large chord thickness ratio of 12% and is not swept back. The elevons were controlled using a steel wire pulley system. The Natter did not have a trim tab, requiring the pilot to maintain a constant force on the stick to maintain steady flight. Even for the Me-163, an aircraft with swept wings and a sleek unibody design, pilots noted control lock and a severe pitch down moment when entering the transonic range. Me-163 pilots would throttle down during attack phases in order to maintain some degree of control and save fuel. Despite the German Research Institude for Aviation’s (DVL) wind tunnel tests stating the Natter was stable up to 1100 km/h (594 knots)[1], it’s likely the pilot would not have had enough strength or dexterity to use the controls at these speeds.

### 5.2.2 Natter Acceleration and G Forces

As shown in Figure 5.5, the aircraft experiences on average 2.5 g’s during its ascent. A spike in g’s at 40 seconds is the aircraft leaving the stall region and experiencing a large increase in lift as it speeds up. Acceleration remains relatively constant for the fixed pitch model. For the variable pitch model, the aircraft quickly pitches up and experiences a large increase in lift. The total lift force and subsequent acceleration drops as the aircraft’s pitch more closely resembles its trajectory. This exceeds the fuselage’s operational limit of 6 g’s but is less than the design limit of 9 [1]. Assuming there’s a proportional decrease in adhesive strength to a maximum load factor, if there’s a 50% reduction in adhesive strength over successive launches [20], then the operational and design limit would be 3 and 4.5 g’s respectively. Any large turns or pitch up maneuvers could possibly cause the airframe to fail, especially of the kind seen in the variable pitch model.

### 5.2.3 Natter Combat Radius

Figure 5.6 gives a visual perspective of the Natter's combat radius. Centered on San Jose State's campus, it can easily cover the entirety of San Jose. During the latter phases of the war, bomber formations attacked from two major approaches: from the north after crossing the north sea and from the west after overflying Belgium and the Netherlands. This means that a defensive line along these approaches would have been 534 km (332 miles) long as seen in Figure 5.7 For full coverage, 37 Natter's could line the length of this defensive line but one Natter vs an entire formation would have been ineffective. Like the Me-163 squadron, Natter launch sites would have been assembled in groups on the approaches to critical areas. There would have been additional logistics issues with supplying a line of Natter's that long. C-stoff and T-stoff deliveries were hampered by continual bombing of the German rail system. Launches of the V-2, which used the same fuel as the Natter, were continually delayed by lack of fuel shipments. If Natter squadrons were dotted along the length of north-west Germany, it's difficult to imagine the existence of a well functioning logistics system that could supply all of them.

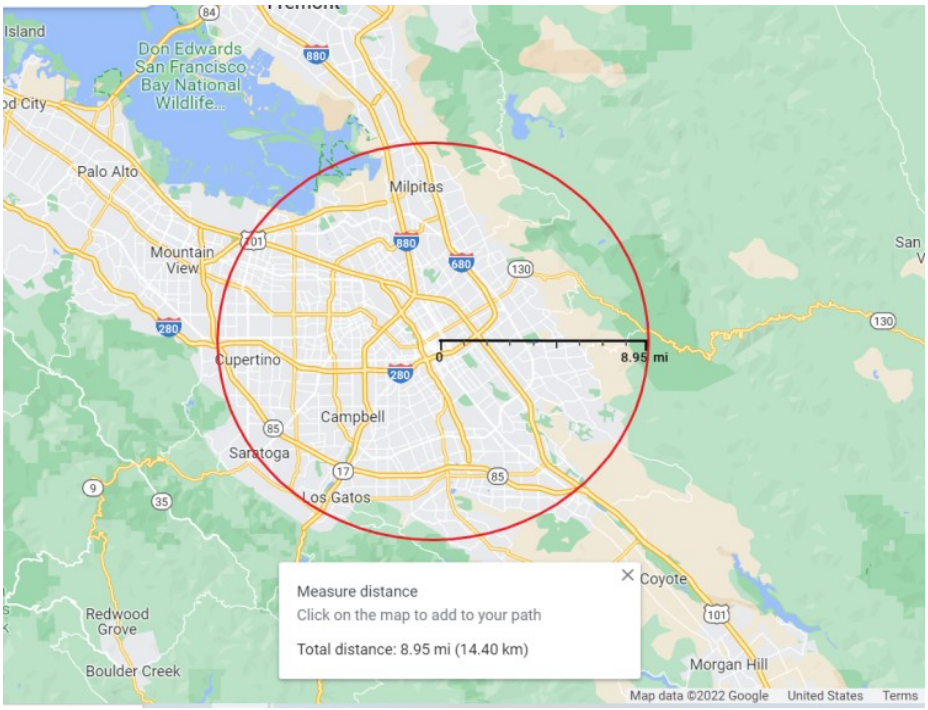

Figure 5.6 Natter combat radius (San Jose State)


Figure 5.7 German air defense line

5.2.4 Natter Drag Forces

As shown in Figure 5.8, the drag forces experienced by the Natter for both fixed and variable pitch flight consists of three phases.

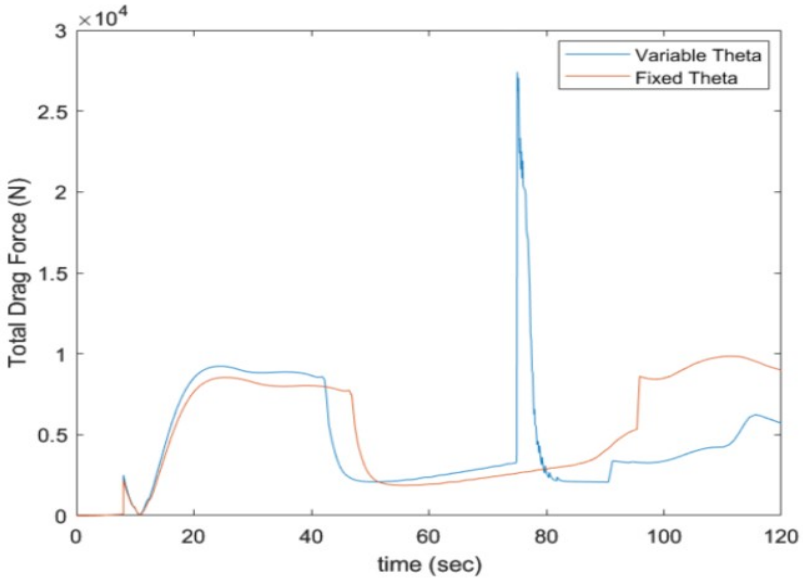


Figure 5.8 Natter drag force for fixed/variable pitch model

At 8 seconds, there is an instantaneous change in the Natter's pitch with no change in horizontal speed. This simplifies the model but it results in a non-physical instantaneous change in drag. The angle of incidence at each step is calculated using Equation 5.1. When the aircraft pitches down, the angle of incidence is exactly 45 degrees, well within post stall territory for a NACA 0012 airfoil. This causes a prompt jump in drag. As the aircraft gains horizontal speed, the drag force plateaus at around 8000 N (1800 lbf). Even though speed is increasing, total drag remains relatively constant as air density decreases with altitude.

$$\gamma = atan(\frac{V_z}{V_x}) \tag{5.1}$$

At roughly 50 seconds, drag rapidly decreases as α gets smaller and the aircraft leaves the post stall region. The aircraft's pitch and trajectory are nearly the same so induced drag and wing drag are nearly zero. For the variable pitch model, once the aircraft pitches up, it creates a large angle of attack and thus large increase in wing and induced drag. Drag will once again increase as the Natter exceeds Mdd. The variable pitch model has lower final drag because of its higher altitude and lower lift force.

## 5.3 Glide Phase

The third and final phase of the Natter's flight is the glide phase. As shown in Figure 1.5, the pilot would fire the Natter's rockets and then perform a near nose dive to decrease altitude. At 3000 meters (9842 ft), the pilot would pull a lever that separated the nose and fuselage and then eject from the aircraft. Though reusable, losing altitude and having a successful ejection was more important than gliding back to the launch site. A slow glide back to the launch site could open the Natter to attack from escort fighters. The Me-163 was particularly vulnerable while gliding back to its airfield.

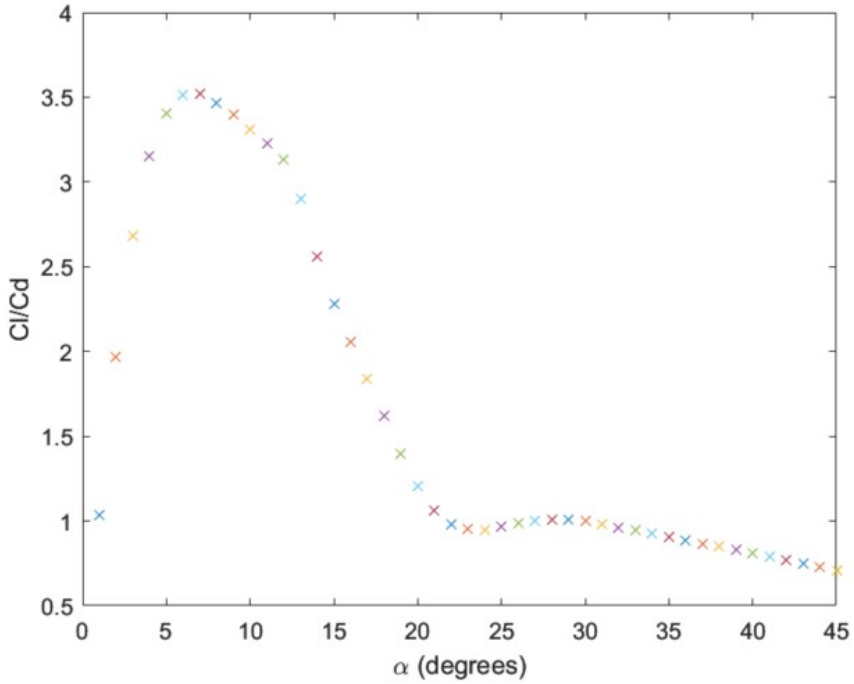

Figure 5.9 L/D for varying angles of attack

Even though the aircraft was not designed for gliding, it's important to know if it was achievable. Glide ratio is the ratio for how much the aircraft moves forward versus how much it descends in altitude. It is a dimensionless parameter and can be found by dividing the lift coefficient by the drag coefficient.

Figure 5.9 is the lift-to-drag (L/D) ratio for different angles of attack for a Natter traveling at 100 m/s (328 ft/s) at 9700 m (31824 ft). An angle of attack of 6 degrees has an L/D ratio of 3.53. To put this in perspective, a Cessna Skyhawk has a maximum L/D of 10.9 [27] while a modern wingsuit has an L/D ratio of approximately 2.5 [28]. Though 3.53 seems low, the aircraft has a large empty cylinder at the nose of the airplane that acts as a rigid parachute. This adds a substantial amount of drag. Starting at an altitude of 9700 m (31824 ft), the Natter could return to its launch point if required but the risk to the pilot and aircraft from attack during this time would have been too great. The Me-163 was frequently shot down during this vulnerable glide phase. Given the risk, the designers did not design for gliding flight, instead opting to simply nosedive and recover the aircraft after the danger of attack had passed.

# 6.0 Stability Analysis

There are three possible stability conditions for an aircraft: stable, neutrally stable, and unstable. An aircraft that is stable is able to "correct" itself following a perturbation and return to steady state flight without any operator input. An aircraft is stable if the CG is located forward of the NP. The longitudinal distance between the CG and the aircraft's neutral point is known as the static margin. For safety, aircraft designers usually define a minimum static margin to ensure longitudinal stability in all flight configurations and scenarios. The neutral point of the aircraft is the furthest aft position that the CG can be before the aircraft becomes unstable. An unstable aircraft would require constant actuation of the flight controls to maintain steady flight. This can be achieved using computerized flight controls but this level of sophistication did not exist during WWII and designers needed to create a stable aircraft.

When the Natter fired its 24 rockets, its CG would have dramatically shifted aft. If the CG shifted aft of the NP, the Natter would be unstable. In this case the pilot would have to bail immediately since the aircraft would be uncontrollable. If the Natter was still stable, the pilot would have to quickly find the next trimmed elevator deflection angle to prevent the aircraft from pitching up. Knowing how the Natter reacted after firing its rockets is critical to knowing if it could accomplish its mission as designed. This chapter will calculate the aircraft's stability derivatives using analytical and numerical techniques and compare these results by simulating the longitudinal response of the aircraft after firing its rockets.

## 6.1 Analytical Neutral Point Determination

There are many ways to calculate the neutral point of an aircraft. Most require a numerical process to fully calculate the effectiveness of the horizontal stabilizer. This requires knowing the downwash angle ($d\varepsilon/d\alpha$) or the angle that external flow approaches the horizontal stabilizer for a given angle of attack. This quantity is difficult to determine due to multiple factors such as tail location, wing size, and calculating the correct amount of induced drag from the main wing.

Two programs are used to determine the NP of the aircraft. The first is Aerotrim©, an analytical program developed by M.V Cook [17] that solves for the downwash angle using an algorithm developed by Stribling [29]. The program has since been converted into a Matlab script by O.A Douglas [30]. Equation 6.1 then estimates the NP of the aircraft [17]. It expresses the effectiveness of the horizontal stabilizer in terms of a one dimensional value: meters. A larger stabilizer with a larger $C_{L\alpha t}$ means the aircraft is more stable and the NP is further aft. Note this process does not take into effect wing body interference.

$$h_n = h_0 + \overline{V}_T \frac{C_{L\alpha t}}{C_{L\alpha w}} \left(1 - \frac{d\varepsilon}{d\alpha}\right) \tag{6.1}$$

Raymer introduces an empirical method to calculate the pitching moment from the fuselage. These moments are based on common 1940s aircraft (Figure 6.1) from NACA TR 711 [31]. $K_f$ is derived from Figure 6.2 and is 0.02 for the Natter. In order to derive the change in static margin from the fuselage pitching moment coefficient, divide by $C_{L\alpha}$ and subtract the result from Equation 6.1 to get Equation 6.3. All NP calculations are located in Appendix B.4.

$$C_{m\alpha f} = \frac{K_f W_L^2 L_f}{c S_{ref}} (per\ degree) \tag{6.2}$$

$$h_n = h_0 + \overline{V}_T \frac{C_{L\alpha t}}{C_{L\alpha w}} \left(1 - \frac{d\varepsilon}{d\alpha}\right) - \frac{C_{m\alpha f}\left(\frac{180}{\pi}\right)}{C_{L\alpha}} \tag{6.3}$$

The analytical NP is 72.5% MAC which is very far aft compared to other aircraft. The Natter's horizontal stabilizer area is large compared to its wing area. It's horizontal stabilizer to wing area ratio is ~2:3 where a Boeing 737-100 is ~1:4. A Boeing 737's NP is usually within 40% MAC [32]. The large stabilizer area acts to prevent longitudinal movement and increase stability. After several tests, Bachem extended the elevon's length by 10 cm (3.93 in), possibly in an attempt counteract the effects from such a large static margin. A large stabilizer like the kind seen on the Natter may also be at the extreme limit for what Equation 6.3 could calculate.

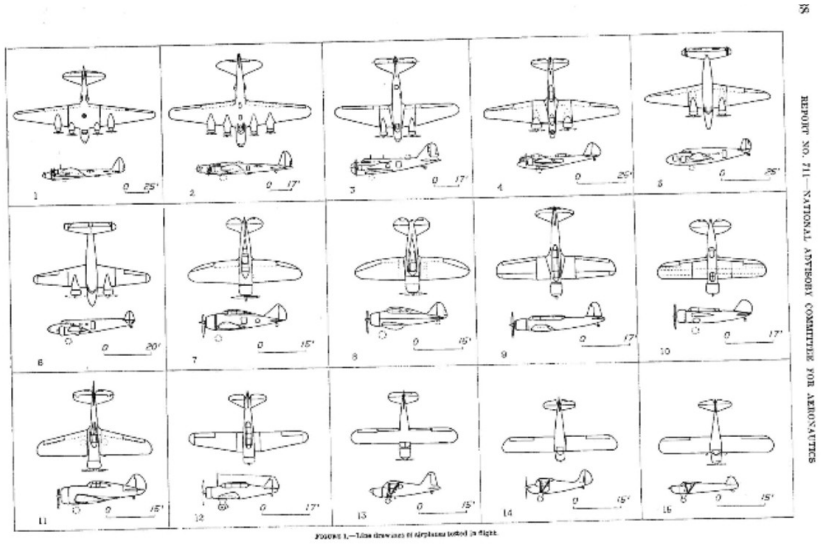

Figure 6.1 Aircraft analyzed in NACA TR 711 [31]

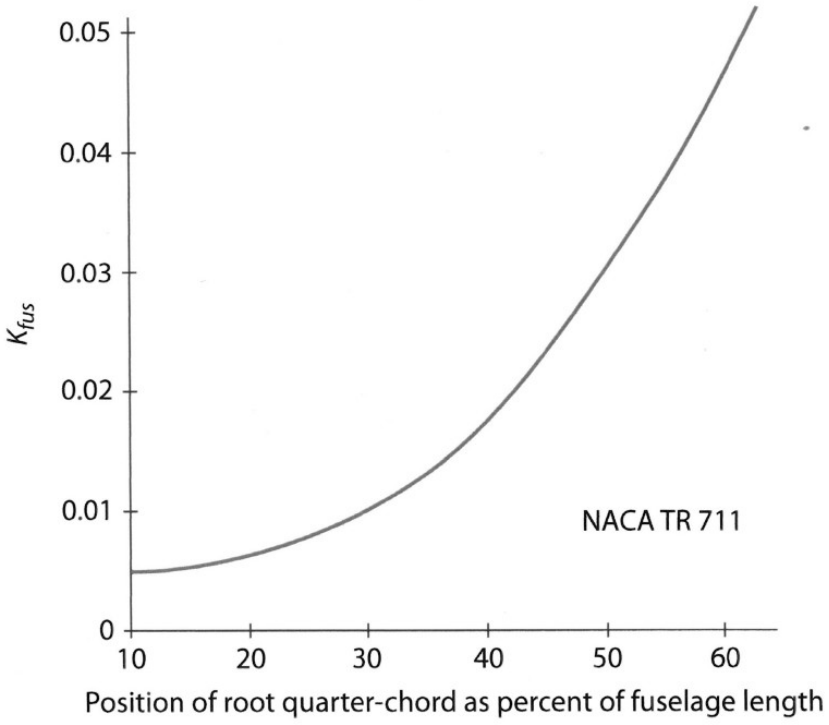


Figure 6.2 Kf vs. root quarter chord location [11]

## 6.2 Numerical Neutral Point Determination

AVL is a program used to derive stability and control derivatives of the aircraft including the NP. It uses VLM in order to estimate pressure, lift and flow for finite 3D bodies. Aerodynamic properties such as lift, drag and moment and their associated coefficients are calculated for different values of α. The program determines the NP numerically by moving the CG aft until $C_{m\alpha} = 0$. When the CG is located exactly at the NP, the aircraft is neutrally stable. AVL's documentation states that including bodies in models can result in instabilities in the solution. VLM is best suited for slender bodies and can not account for flow separation. It's recommended to analyze aircraft with wings and tails only. Though this will have an effect on final stability values, this can be mitigated by hard-coding drag values into the input parameters to simulate the missing fuselage. Figure 6.3 is the geometric model to be analyzed in AVL.

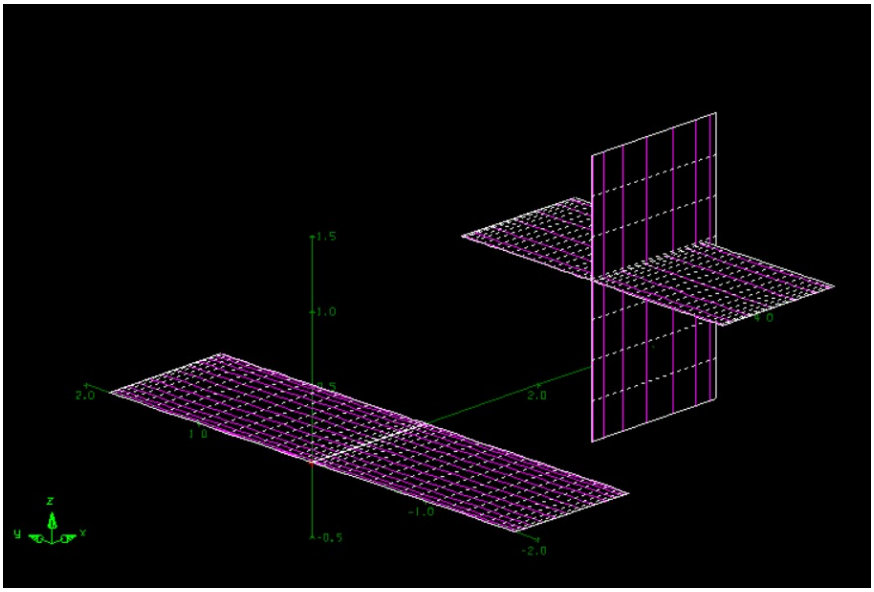

Figure 6.3 AVL wing & tail surfaces geometric plot

AVL gives the NP of 80.1%. This is also well aft of other contemporary aircraft but trends with the analytical value. It may be tempting to apply Raymer's $C_{m\alpha f}$ to reduce this but any change in one coefficient would affect another such as $C_{m\dot{\alpha}}$ and $C_{mq}$. It is not possible for AVL to retroactively calculate new coefficients with a manual change in one parameter. AVL geometry and run files are location in Appendix C.1 and C.2.

## 6.3 Trimmed State Conditions

The goal of this analysis is to first determine how stable the Natter is before and after firing its rockets. This analysis will only study longitudinal stability. There are two quantities that need to be determined to model the response of the Natter after firing its rockets: the trimmed condition angle of attack before and after firing and the longitudinal stability derivatives with its rockets expended. A trimmed condition is when there is no rotation about the aircraft's CG and the aircraft is in level flight. Calculating elevator deflection will also provide a means to validate the solution and model the response. Elevator deflection is calculated analytically by summing the forces and moments of the aircraft as shown in Equations 6.4 and 6.5. These forces are displayed in Figure 6.4. The change in lift for a NACA 0012 airfoil due to elevator deflection is $C_{Lt\delta e}$ and is derived from Reference [33]. Reference [33] studies an airfoil with an elevator that comprises the last 30% of the stabilizer chord. The Natter's elevator comprises the last 33%. This difference is assumed to be negligible for $C_{Lt\delta e}$. Calculations for trimmed elevator deflection are located in Appendix B.5. Results from the analytical and numerical models are listed in Tables 6.1.

$$\Sigma F = 0 = (C_{L\alpha w} q S_W)\alpha + (C_{L\alpha t} q S_t)\alpha + (C_{Lt\delta e} q S_t)\delta e - mg \quad (6.4)$$

$$\Sigma M = 0 = (C_{L\alpha w} q S_W X_W)\alpha + (C_{L\alpha t} q S_t X_t)\alpha + (C_{Lt\delta e} q S_t X_t)\delta e - mg X_{CG} \quad (6.5)$$

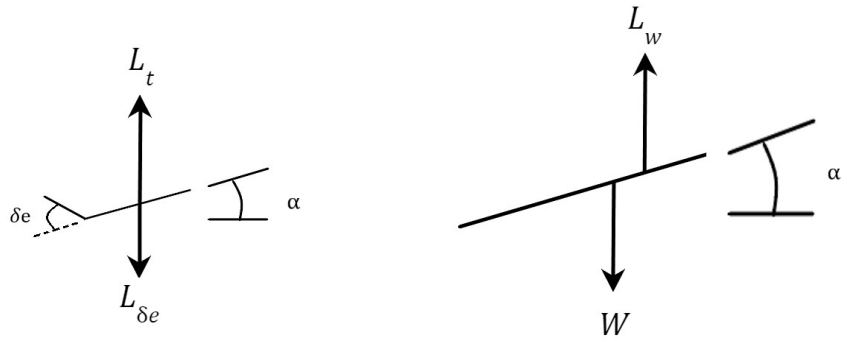


Figure 6.4 Trimmed state free body diagram [17]

Table 6.1 - Trimmed state condition before & after firing rockets

| | Analytical | | AVL | |
|---|---|---|---|---|
| | Before | After | Before | After |
| Trimmed AOA (°) | 2.99 | 2.45 | 3.35 | 2.89 |
| Trimmed δe (°) | -7.15 | -5.96 | -7.17 | -3.85 |
| Neutral Point (% MAC) | 72.5 | | 80.1 | |

## 6.4 Stability Derivatives

Stability derivatives are calculated using Reference [34]. Longitudinal stability derivatives can be approximated using Table 6.2. It's assumed that $C_{Xu}$, $C_{Zu}$, $C_{mu}$ are zero because the change in velocity is small compared to the total speed of the aircraft. Additionally, the lift is the only force acting in the z-direction. Flight conditions for the aircraft are located in Table 6.3. The aircraft is at 9700 m (31824 ft) traveling at 275 m/s (902 ft/s). It has just fired its rockets and has 16 seconds of fuel remaining.

Table 6.2 Analytical stability derivative approximations [34]

| Variable | $X$ | $Z$ | $M$ |
|---|---|---|---|
| $u$ | $X_u = \frac{QS}{mu_0}[2\mathbf{C}_{X0} + \mathbf{C}_{Xu}]$ | $Z_u = \frac{QS}{mu_0}[2\mathbf{C}_{Z0} + \mathbf{C}_{Zu}]$ | $M_u = \frac{QS\bar{c}}{I_y u_0}\mathbf{C}_{mu}$ |
| $w$ | $X_w = \frac{QS}{mu_0}\mathbf{C}_{X\alpha}$ | $Z_w = \frac{QS}{mu_0}\mathbf{C}_{Z\alpha}$ | $M_w = \frac{QS\bar{c}}{I_y u_0}\mathbf{C}_{m\alpha}$ |
| $\dot{w}$ | $X_{\dot{w}} = 0$ | $Z_{\dot{w}} = \frac{QS\bar{c}}{2mu_0^2}\mathbf{C}_{Z\dot{\alpha}}$ | $M_{\dot{w}} = \frac{QS\bar{c}^2}{2I_y u_0^2}\mathbf{C}_{m\dot{\alpha}}$ |
| $q$ | $X_q = 0$ | $Z_q = \frac{QS\bar{c}}{2mu_0}\mathbf{C}_{Zq}$ | $M_q = \frac{QS\bar{c}^2}{2I_y u_0}\mathbf{C}_{mq}$ |

Table 6.3 - Natter flight conditions

| | |
|---|---|
| u=275 m/s (902 ft/s) | ρ=0.428 $kg/m^3$ (0.027 $lbm/ft^3$) |
| $S_{ref}$=3.6 $m^2$ (38.75 $ft^2$) | c=1 m (3.28 ft) |
| m= 926 kg (2041 lbm) | $I_{yy}$=986.5 $kg \cdot m^2$ (282.1 $lbm \cdot ft^2$) |
| $X_{CG}$= 33% MAC | Q=16184 $N/m^2$ (338 $lbf/ft^2$) |

$C_X$ and $C_Z$ represent the force coefficients acting in the x and z directions. These are equivalent to $C_{D0}$ and $C_L$ respectively. $C_{X\alpha}$ is the change in drag with respect to the α This is directly calculated from Reference [14]. $C_{m\alpha}$ is calculated using Equation 6.6. An accurate calculation of the NP is important and this is where the analytical and numerical derivatives start to differ.

$$C_{m\alpha} = [\frac{X_{CG}}{c} - \frac{X_{NP}}{c}]C_{L\alpha w} \tag{6.6}$$

$C_{L\dot{\alpha}}$ and $C_{Lq}$ are calculated using Equations 6.7 and 6.8. Even though the tail has the same airfoil as the wing, $C_{L\alpha t}$ is smaller due to its smaller aspect ratio. $C_{m\dot{\alpha}}$ and $C_{mq}$ are calculated by multiplying $C_{L\dot{\alpha}}$ and $C_{Lq}$ by the chord-normalized distance between the wing and tail.

$$C_{L\dot{\alpha}} = -2\eta \overline{V}_t \frac{dC_{Lt}}{d\alpha_t}\frac{d\epsilon}{d\alpha} \tag{6.7}$$

$$C_{Lq} = 2\eta \overline{V}_t \frac{dC_{Lt}}{d\alpha_t} \tag{6.8}$$

$$C_{M\dot{\alpha}} = -2\eta \frac{l_t}{c} \overline{V_t} \frac{dC_{Lt}}{d\alpha_t} \frac{d\epsilon}{d\alpha} = [\frac{l_t}{c}] C_{L\dot{\alpha}} \tag{6.9}$$

$$C_{M\dot{\alpha}} = -2\eta \frac{l_t}{c} \overline{V_t} \frac{dC_{Lt}}{d\alpha_t} = -[\frac{l_t}{c}] C_{Lq} \tag{6.10}$$

Aerodynamic coefficients are located in Table 6.4. AVL calculates some but not all coefficients. AVL coefficients denoted with an asterisk are calculated using quantities such as $\overline{V_t}$ and $l_t/c$ from the analytical equations.

Table 6.4 - Non-dimensional aerodynamic coefficients (analytical v. AVL)

| | Aerodynamic Coefficient | Analytical | AVL |
|---|---|---|---|
| $C_X$ | $C_D$ | 0.103 | 0.106 |
| | $C_{D\alpha}$ | 0.083 | 0.083* |
| | $C_{D\dot{\alpha}}$ | ≈ 0 | ≈ 0 |
| | $C_{Dq}$ | ≈ 0 | ≈ 0 |
| $C_Z$ | $C_L$ | 0.156 | 0.187 |
| | $C_{L\alpha}$ | 3.574 | 4.522 |
| | $C_{L\dot{\alpha}}$ | -3.017 | -3.017* |
| | $C_{Lq}$ | 9.170 | 12.950 |
| $C_M$ | $C_{mu}$ | ≈ 0 | ≈ 0 |
| | $C_{m\alpha}$ | -1.412 | -2.130 |
| | $C_{m\dot{\alpha}}$ | -7.512 | -7.512* |
| | $C_{mq}$ | -22.833 | -23.360 |

Table 6.5 - Dimensional stability coefficients (analytical v. AVL)

| | Aerodynamic Coefficient | Analytical | AVL |
|---|---|---|---|
| $C_X$ | $X_u$ | -0.0471 | -0.0485 |
| | $X_\alpha$ | 0.0190 | 0.0190* |
| | $X_{\dot{\alpha}}$ | 0 | 0 |
| | $X_q$ | 0 | 0 |
| $C_Z$ | $Z_u$ | -0.0713 | -0.0856 |
| | $Z_\alpha$ | -0.8176 | -1.0345 |
| | $Z_{\dot{\alpha}}$ | 0.0013 | 0.0013* |
| | $Z_q$ | -1.0488 | -1.4812 |
| $C_M$ | $M_u$ | ≈ 0 | ≈ 0 |
| | $M_\alpha$ | -0.3033 | -0.4576 |
| | $M_{\dot{\alpha}}$ | -0.0029 | -0.0029* |
| | $M_q$ | -2.4527 | -2.5093 |

To determine if the Natter is longitudinally stable, the stability derivatives are arranged in state space representation where A is the stability matrix, B is the control matrix and C and D are identity and feed forward matrices respectively [34].

$$\dot{\vec{x}} = A\vec{x} + B\vec{u} \tag{6.11}$$

$$\vec{y} = C\vec{x} + D\vec{u} \tag{6.12}$$

$$A = \begin{bmatrix} X_u & X_a & 0 & -g \\ Z_u/U_1 & Z_\alpha/U_1 & 1 & 0 \\ (M_u + \frac{M_{\dot{\alpha}} Z_u}{U_1}) & (M_\alpha + \frac{M_{\dot{\alpha}} Z_u}{U_1}) & M_q + M_\alpha & 0 \\ 0 & 0 & 1 & 0 \end{bmatrix} \tag{6.13}$$

$$B = \begin{bmatrix} X_{\delta e} \\ Z_{\delta e}/U_1 \\ M_{\delta e} + \frac{M_{\dot{\alpha}} Z_{\delta e}}{U_1} \\ 0 \end{bmatrix} \tag{6.14}$$

$$\vec{x} = \begin{bmatrix} u \\ \alpha \\ q \\ \theta \end{bmatrix} \tag{6.15}$$

The A and B matrices are shown above. Deriving the eigenvalues of the analytical and AVL A matrices gives the following eigenvaules.

Table 6.6 - Analytical longitudinal mode characteristics

| Mode | Pole | Damping | Frequency (Rad/sec) | Time Constant (sec) |
|---|---|---|---|---|
| Short Period | $-1.30\,x\,10^{-2} \pm i\,4.45\,x\,10^{-2}$ | 0.280 | $4.63\,x\,10^{-2}$ | 77.1 |
| Phugoid | $-0.155$ | 1 | 0.155 | 6.46 |
| | $-2.32$ | 1 | 2.32 | 0.430 |

Table 6.7 - AVL longitudinal mode characteristics

| Mode | Pole | Damping | Frequency (Rad/sec) | Time Constant (sec) |
|---|---|---|---|---|
| Short Period | $-1.55\,x\,10^{-2} \pm i\,5.01\,x\,10^{-2}$ | 0.295 | $5.24\,x\,10^{-2}$ | 64.7 |
| Phugoid | $-0.220$ | 1 | $2.20\,x\,10^{-2}$ | 4.56 |
| | $-2.50$ | 1 | 2.31 | 0.432 |

The Natter is longitudinally stable since the short period and phugoid are both negative. Aircraft operating at high speed usually have lightly damped phugoids [34]. The eigenvalues of the A matrix presented a unique situation where two of the four roots of $det[A-\lambda I]$ were real with no non-real component. When this is the case, Matlab's "damp()" function assumes a damping factor of 1, indicating that it's critically damped. The response discussed though in section 6.5 shows this is not the case. Caughey [34] provides an approximation of the natural frequency and period for the phugoid mode as seen in Equations 6.16 and 6.17.

$$W = \sqrt{2}\frac{g}{U} \tag{6.16}$$

$$\zeta = \frac{1}{\sqrt{2}}\frac{C_D}{C_L} \tag{6.17}$$

The resultant frequency and damping ratio is 0.05 rad/sec and 0.4 respectively. A damping ratio less that 1 means that there is oscillation following a perturbation.

## 6.5 Longitudinal Response

The longitudinal response of the Natter is simulated using an open loop system where δe is the input and Equation 6.15 is the output. Figure 6.7 represents the Natter's response to a sudden change in CG with the prior trimmed state δe. After 5 seconds, δe is reduced to the trimmed state value for the new CG. For both the analytical and AVL model, the aircraft pitches up. If δe doesn't change and the CG moves aft, the δe angle is too large and the aircraft begins to pitch up. Once the δe is reduced, the aircraft returns to its new steady state flight condition.

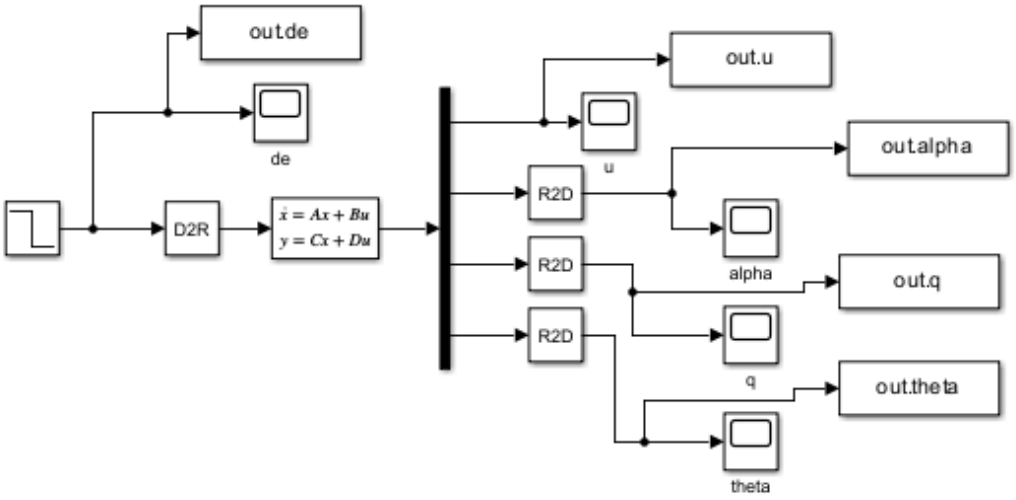


Figure 6.5 Natter open loop longitudinal model

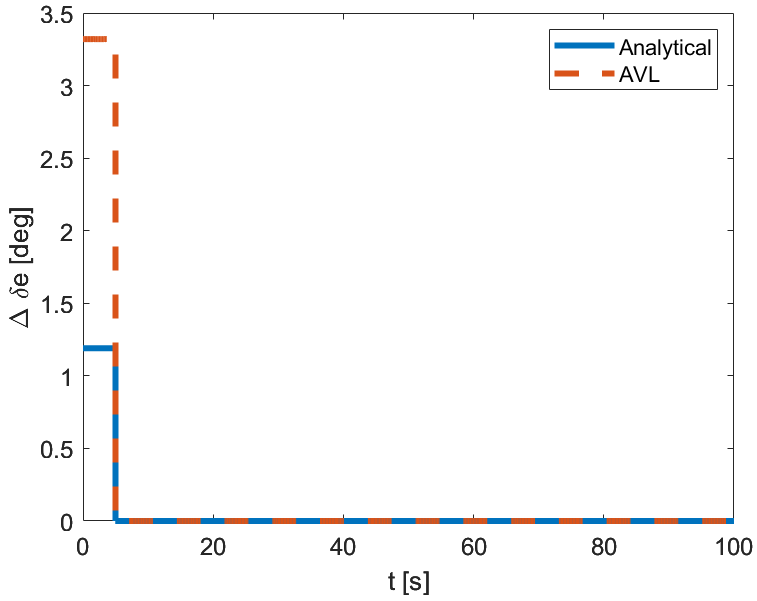


Figure 6.6 Natter elevator deflection (analytical vs. AVL)

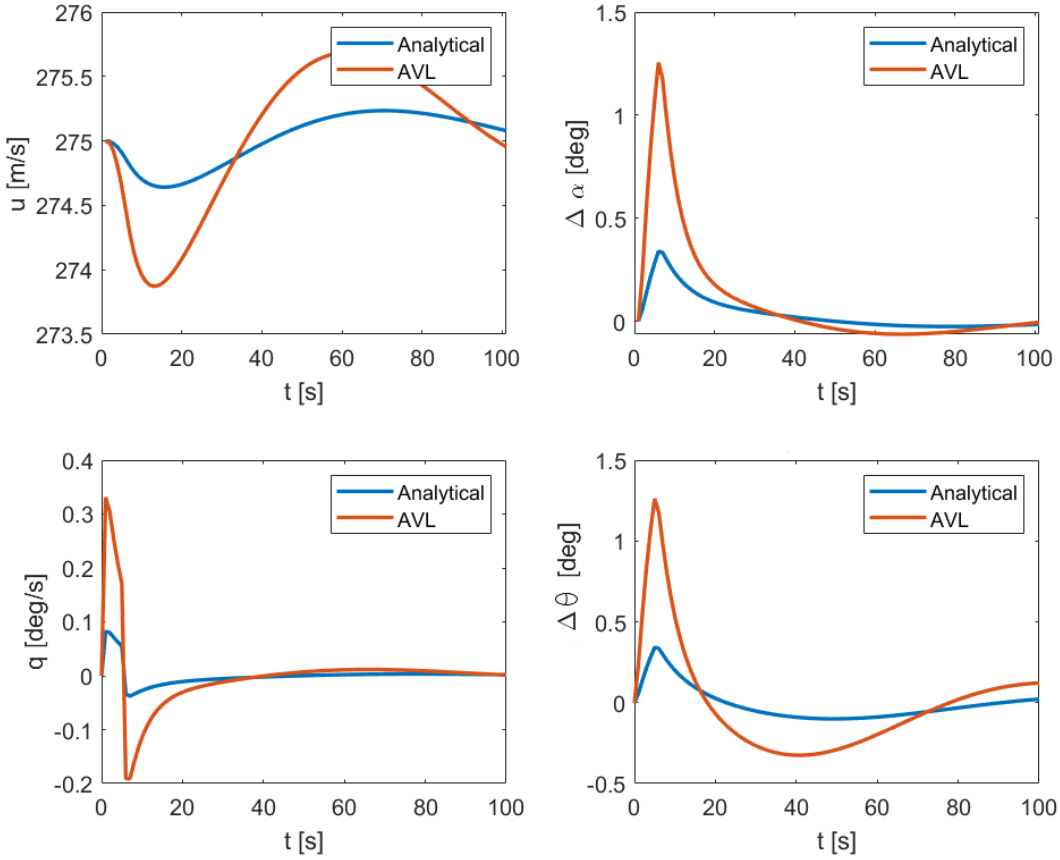


Figure 6.7 Natter open loop response (Δδe = 0, t = 5 sec) (analytical vs. AVL)

For Figure 6.7, the rate of change in α and θ is much less in the analytical model than in the AVL one. The AVL NP is approximately 8% further aft which makes recovery from any perturbation quicker. There is a larger δe for the AVL model which results in a larger pitch up.

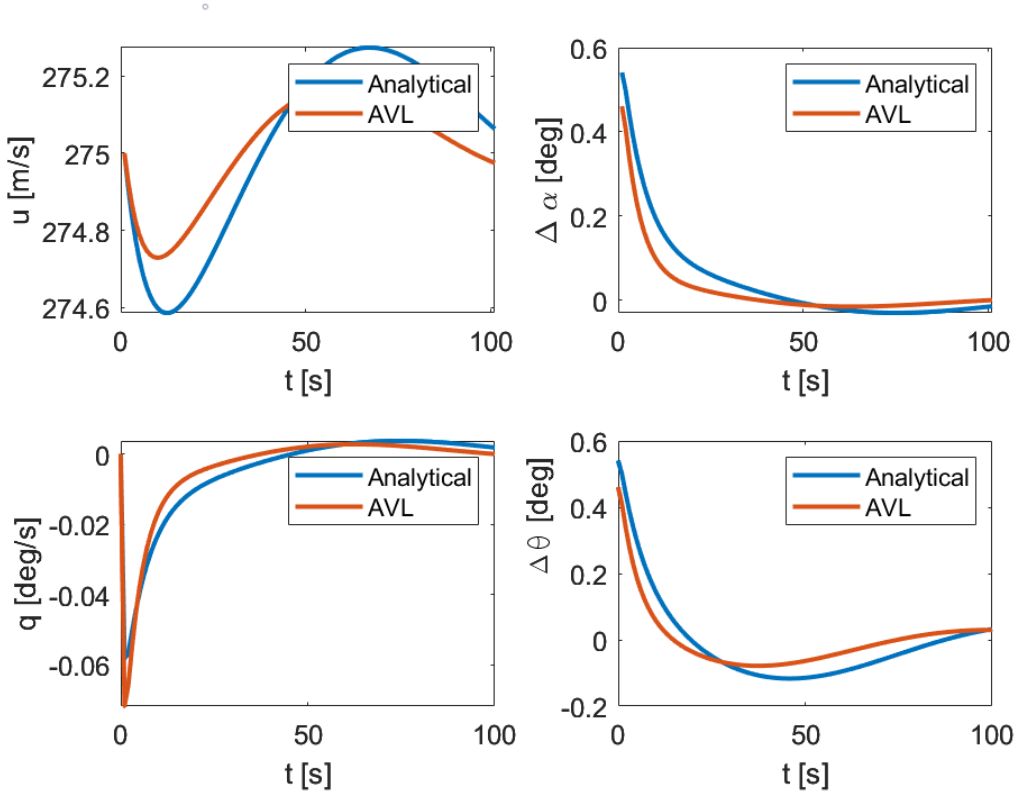


Figure 6.8 Natter open loop response (Δδe = 0, t = 0 sec) (analytical vs. AVL)

Figure 6.8 represents the longitudinal response if the pilot immediately reduced δe after the rockets were fired and the CG moved aft. The aircraft pitches down and settles at its new trimmed state α and θ. The change in α and θ is less than one degree and takes approximately 60 seconds to settle at its new trimmed state. For both cases presented in Figures 6.7 and 6.8, the pilot would not have had any issue with controlling the Natter after firing its rockets.

# 7. Energy & Maneuverability

## 7.1 Energy-Maneuverability (EM) Background

For the Natter to line up its shot, it needs to be able to turn. Unlike contemporary fighter aircraft of the time, the Natter was not designed with high performance maneuvers in mind. Its frame was made of wood and its pilot given the most basic of amenities for the harsh high altitude conditions. Bachem personally states that the design was meant to withstand 6g's with a safety factor of 1.5 [1]. The maneuverability of combat aircraft is calculated and displayed by "Energy-Maneuverability" diagrams. These diagrams display the turn rate, speed and g-force a pilot could expect when maneuvering. The embolded curves with values "0","+2.5", etc. are specific excess energy (PS) curves. These indicate the maximum speed an aircraft could maintain a sustained turn and still be able to accelerate. Any condition above and to the right of the "0" PS curve means the aircraft is unable to speed up. Any condition below and to the left means the aircraft has some remaining energy to speed up. Analytical methods for this were developed by USAF Col. John Boyd beginning in the 1960s [35], well after WWII. Figure 7.1 is an EM chart for an F-4J Phantom II (Figure 7.2).

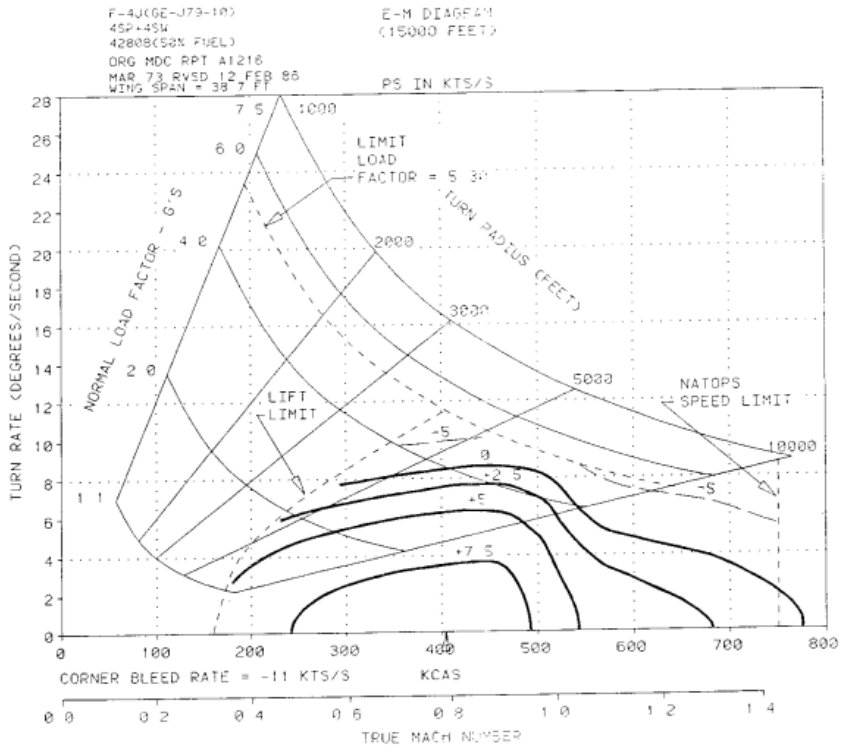


Figure 7.1 F-4J Phantom II EM diagram [35]

Figure 7.2 F-4J Phantom II, U.S Navy [36]

A pilot would reference the diagram to manage the aircraft's speed in order to find the best turn rate while not exceeding the aircraft's load limits. The thrust and control capabilities of a fighter aircraft could well cause a load factor that exceeded the airframe's and pilot's physiology limits. It's necessary for a pilot to know these limits in order to efficiently execute a turn. WWII era designers *did* take parameters such as thrust, weight, and load factor into account while designing an aircraft but the EM framework that combined these did not exist.

## 7.2 EM Analysis

In EM analysis, there are two performance metrics that can describe the maximum turn rate of the aircraft: instantaneous and sustained turn rate. Turn rate is in units of degrees per second. The aircraft banks over and a portion of the lift from the wings and elevator input from the pilot causes the aircraft to turn and change heading. Instantaneous turn rate is where a pilot banks over but the aircraft is unable to maintain a steady speed. Sustained turn rate is the turn rate where the aircraft can maintain the same speed throughout the turn [37].

Instantaneous turn rate is determined by first calculating the maximum lift coefficient at stall and plotting the resultant turn rate for a given load factor. Figure 7.3 represents the forces on the aircraft as it turns [11]. For every bank angle during level flight, the aircraft always maintains a constant weight. As bank angle increases, the pilot needs to increase the force on the elevator in order to compensate for the loss of lift in the z-direction.

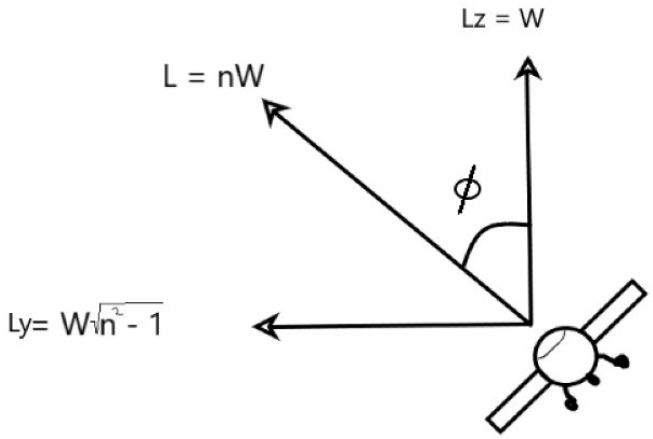


Figure 7.3 Free body diagram of turning aircraft [11]

Turn rate is defined in Equation 7.1, where the top term is the radial force felt by the aircraft and the bottom is the aircraft's momentum. The instantaneous turn rate is determined by deriving an equation for the turn rate of the aircraft for maximum lift at a given bank angle ($\phi$) for the lowest speed possible. The maximum bank angle for a given speed can be derived from the total weight of the aircraft and maximum lift coefficient since the lifting force in the z-direction must equal the weight of the aircraft. The radial force term is and then divided by the aircraft's momentum to get the instantaneous turn rate as shown in Equation 7.3. This is the turn rate at which the aircraft is just before stalling.

$$\dot{\psi} = \frac{W\sqrt{n^2-1}}{(W/g)V} = \frac{W\sqrt{n^2-1}}{mV} \tag{7.1}$$

$$\phi = cos^{-1}\frac{mg}{(C_{L_{max}}\rho SV^2)/2} \tag{7.2}$$

$$\dot{\psi}_{instant} = \frac{sin(\beta)\frac{Cl_{max}\rho SV^2}{2}}{mV} \tag{7.3}$$

Sustained turn rate is when the aircraft is able to turn while maintaining level flight and the lowest constant speed. Thrust must equal drag and lift must equal the aircraft's weight [37]. The load factor for these values can be simplified to Equation 7.4. It's important to note that this simplification assumes that no thrust is used for lift.

$$n = \frac{TL}{WD} = \frac{F_{thrust} C_L}{(mg) C_D} \tag{7.4}$$

## 7.3 Results

The load factor is solved for level flight at 9700 m (31824 ft) for speeds between 100 (328.1) and 400 m/s (1312.3 ft/s). This is then plugged into Equation 7.1 to solve for the maximum ("0") PS contour line. This process is repeated for different drag values based on possible nose configurations. The instantaneous and sustained turn rate, and PS contour lines for all aircraft configurations are shown in Figure 7.4.

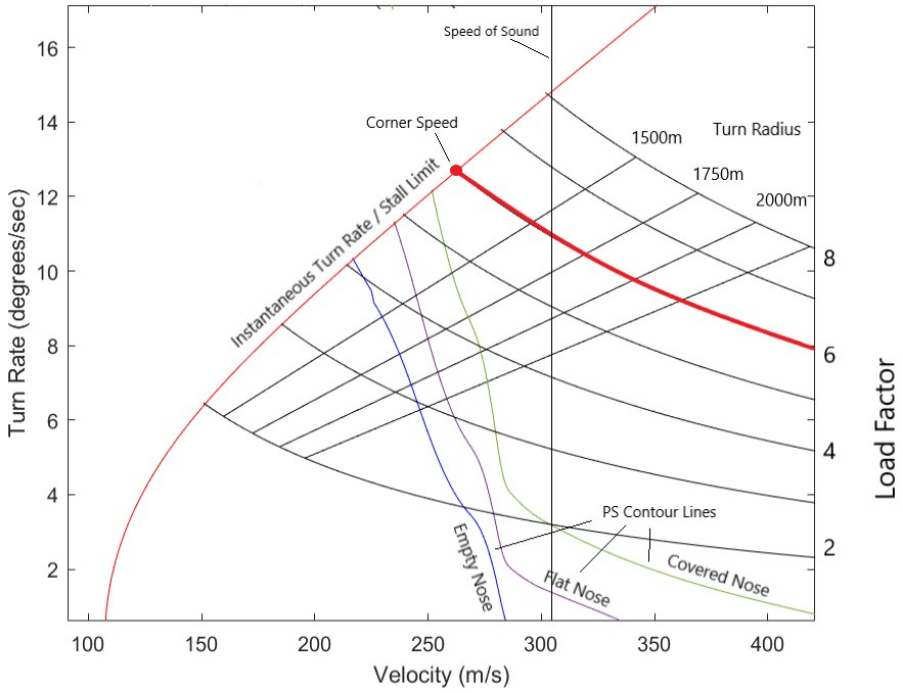


Figure 7.4 Natter EM diagram

The corner speed (speed for highest turn rate) is approximately 275 m/s (902 ft/s) with a turn radius of 1300 m (4265 ft). The maximum achievable turn rate is 13 °/sec. At 9700 m (31824 ft), Mach 1 is approximately 300 m/s (984 ft/s). Assuming that this is the top speed of the aircraft, the Natter only has a 50 m/s (164 ft/s) window where it could maintain a steady speed, not be stalling, exceeding the speed of sound or exceeding its maximum load factor.

The Natter has a relatively high stall speed compared to other aircraft, especially at 9700 m (31824 ft). A large change in bank angle means that the aircraft has to speed up in order to maintain level flight. The NACA 0012 does not have any camber nor was the Natter equipped with any lift devices such as slats or Krueger flaps. It wasn't meant to dogfight other aircraft. It was only meant to shoot down bombers on a single pass. As the nose configuration changes and drag increases, the maximum allowable speed in a sustained turn decreases and the PS curve moves to the left. There is less and less remaining energy for a high drag configuration until the Natter could no longer maintain a sustained turn.

If the Natter did reach 9700 m (31824 ft), it would only have 16 seconds left of fuel at full throttle. If it found itself past a bomber without expending its rockets it could attempt to turn in order to make a second pass. With 16 seconds left of fuel, it would require a 11.25 °/sec turn rate with a turn radius of 1250 m. A B-29 cruises at 191 knots (100 m/s). Natter pilots were trained to approach the bomber directly from the side. If a pilot could not line up a shot and wanted to make a 180° turn for a second try, the Natter would find itself well ahead of the original bomber as seen in Figure 7.5.

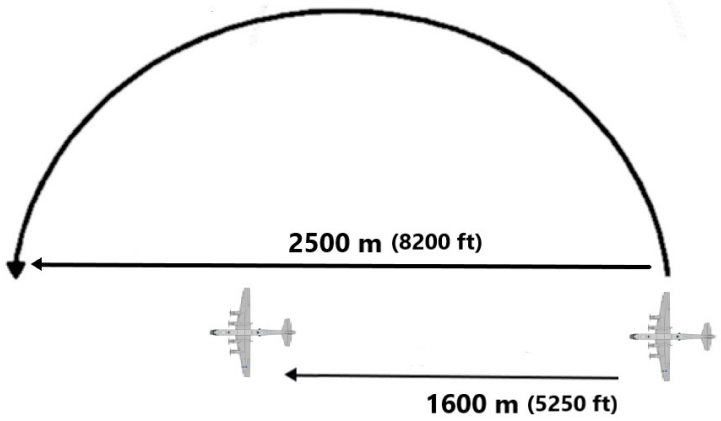


Figure 7.5 Natter 180° in 16 seconds

The maximum sustained turn rate for the Natter in the “flat nose” configuration is approximately 11.5 °/sec at 250 m/s (820 ft/s). Any slower velocity would mean that the aircraft would begin to stall and maintaining the turn by using more and more elevator would slow the aircraft even more. The Natter would have to halve its speed in less than a few seconds to first enter this instantaneous turn region and then conduct a turn while continuing to lose velocity. This may have been all too impossible for a pilot to achieve.

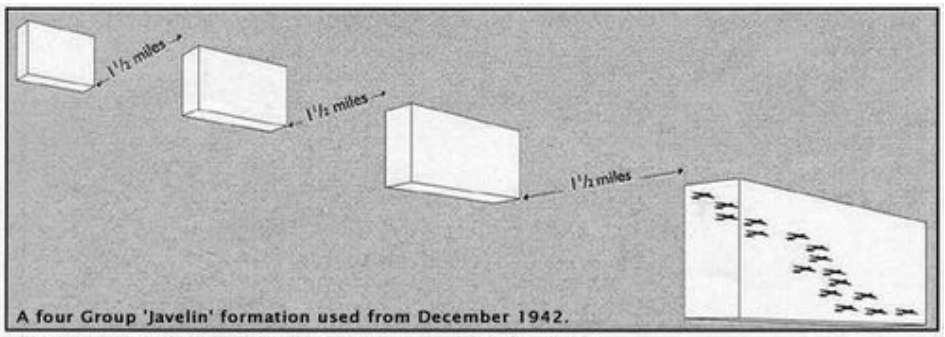

Figure 7.6 WWII bomber “javelin” formation [38]

The only chance the Natter may have had to make a second attack following a failed first pass was to attack another bomber in the formation. In 1942, The U.S 8th Air Force introduced the “Javelin” formation where bomber groups would be staggered in formations, each trailing the last by 1.5 miles (2400 m) [38]. At 250 m/s (820 ft/s), the Natter could cover this distance in 10 seconds.

# 8. Conclusion

## 8.1 Summary of Results

The Natter was not a cutting edge machine. It was hastily created using substandard materials and rushed labor. The requirements handed down to the designers were based off conjecture on the B-29's capabilities. Physically, the Natter could achieve many of these requirements. From the numerical modeling of its trajectory, it could have taken off and accelerated enough to prevent it from stalling in level flight. The aircraft could reach the required altitude and shoot down bombers. Unlike other aircraft, the CG and static margin of the Natter varies widely throughout its flight. The 833 kg (1836 lbm) of fuel and 185 kg (407.8 lbm) payload accounts for nearly half its weight. The aircraft is stable throughout its flight but the NP from both the analytical and numerical calculations are relatively far aft compared to other aircraft. Finally the aircraft can maneuver at high speeds but the limitations on the air frame would severely limit the aircraft while at full throttle flight.

## 8.2 Transonic Limitations

The highest speed the Natter can theoretically achieve is just below Mach 1. Entering the transonic region greatly increases drag, preventing the aircraft from breaking the sound barrier but the compressibility effects on the control surfaces would have surely prevented the pilot from controlling the aircraft at all. The P-38 Lightning, another WWII era aircraft, suffered from this same problem. If the pilot entered a dive at too high a speed, the controls would lock up or become wholly ineffective [39]. Pilots would report their control stick seemed as if it was "encased in two feet of concrete" until slowing to a speed where they could recover. Many died as a result of this issue. These effects can be mitigated by using swept wings and thin airfoils with sharp leading edges. The NACA 0012 lacks that last quality. A pilot would have to prevent the aircraft from entering this region in the first place. Rolling back on the throttle could save fuel, increase endurance and prevent these negative control effects.

## 8.3 Human Limitations

The maximum achievable altitude was almost 14,000 m (45931 ft). To put this into perspective, Mt. Everest is nearly 9000 m (29527 ft) tall. Commercial airliners cruise at about 10,000 m (32808 ft). An additional 4000 m (13123 ft) places this at the upper reaches of the troposphere. According to Figure 2.1, atmospheric pressure at 14,000 m (45931 ft) is 25% of sea level. The pressure at 9700 m (31824 ft) is 42% of sea level. The B-29 was pressurized meaning pilots did not have to wear oxygen masks at high altitudes. The Natter was not pressurized but pilots had supplemental oxygen but the quick ascent to altitude would have negated this. For an oxygen mask to be effective, a person needs to breath supplemental oxygen for a long period of time prior to an ascent in altitude. B-17 bombers were not pressurized and crews used oxygen masks but the B-17's

long ascent time meant the crew had time to adjust to the lowering pressure. This prevented them from suffering from decompression sickness or hypoxia.

The Natter pilot would also have to contend with a 2-3 g force throughout the ascent. An additional spike in g force if the pilot pulled up like in the variable pitch model would have required an exceptionally trained pilot. This constant acceleration throughout the flight would have made dexterous movement by the pilot difficult, especially when attempting to line up a shot. Even if the aircraft could be controlled at high speeds and high altitudes, the combination of decompression and g-forces on the pilot would have made this exceedingly difficult. A pilot would need advance warning of an incoming air raid in order to have enough time to breath pure oxygen. A pilot would also need multiple training flights to become proficient and acclimate to the harsh conditions, something that the disposable nature of the Natter couldn't afford.

## 8.4 Stability and Maneuvering Limitations

Many of the coefficients and stability derivatives are derived from assumptions and rules of thumb. These *may* give quantities such as the period and damping ratio of a system, but the compounding assumptions at each step of the calculation process may not give an exact or realistic quantitative result. These types of analyses may only be good for determining basic quantities like if an aircraft is stable or unstable. Values for the NP are comparatively further aft than other aircraft of the day. It's difficult to calculate the NP without physically verifying a real life or scale model. It's not inconceivable that the NP could be this far aft. The Natter is a very short aircraft with a large stabilizer closely following the wing. Aerotrim's analytical approach and Raymer's empirical method are based on aircraft designs like the kind seen in Figure 6.1. The small moment arm between the wing and stabilizer and high tail-to-wing area ratio pulls the NP further back. The result of all this is a large static margin and a more stable aircraft. The Natter can resist changes in pitch due to external factors such as wind gusts or a change in elevator deflection. It can more quickly correct itself following one of these disturbances. This may have been the reason why Bachem added an additional 10 cm (3.93 in) to the rear elevon following the first few flight tests. The large static margin creates a very large downward pitching moment when the aircraft is above its trimmed angle of attack. A pilot attempting a sharp turn could have the elevon at full rise but not at the aircraft's theoretical corner turn rate shown in Figure 7.4. This would limit the total lift and g-force the Natter could produce in a turn.

The speeds involved and turn rate needed to attack a single bomber formation would have been prohibitively taxing on the airframe as well. Assuming that the strength of the wood and UF built components was proportional to the maximum design load factor, an airframe like the one tested in Reference [13] would only have a maximum limit of 4.5 g's. The Natter was capable of exceeding this in sustained turns. If the Natter was in good enough condition to be recovered and be reused, its likely the needs of the war would have pushed the airframe to its breaking point over multiple launch and recovery cycles.

## 8.5 Final Remarks

The Natter was a rushed concept that used substandard materials and designs to accomplish an impossible task of defending Germany from hundreds of bombers. Lack of quality control compounded issues with testing and led to the death of one test pilot. The rocket powered interceptor was created in a transitional phase between piston and jet powered aircraft. Designers used 1940s era design techniques for requirements that would eventually be met and exceeded by jet powered aircraft. The Natter is simple in design but unconventional in application. Characteristics like the CG, NP and control surface layout make it difficult to apply an analytical approach. Future work with wind tunnel tests on a scale model like the kind performed by Bachem at DVL would validate results from the methods discussed in this paper.

# 9.0 References

[1] Forsyth, R, “Bachem Ba-349 Natter”, Bloomsbury Publishing, United Kingdom, 2018.

[2] Myhra, D., “Bachem Ba-349 Natter, An Illustrated Series on Germany’s Experimental Aircraft of World War II”, Schiffer Publishing Ltd, United States, 1999.

[3] Dressel, J., “Natter Ba-349 und Andere Deustche Kleinstraketenjäeger”, Podzun-Pallas-Verlag GmbH, Dorheim, Germany, 1989.

[4] Sharp, D, “The Fatal Mistake of Lothar Sieber, Spitfires Over Berlin, The Airwar over Europe 1945”, Mortons Media Group Ltd, United Kingdom, 2015.

[5] Schwantes, B., “United States Rocket Research and Development During World War II”, *Joint Army Navy NASA Airforce Interagency Propulsion Committee*, United States, 2021. URL https://www.jannaf.org/ sites/default/files/jannaf/WWII_Rocketry_Distro-A.pdf.

[6] Yefim, G, “Soviet Rocket Fighter”, Midland Publishing LTD, UK, 2006

[7] Johnson, D, “Heinkel He-176,” *Luft 46*, URL http://www.luft46.com/prototyp/he176.html, Accessed: 2022-06-30.

[8] Piccirillo, A, “The Me 163B Komet, Development and Operational Experience,” *SAE Transactions*, Vol. 106, 1997, pp. 1828–1845, https://doi.org/10.2514/6.1997-5627

[9] Joburgess, A, “RAF Bomber Command’s first 1,000 bomber raid May 1942,” , 2017. URL: https:// www.memorialflightclub.com/bomber-command-first-bomber-raid, Accessed: 2022-06-28.

[10] “B-24 Liberator Assembly Line at Ford Willow Run Bomber Plant, 1944, RAF Bomber Command’s first 1,000 bomber raid May 1942”, *The Henry Ford*, United States 1942. URL https://www.thehenryford.org/collections-and-research/digital-collections/expertsets/101765, Accessed: 2022-06-28.

[11] Raymer, D, “Aircraft design: A Conceptual Approach 5$^{th}$ Edition”, American Institute of Aeronautics and Astronautics, Inc., United States, 2012.

[12] Essuri, M, Addeep, S., Afolabi, L., and Elfaghia, A., “Effect of Mesh Type on Numerical Computation of Aerodynamic Coefficients of NACA 0012 Airfoil,” *Journal of Advanced Research in Fluid Mechanics and Thermal Sciences*, Vol. 87, 2021, pp. 31–39, https://doi.org/10.37934/arfmts.87.3.3139

[13] Fernando, V. N, and Mudunkotuwa, D. Y, “Bio-Inspired Aircraft Wing Modification Analysis in ANSYS Fluent”, *10th International Conference on Information and*

*Automation for Sustainability (ICIAfS)*, IEEE, 2021, pp. 316–321, https://doi.org/10.1109/ICIAfS52090.2021.9605821

[14] Critzos, C. C., Heyson, H. H., and Boswinkle Jr, R. W., “Aerodynamic characteristics of NACA 0012 airfoil section at angles of attack from 0 deg to 180 deg,” *Tech. Rep 3361*, National Aeronautics and Space Administration Washington DC, United States, 1955.

[15] Lednicer, D., “World War II Fighter Aerodynamics,” EAA Sport Aviation Magazine, 1997, pp. 85–91.

[16] Barnes, P., “Aerodynamic and Artistic Study of the German Jets,” Pelican Aero Group, www.howfliesthealbatross.com, Accessed: 2022-07-25.

[17] Cook, M. V., “Flight Dynamics Principles: A Linear Systems Approach to Aircraft Stability and Control”, Butterworth-Heinemann, 2012.

[18] Peterson, I. C., “Problems in Wood Aircraft,” *SAE Transactions*, 1943, pp. 369–380, https://doi.org/10.4271/430159

[19] Konnerth, J., Müller, U., Gindl, W., and Buksnowitz, C., “Reliability of wood adhesive bonds in a 50 year old glider construction,” *European Journal of Wood and Wood Products*, Vol. 70, No. 1, 2012, pp. 381–384, https://doi.org/10.1007/s00107-011-0536-0

[20] Müller, U., Müller, H., and Teischinger, A., “Durability of wood adhesives in 50-year-old aircraft and glider Constructions,” *Wood Res*, Vol. 49, No. 3, 2004, pp. 25–34.

[21] Benson, T., “Shape Effects on Drag,” NASA Glenn Research Center, https://www.grc.nasa.gov/www/k12/rocket/shaped.html, Accessed: 2022-07-04.

[22] Benson, T., “Earth Atmospheric Model (Metric)” NASA Glenn Research Center, https://www.grc.nasa.gov/ www/k-12/rocket/atmosmet.html, Accessed: 2022-07-04.

[23] Hoerner, S. F., “Fluid Dynamic Drag, Theoretical, Experimental and Statistical Information,” 1965.

[24] Loftin, L., “Quest for Performance: The Evolution of Modern Aircraft, Chapter 10: Technology of the Jet Airplane”, *NASA Special Publication*, NASA, United States, 1985, https://books.google.com/books?id=fQg_AQAAMAAJ.

[25] Lunmitos AG, “List of Stoffs”, Chemeurope.com, https://www.chemeurope.com/en/encyclopedia/List_of_stoffs.html, Accessed: 2022-07-15

[26] Dormand, J. R., and Prince, P. J., “A Family of Embedded Runge-Kutta Formulae”, *Journal of Computational and Applied Mathematics*, Vol. 6, No. 1, 1980, pp. 19–26, https://doi.org/10.1016/0771-050X(80)90013-3

[27] McIver, J., “Cessna Skyhawk II/100 Performance Assessment”, http://temporal.com.au/c172.pdf, Accessed: 2022-08-22.

[28] Berry, M., Las Fargeas, J., and Blair, K. B., “Wind Tunnel Testing of a Novel Wingsuit Design”, *Procedia Engineering*, Vol. 2, No. 2, 2010, pp. 2735–2740, https://doi.org/10.1016/j.proeng.2010.04.059

[29] Stribling, C. B, “Basic Aerodynamics”, Butterworth-Heinemann, United Kingdom, 1984.

[30] Douglas, O., “Aerotrim, MATLAB”, 2017. https://www.mathworks.com/matlabcentral/answers/uploaded_files/95173/AEROTRIM.m, Accessed: 2022-09-15.

[31] Gilruth, R, and White, M, “Analysis and Prediction of Longitudinal Stability of Airplanes, No. NACA-TR-711”, Tech. rep., United States, 1941.

[32] Brady, C., “Boeing 737-100 Technical Specifications”, 1999, http://www.b737.org.uk/techspecsoriginals.html, Accessed: 2022-11-01.

[33] Fatahian, E., Lohrasbi Nichkoohi, A., Salarian, H., and Khaleghinia, J., “Comparative study of flow separation control using suction and blowing over an airfoil with/without flap”, *Sadhana*, Vol. 44, No. 11, 2019, pp. 1–19, https://doi.org/10.1007/s12046-019-1205-y

[34] Caughey, D.A, “Introduction to aircraft stability and control course notes for M&AE 5070”, *Sibley School of Mechanical & Aerospace Engineering Cornell University*, United States, 2011

[35] Neufeld, J., “Technology and the Air Force: A Retrospective Assessment”, DIANE Publishing, United States, 2009.

[36] “F-4J Phantom II,” U.S Archives, https://catalog.archives.gov/id/6393002, Accessed: 2022-08-22.

[37] Caddy, M. J., and Arnold, W. K., “Energy Maneuverability and Engine Performance Requirements,” *Turbo Expo: Power for Land, Sea, and Air*, Vol. 79191, American Society of Mechanical Engineers, 1988, p. V002T02A018, https://doi.org/10.1115/88-GT-303

[38] Zhou, J, “Flying Formation, B-17 Bomber Flying Fortress – The Queen of the Skies”, https://b17flyingfortress.de/en/details/formationsflug, Accessed: 2022-11-17

[39] Anderson, J. D., “Breaking the Sound Barrier,” *AIAA Scitech 2019 Forum*, 2019, p. 2194, https://doi.org/10.2514/6.2019-2194

# Appendix A – Aircraft Characteristics

Table A.1 – Natter Weight Distribution 104 seconds into Flight

| Component | Weight (kg) | Arm (m) (From nose) | Moment $(kg \cdot m)$ | Inertia $(kg \cdot m^2)$ |
|---|---|---|---|---|
| Wooden Frame | 206 | 3.13 | 644.78 | 26.7 |
| Control Parts | 25 | 2.04 | 51 | 13.32 |
| Course Control | 35 | 0.92 | 32.2 | 119.79 |
| Crew & Equipment | 100 | 1.74 | 174 | 106.09 |
| Pilot Seat | 4 | 1.74 | 6.96 | 4.24 |
| Weapons and Ammunition | 0 | 0.31 | 0 | 0 |
| Bulletproof Glass | 25 | 1.33 | 33.25 | 51.84 |
| Instrument | 6 | 0.92 | 5.52 | 20.54 |
| Armor Plate | 139 | 1.61 | 223.79 | 187.04 |
| Accumulator | 25 | 3.66 | 91.5 | 19.8 |
| Tanks and Fuel | 111 | 2.75 | 305.25 | 0.04 |
| Engine | 170 | 3.6 | 612 | 117.11 |
| Fuselage Rescue Parachute | 80 | 4.77 | 381.6 | 320 |
| Total Weight | 926 | - | 2561.85 | 986.51 |
| | | CG (m) (From nose) | 2.77 | |
| | | CG (% MAC) | 33 | |

Table A.2 – Natter Weight Distribution, Full Fuel/Rockets Not Fired

| Component | Weight (kg) | Arm (m) (From nose) | Moment $(kg \cdot m)$ | Inertia $(kg \cdot m^2)$ |
|---|---|---|---|---|
| Wooden Frame | 206 | 3.13 | 644.78 | 26.7 |
| Control Parts | 25 | 2.04 | 51 | 13.32 |
| Course Control | 35 | 0.92 | 32.2 | 119.79 |
| Crew & Equipment | 100 | 1.74 | 174 | 106.09 |
| Pilot Seat | 4 | 1.74 | 6.96 | 4.24 |
| Weapons and Ammunition | 185 | 0.31 | 57.35 | 895.4 |
| Bulletproof Glass | 25 | 1.33 | 33.25 | 51.84 |
| Instrument | 6 | 0.92 | 5.52 | 20.54 |
| Armor Plate | 139 | 1.61 | 223.79 | 187.04 |
| Accumulator | 25 | 3.66 | 91.5 | 19.8 |
| Tanks and Fuel | 833 | 2.75 | 2290.75 | 47.98 |
| Engine | 170 | 3.6 | 612 | 117.11 |
| Fuselage Rescue Parachute | 80 | 4.77 | 381.6 | 320 |
| Total Weight | 1833 | - | 4604.7 | 1984.45 |
| | | CG (m) (From nose) | 2.51 | |
| | | CG (% MAC) | 7 | |

Table A.3 – Natter Weight Distribution, Empty Fuel/Rockets Not Fired

| Component | Weight (kg) | Arm (m) (From nose) | Moment $(kg \cdot m)$ | Inertia $(kg \cdot m^2)$ |
|---|---|---|---|---|
| Wooden Frame | 206 | 3.13 | 644.78 | 26.7 |
| Control Parts | 25 | 2.04 | 51 | 13.32 |
| Course Control | 35 | 0.92 | 32.2 | 119.79 |
| Crew & Equipment | 100 | 1.74 | 174 | 106.09 |
| Pilot Seat | 4 | 1.74 | 6.96 | 4.24 |
| Weapons and Ammunition | 185 | 0.31 | 57.35 | 754.87 |
| Bulletproof Glass | 25 | 1.33 | 33.25 | 51.84 |
| Instrument | 6 | 0.92 | 5.52 | 20.54 |
| Armor Plate | 139 | 1.61 | 223.79 | 187.04 |
| Accumulator | 25 | 3.66 | 91.5 | 19.8 |
| Tanks and Fuel | 50 | 2.75 | 137.5 | 8.82 |
| Engine | 170 | 3.6 | 612 | 117.11 |
| Fuselage Rescue Parachute | 80 | 4.77 | 381.6 | 320 |
| Total Weight | 1050 | - | 2451.45 | 1907.1 |
| | | CG (m) (From nose) | 2.33 | |
| | | CG (% MAC) | -11 | |

Table A.4 – Natter Weight Distribution, Empty Fuel/Rockets Fired

| Component | Weight (kg) | Arm (m) (From nose) | Moment $(kg \cdot m)$ | Inertia $(kg \cdot m^2)$ |
|---|---|---|---|---|
| Wooden Frame | 206 | 3.13 | 644.78 | 26.7 |
| Control Parts | 25 | 2.04 | 51 | 13.32 |
| Course Control | 35 | 0.92 | 32.2 | 119.79 |
| Crew & Equipment | 100 | 1.74 | 174 | 106.09 |
| Pilot Seat | 4 | 1.74 | 6.96 | 4.24 |
| Weapons and Ammunition | 0 | 0.31 | 0 | 0 |
| Bulletproof Glass | 25 | 1.33 | 33.25 | 51.84 |
| Instrument | 6 | 0.92 | 5.52 | 20.54 |
| Armor Plate | 139 | 1.61 | 223.79 | 187.04 |
| Accumulator | 25 | 3.66 | 91.5 | 19.8 |
| Tanks and Fuel | 50 | 2.75 | 137.5 | 8.82 |
| Engine | 170 | 3.6 | 612 | 117.11 |
| Fuselage Rescue Parachute | 80 | 4.77 | 381.6 | 320 |
| Total Weight | 865 | - | 2394.1 | 986.49 |
| | | CG (m) (From nose) | 2.77 | |
| | | CG (% MAC) | 33 | |

# Appendix B.1 – Atmospheric Conditions Code

```
%Benjamin S Hopkins Atmospheric Conditions, Chapter 2.0
%11/25/22

altitude = linspace(0,15000,100);

T_amb = 15 + 273.15;%Kelvin, Ambient Ground Temperature (15 Celsius)
T = T_amb - 0.00649.*altitude; %Kelvin, Temperature w/ Altitude, Reference 1
P = 101325*(T./288.08).^5.256; %Pascals, Pressure w/ Altitude, Reference 1
rho = P./(286.9.*T); %kg/m^3, Denisity of Air, Reference 1
mu = 1.789E-5.*((T./T_amb).^1.5).*((T_amb + 110.4)./(T + 110.4)); %Pa*s Dynamic viscosity, Reference
2
k = 1.015E-5; %Skin Roughness Value (Camouflage), Raymer Page 435 Table 12.5
c = sqrt(1.4*8.3145*T/0.0289645);%m/s Speed of Sound in Air, Reference 3

figure(1)
set(gcf,'color','w');
subplot(1,3,1)
plot(altitude,T-273.15)
ylabel('Temperature (Celsius)')
xlabel('Altitude (m)')
subplot(1,3,2)
plot(altitude,rho)
ylabel('Density (kg/m^3)')
xlabel('Altitude (m)')
subplot(1,3,3)
plot(altitude,c)
ylabel('Speed of Sound (m/s)')
xlabel('Altitude (m)')
```

# Appendix B.2 – Fixed Pitch Trajectory Code

```
%Benjamin S. Hopkins Fixed Pitch Trajectory Model, Chapter 2.0, 4.0 & 5.0
%11/25/22

close all
clear all
clc

%for pitch = 30:90

pitch = 43; %Degrees, Pitch
transition_time = 8; %Seconds, Time after plane goes to AOA from vertical position
g = 9.81; %m/s^2 Gravitational Acceleration
Sref = 3.6; % m^2 Planform Area of Wing
Mdd = 0.75; %Drag-Divergence Mach Number t/c = .12 Raymer Page 450, Fig 12.29

%Initial Conditions
y0 = [0 0 0 .001]; %Plane is at rest. Small dy/dt prevent ODE45 overflow NaN error
tspan = [0 120]; %120 seconds of fuel. Simulate for only 120 seconds.
[t,x] = ode45(@(t,y)flightode(t,y,g,Sref,transition_time,pitch,Mdd),tspan,y0); %Solver

figure(1)
set(gcf,'color','w');
plot(t,sqrt(x(:,4).^2+x(:,2).^2))
%legend('Vertical Speed','Horizontal Speed')
ylabel('Velocity (m/s)')
xlabel('time(sec)')

figure(2)
set(gcf,'color','w');
plot(x(:,1),x(:,3),'-')
hold on
xlabel('Range(m)')
ylabel('Altitude (m)')

coef_drag = zeros(1,length(t));
coef_lift = zeros(1,length(t));
force_drag_y = zeros(1,length(t));
force_drag_x = zeros(1,length(t));
force_lift_y = zeros(1,length(t));
force_lift_x = zeros(1,length(t));
force_thrust_y = zeros(1,length(t));
force_thrust_x = zeros(1,length(t));
y_accel_plot = zeros(1,length(t));
x_accel_plot = zeros(1,length(t));

mass = zeros(1,length(t));
density = zeros(1,length(t));
Mach = zeros(1,length(t));
speed_sound = zeros(1,length(t));

for i = 1:length(t)
```

```
u = sqrt(x(i,2)^2+x(i,4)^2); %m/s, Flowspeed of Air
[F,m,Cd,rho,T,M,c,theta] = properties(t(i), x(i,3), u,transition_time,pitch,Mdd); %Obtain atmopheric...
%speed and drag properties of aircraft for given time/height
gamma = atand(x(i,4)/x(i,2)); %Degrees, Angle between horizon & flowspeed
alpha = theta - gamma; %Degrees, Angle of Incidence
[Cl, Cd_wing] = Natter_Splines(real(alpha)); %Obtain Cl and Cd for given Alpha
e = .95; %Oswald Efficiency Factor AR = 3.6, Raymer Page 456 Eq 12.48
K_wing= 1/(pi*e*(3.6^2/Sref)); %Raymer Page 456 Eq 12.47
K_tail = 1/(pi*e*(2.3^2/2.53)); %Raymer Page 456 Eq 12.47
Cdi = K_wing*(Cl^2) + K_tail*(2.53/Sref)*(Cl^2); %Trimmed Cdi, Raymer Page 624 Eq 16.34
Cd = Cd*Natter_transonicdrag(M,Mdd); %Transonic Cd Modifier
x_accel = (F*cosd(theta) - (Cl*rho*Sref*(u^2)/2)*sind(gamma) -
((Cd+Cd_wing+Cdi)*rho*Sref*(u^2)/2)*cosd(gamma))/m;
y_accel = (F*sind(theta) + (Cl*rho*Sref*(u^2)/2)*cosd(gamma) -
((Cd+Cd_wing+Cdi)*rho*Sref*(u^2)/2)*sind(gamma))/m;% - g;
%Store values which will be plotted later
coef_drag(i) = Cd+Cd_wing+Cdi;
coef_lift(i) = Cl;
mass(i) = m;
force_thrust_y(i) = F*sind(theta);
force_thrust_x(i) = F*cosd(theta);
force_lift_y(i) = (coef_lift(i)*rho*Sref*(u^2)/2)*cosd(gamma);
force_lift_x(i) = (coef_lift(i)*rho*Sref*(u^2)/2)*sind(gamma);
force_drag_y(i) = (coef_drag(i)*rho*Sref*(u^2)/2)*sind(gamma);
force_drag_x(i) = (coef_drag(i)*rho*Sref*(u^2)/2)*cosd(gamma);
y_accel_plot(i) = y_accel;
x_accel_plot(i) = x_accel;
density(i) = rho;
Mach(i) = M;
speed_sound(i) = c;
end

Plot values
figure(3)
set(gcf,'color','w');
plot(t,Mach)
title('Natter Takeoff')
xlabel('time (sec)')
ylabel('Mach Number')

figure(4)
set(gcf,'color','w');
plot(t,coef_drag)
xlabel('time (sec)')
ylabel('Cd')

figure(5)
set(gcf,'color','w');
plot(t,force_thrust_y,t,force_lift_y,t,force_drag_y,t,mass*9.81)
legend('Thrust','Lift','Drag','Weight')
title('Natter Takeoff (Y)')
xlabel('time (sec)')
ylabel('Total Force')
```

```
figure(6)
set(gcf,'color','w');
plot(t,force_thrust_x,t,force_lift_x,t,force_drag_x)
legend('Thrust','Lift','Drag')
title('Natter Takeoff (X)')
xlabel('time (sec)')
ylabel('Total Force')

figure(7)
set(gcf,'color','w');
plot(t,force_thrust_y+force_lift_y,t,force_drag_y+mass*9.81)
legend('Thrust+Lift','Drag+Weight')
title('Natter Takeoff (Y-Forces)')
xlabel('time (sec)')
ylabel('Total Force')

figure(8)
set(gcf,'color','w');
plot(t,sqrt((force_drag_x.^2)+(force_drag_y.^2)))
title('Natter Takeoff')
xlabel('time (sec)')
ylabel('Total Drag Force (N)')

figure(9)
set(gcf,'color','w');
plot(t,1+sqrt((x_accel_plot.^2)+(y_accel_plot.^2))/g)
title('Natter Takeoff')
xlabel('time (sec)')
ylabel('Acceleration (g)')



%Function for Equations of Motion
function dy = flightode(t,y,g,Sref,transition_time,AOA,Mdd)

u = sqrt(y(2)^2+y(4)^2); %m/s, Flowspeed of Air
[F,m,Cd,rho,T,M,c,theta] = properties(t, y(3), u, transition_time,AOA,Mdd);%Obtain atmopheric...
%speed and drag properties of aircraft for given time/height
gamma = abs(atand(y(4)/y(2))); %Degrees, Angle between horizon & flowspeed
alpha = theta - gamma; %Degrees, Angle of Incidence
[Cl, Cd_wing] = Natter_Splines(real(alpha)); %Obtain Cl and Cd for given Alpha
e = .95; %Oswald Efficiency Factor AR = 3.6, Raymer Page 456 Eq 12.48
K_wing= 1/(pi*e*(3.6^2/Sref)); %Raymer Page 456 Eq 12.47
K_tail = 1/(pi*e*(2.3^2/2.53)); %Raymer Page 456 Eq 12.47
Cdi = K_wing*(Cl^2) + K_tail*(2.53/Sref)*(Cl^2); %Trimmed Cdi, Raymer Page 624 Eq 16.34
Cd = Cd*Natter_transonicdrag(M,Mdd);  %Transonic Cd Modifier
%Solve the Equations of Motions
%dy = [x-velocity, x-accel, y-velocity, y-accel]
dy = [y(2);
    (F*cosd(theta) - (Cl*rho*Sref*(u^2)/2)*sind(gamma) -
((Cd+Cd_wing+Cdi)*rho*Sref*(u^2)/2)*cosd(gamma))/m;
    y(4);
```

```
    (F*sind(theta) + (Cl*rho*Sref*(u^2)/2)*cosd(gamma) -
((Cd+Cd_wing+Cdi)*rho*Sref*(u^2)/2)*sind(gamma))/m - g];
end

%Obtain atmopheric speed and drag properties of aircraft for given time/height
function [F,m,Cd,rho,T,M,c,theta] = properties(t, altitude, flowspeed, transition_time,AOA,Mdd)
% Flat plate skin friction coefficient (Cf) Appoximation, Raymer Section 12.5.3 Page 433
L = 6.02; %m, Characteristic Aircraft Length
u = flowspeed;%m/s, Flowspeed
T_amb = 15 + 273.15;%Kelvin, Ambient Ground Temperature (15 Celsius)
T = T_amb - 0.00649.*altitude; %Kelvin, Temperature w/ Altitude, Reference 1
P = 101325*(T./288.08).^5.256; %Pascals, Pressure w/ Altitude, Reference 1
rho = P./(286.9.*T); %kg/m^3, Denisity of Air, Reference 1
mu = 1.789E-5.*((T./T_amb).^1.5).*((T_amb + 110.4)./(T + 110.4)); %Pa*s Dynamic viscosity, Reference
2
k = 1.015E-5; %Skin Roughness Value (Camouflage), Raymer Page 435 Table 12.5
c = sqrt(1.4*8.3145*T/0.0289645);%m/s Speed of Sound in Air, Reference 3
M = u/c; %Mach Number

%Determine Reynold's Number
if M < Mdd
Re_cutoff = 38.21*(L/k)^1.053; %Subsonic, Raymer Page 434 Eq 12.28
elseif M >= Mdd
Re_cutoff = 44.62*((L/k)^1.053)*M^1.16; %Transonic, Raymer Page 434 Eq 12.29
end

Cf = 0.455 / ((log10(Re_cutoff)^2.58)*(1+0.144*M^2)^0.65); %Turbulent Flow Cf, Raymer Page 433, Eq
12.27


% Form Factor and Adjustments Section 12.5.4 Page 435
Amax = 0.819; %m^2, wing, tail strut and pylon
xc = 0.3; %chordwise location at max thickness
tc = 0.12; %thickness to chord ratio
FF_wingtail = (1 + ((0.6/xc)*(tc)) + 100*((tc)^4))*(1.34*(M^0.18)); %Form Factor Raymer Page 435 Eq
12.30
f = L/sqrt((4/pi)*Amax); %Raymer Page 436 Eq 12.33
FF_fuselage = 1 + (60/(f^3)) + (f/400); %Form Factor Raymer Page 435 Eq 12.31

Swet_fuselage = 17.84; %m^2, Wetted area (Derived from Solidworks Model)
Swet_wingtail = 6.18 + 5.26 + 4.1; %m^2, wing + elevator + tail wetted area (Derived from Solidworks
Model)
Sref = 3.6; %m^2, Planform area of wing

%Interference Factors Raymer Page 437 Section 12.5.5
Q_fuselage = 1.0; %Interference Factor
Q_wingtail = 1.03;%Interference Factor

Cd_canopy = 0.15*0.137/Sref; %Sharp edged windshield w/ 0.137m^2 frontal area, Raymer Page 442
Table 12.6
Cd_VTO = 0.3*.051/Sref; %bullet w/ 0.051m^2 frontal area, Raymer Page 442 Table 12.6

%Time Dependent Properties
```

```
if t < transition_time
   theta = 90;
elseif t >= transition_time
   theta = AOA;
end

%Full throttle, VTO Boosters
if t < 8
   m = 2293 - 20*t - 6.94*t; %kg, Initial Mass with 20 kg/s for VTO, 6.94 kg/s for HWK
   F = 2900*9.81; %Newtons, 2900 kg of total thrust
   %Sum Drag Components, Raymer Page 430 Eq 12.24
   Cd = (Cf*FF_fuselage*Q_fuselage*Swet_fuselage/Sref) + ...
        (Cf*FF_wingtail*Q_wingtail*Swet_wingtail/Sref) + ...
        Cd_canopy + ...
        4*Cd_VTO; %<- 4 VTO boosters

%Full Throttle, No VTO Boosters
elseif t >= 8 & altitude < 7000
   m = 1833 - (8*6.94) - 6.94*(t-8); %1810 kg weight - burnt fuel - burning fuel
   F = 1700*9.81; %Newtons, HWK109-509 Rocket produces 1700kg
   %Sum drag components but no boosters
   Cd = (Cf*FF_fuselage*Q_fuselage*Swet_fuselage/Sref) + ...
        (Cf*FF_wingtail*Q_wingtail*Swet_wingtail/Sref) + ...
        Cd_canopy;
%Full Throttle, No VTO Boosters, Blunt Nose
elseif t >= 8 & altitude > 7000 %Estimating 7000m is when he ejects the nosecap
   m = 1833 - (8*6.94) - 6.94*(t-8); %1810 kg weight - burnt fuel - burning fuel
   F = 1700*9.81; %Newtons
   Cd = (2.608)*(Cf*FF_fuselage*Q_fuselage*Swet_fuselage/Sref) + ... % 2.608 is the ratio of Cd for
smooth and flatnose fuselage
        (Cf*FF_wingtail*Q_wingtail*Swet_wingtail/Sref) + ...
        Cd_canopy;
end

Cd =  Cd + 0.05*Cd; %Add L&P Drag, 5% increase, Raymer Page 444 Table 12.8

end

%Obtain Cl,Cd for given Angle of Attack
function [Cl, Cd_wing] = Natter_Splines(alpha)
x_l = [0 68.18 71.51 77.23 79.62 105.83 145.87 171.61 210.89 260.26 403.9 472.23]*(90/472.23);
y_l = [0 324.09 331.24 330.29 324.09 177.29 231.15 266.9 294.07 286.92 129.49 23.05]*(1.275/331.24);

x_d = [0 64.97 76.08 84.53 179.86 446.53 504.91 530.19]*(90/530.19);
y_d = [0 4.63 11.43 32.34 189.88 635.19 670.87 675.68]*(2.35/675.68);

yy_l = spline(x_l , [4.75*(1.275/331.24)/(90/472.23) y_l -1.55*(1.275/331.24)/(90/472.23)]);
yy_d = spline(x_d ,[0 y_d 0]);

Cl = ppval(yy_l,abs(alpha));
Cl = Cl/(1+Cl/(pi*3.6));
Cd_wing = ppval(yy_d,abs(alpha));
end
```

```
%Obtain Transonic Drag Increase for given Mach Number
function [transonic_ratio] = Natter_transonicdrag(M,Mdd)

x_d = [0 32.19 76.09 101.01 107.53 113.47 131.26 139.82]*(1-Mdd)/139.82;
y_d = ([0 15.49 73.03 153.71 211.26 227.87 240.92 242.67]*2/242.67)+1;

yy_d = spline(x_d , [0 y_d 0]);
xx_d = linspace(0,1-Mdd,50);

if M <= Mdd
   transonic_ratio = 1;
elseif M > Mdd & M < 1
   transonic_ratio = ppval(yy_d,M-Mdd);
elseif M >= 1
   transonic_ratio = 3;
end
end
```

# Appendix B.3 – Variable Pitch Trajectory Code

```
%Benjamin S. Hopkins Variable Pitch Trajectory Model, Chapter 2.0, 4.0 & 5.0
%11/25/22

clear all
close all
clc

pitch = 45; %Degrees, Pitch
transition_time = 8; %Seconds, Time after plane goes to AOA from vertical position
g = 9.81; %m/s^2 Gravitational Acceleration
Sref = 3.6; % m^2 Planform Area of Wing
Mdd = 0.75; %Drag-Divergence Mach Number t/c = .12 Raymer Page 450, Fig 12.29

%Initial Conditions
y0 = [0 0 0 .001]; %Plane is at rest. Small dy/dt prevent ODE45 overflow NaN error
tspan = [0 120]; %120 seconds of fuel. Simulate for only 120 seconds.
[t,x] = ode45(@(t,y)flightode(t,y,g,Sref,transition_time,pitch,Mdd),tspan,y0); %Solver

% figure(1)
% set(gcf,'color','w');
% plot(t,sqrt(x(:,4).^2+x(:,2).^2))
% %legend('Vertical Speed','Horizontal Speed')
% title('Natter Takeoff')
% ylabel('Velocity (m/s)')
% xlabel('time(sec)')
%
% figure(2)
% set(gcf,'color','w');
% plot(x(:,1),x(:,3),'-')
% hold on
% title('Natter Takeoff')
% xlabel('Range(m)')
% ylabel('Altitude (m)')

theta_natter = zeros(1,length(t));
coef_drag = zeros(1,length(t));
coef_lift = zeros(1,length(t));
force_drag_y = zeros(1,length(t));
force_drag_x = zeros(1,length(t));
force_lift_y = zeros(1,length(t));
force_lift_x = zeros(1,length(t));
force_thrust_y = zeros(1,length(t));
force_thrust_x = zeros(1,length(t));
y_accel_plot = zeros(1,length(t));
x_accel_plot = zeros(1,length(t));

mass = zeros(1,length(t));
density = zeros(1,length(t));
Mach = zeros(1,length(t));
speed_sound = zeros(1,length(t));
```

```
for i = 1:length(t)
u = sqrt(x(i,2)^2+x(i,4)^2); %m/s, Flowspeed of Air
[F,m,Cd,rho,T,M,c] = properties(t(i), x(i,3), u,transition_time,Mdd); %Obtain atmopheric...

if t(i) < transition_time
   theta = 90;
   [Cl, Cd_total,gamma,alpha] = LiftDrag_Coefficient(theta,x(i,:),M,Mdd,Sref,Cd);

%Aircraft goes from Vertical to preset pritch in order to gain speed in
%x-direction
variable_pitch_time = 75;
elseif t(i) >= 8 && t(i) < variable_pitch_time
   theta = 40;
   [Cl, Cd_total,gamma,alpha] = LiftDrag_Coefficient(theta,x(i,:),M,Mdd,Sref,Cd);

elseif t(i) >= variable_pitch_time
   F_y = zeros(1,89);
   for theta = 1:89
      [Cl, Cd_total,gamma,alpha] = LiftDrag_Coefficient(theta,x(i,:),M,Mdd,Sref,Cd);
      F_y(theta) = (F*sind(theta) + (Cl*rho*Sref*(u^2)/2)*cosd(gamma) -
(Cd_total*rho*Sref*(u^2)/2)*sind(gamma));
   end
   [value, theta] = max(F_y);
   [Cl, Cd_total,gamma,alpha] = LiftDrag_Coefficient(theta,x(i,:),M,Mdd,Sref,Cd);

end

x_accel = (F*cosd(theta) - (Cl*rho*Sref*(u^2)/2)*sind(gamma) -
((Cd_total)*rho*Sref*(u^2)/2)*cosd(gamma))/m;
y_accel = (F*sind(theta) + (Cl*rho*Sref*(u^2)/2)*cosd(gamma) -
((Cd_total)*rho*Sref*(u^2)/2)*sind(gamma))/m;% - g;
%Store values which will be plotted later
theta_natter(i) = theta;
coef_drag(i) = Cd_total;
coef_lift(i) = Cl;
mass(i) = m;
force_thrust_y(i) = F*sind(theta);
force_thrust_x(i) = F*cosd(theta);
force_lift_y(i) = (coef_lift(i)*rho*Sref*(u^2)/2)*cosd(gamma);
force_lift_x(i) = (coef_lift(i)*rho*Sref*(u^2)/2)*sind(gamma);
force_drag_y(i) = (coef_drag(i)*rho*Sref*(u^2)/2)*sind(gamma);
force_drag_x(i) = (coef_drag(i)*rho*Sref*(u^2)/2)*cosd(gamma);
y_accel_plot(i) = y_accel;
x_accel_plot(i) = x_accel;
density(i) = rho;
Mach(i) = M;
speed_sound(i) = c;
end

%Plot values
% figure(3)
% set(gcf,'color','w');
% plot(t,Mach)
```

```
% title('Natter Takeoff')
% xlabel('time (sec)')
% ylabel('Mach Number')
%
% figure(4)
% set(gcf,'color','w');
% plot(t,coef_drag)
% xlabel('time (sec)')
% ylabel('Cd')
%
% figure(5)
% set(gcf,'color','w');
% plot(t,force_thrust_y,t,force_lift_y,t,force_drag_y,t,mass*9.81)
% legend('Thrust','Lift','Drag','Weight')
% title('Natter Takeoff (Y)')
% xlabel('time (sec)')
% ylabel('Total Force')
%
% figure(6)
% set(gcf,'color','w');
% plot(t,force_thrust_x,t,force_lift_x,t,force_drag_x)
% legend('Thrust','Lift','Drag')
% title('Natter Takeoff (X)')
% xlabel('time (sec)')
% ylabel('Total Force')
%
% figure(7)
% set(gcf,'color','w');
% plot(t,force_thrust_y+force_lift_y,t,force_drag_y+mass*9.81)
% legend('Thrust+Lift','Drag+Weight')
% title('Natter Takeoff (Y-Forces)')
% xlabel('time (sec)')
% ylabel('Total Force')
%
% figure(8)
% set(gcf,'color','w');
% plot(t,sqrt((force_drag_x.^2)+(force_drag_y.^2)))
% title('Natter Takeoff')
% xlabel('time (sec)')
% ylabel('Total Drag Force (N)')
%
% figure(9)
% set(gcf,'color','w');
% plot(t,1+sqrt((x_accel_plot.^2)+(y_accel_plot.^2))/g)
% title('Natter Takeoff')
% xlabel('time (sec)')
% ylabel('Acceleration (g)')



%Function for Equations of Motion
function dy = flightode(t,y,g,Sref,transition_time,pitch,Mdd)
```

```
u = sqrt(y(2)^2+y(4)^2); %m/s, Flowspeed of Air
[F,m,Cd,rho,T,M,c] = properties(t, y(3), u, transition_time,Mdd);%Obtain atmopheric...

variable_pitch_time = 75;
if t < transition_time
   theta = 90;
   [Cl, Cd_total,gamma,alpha] = LiftDrag_Coefficient(theta,y,M,Mdd,Sref,Cd);

%Aircraft goes from Vertical to preset pritch in order to gain speed in
%x-direction

elseif t >= 8 && t < variable_pitch_time
   theta = 40;
   [Cl, Cd_total,gamma,alpha] = LiftDrag_Coefficient(theta,y,M,Mdd,Sref,Cd);

elseif t >= variable_pitch_time
   F_y = zeros(1,89);
   for theta = 1:89
      [Cl, Cd_total,gamma,alpha] = LiftDrag_Coefficient(theta,y,M,Mdd,Sref,Cd);
      F_y(theta) = (F*sind(theta) + (Cl*rho*Sref*(u^2)/2)*cosd(gamma) -
(Cd_total*rho*Sref*(u^2)/2)*sind(gamma));
   end
   [value, theta] = max(F_y);
   [Cl, Cd_total,gamma,alpha] = LiftDrag_Coefficient(theta,y,M,Mdd,Sref,Cd);

end

%Solve the Equations of Motions
%dy = [x-velocity, x-accel, y-velocity, y-accel]
dy = [y(2);
    (F*cosd(theta) - (Cl*rho*Sref*(u^2)/2)*sind(gamma) - (Cd_total*rho*Sref*(u^2)/2)*cosd(gamma))/m;
    y(4);
    (F*sind(theta) + (Cl*rho*Sref*(u^2)/2)*cosd(gamma) - (Cd_total*rho*Sref*(u^2)/2)*sind(gamma))/m -
g];
end

function [Cl, Cd_total,gamma,alpha] = LiftDrag_Coefficient(theta,y,M,Mdd,Sref,Cd)
   gamma = abs(atand(y(4)/y(2))); %Degrees, Angle between horizon & flowspeed
   alpha = theta - gamma; %Degrees, Angle of Incidence
   [Cl, Cd_wing] = Natter_Splines(real(alpha)); %Obtain Cl and Cd for given Alpha
   e = .95; %Oswald Efficiency Factor AR = 3.6, Raymer Page 456 Eq 12.48
   K_wing= 1/(pi*e*(3.6^2/Sref)); %Raymer Page 456 Eq 12.47
   K_tail = 1/(pi*e*(2.3^2/2.53)); %Raymer Page 456 Eq 12.47
   Cdi = K_wing*(Cl^2) + K_tail*(2.53/Sref)*(Cl^2); %Trimmed Cdi, Raymer Page 624 Eq 16.34
   Cd = Cd*Natter_transonicdrag(M,Mdd);  %Transonic Cd Modifier
   Cd_total = Cd_wing+Cd+Cdi;
end


%Obtain atmopheric speed and drag properties of aircraft for given time/height
function [F,m,Cd,rho,T,M,c] = properties(t, altitude, flowspeed, transition_time,Mdd)
% Flat plate skin friction coefficient (Cf) Appoximation, Raymer Section 12.5.3 Page 433
L = 6.02; %m, Characteristic Aircraft Length
```

```
u = flowspeed;%m/s, Flowspeed
T_amb = 15 + 273.15;%Kelvin, Ambient Ground Temperature (15 Celsius)
T = T_amb - 0.00649.*altitude; %Kelvin, Temperature w/ Altitude, Reference 1
P = 101325*(T./288.08).^5.256; %Pascals, Pressure w/ Altitude, Reference 1
rho = P./(286.9.*T); %kg/m^3, Denisity of Air, Reference 1
mu = 1.789E-5.*((T./T_amb).^1.5).*((T_amb + 110.4)./(T + 110.4)); %Pa*s Dynamic viscosity, Reference
2
k = 1.015E-5; %Skin Roughness Value (Camouflage), Raymer Page 435 Table 12.5
c = sqrt(1.4*8.3145*T/0.0289645);%m/s Speed of Sound in Air, Reference 3
M = u/c; %Mach Number

%Determine Reynold's Number
if M < Mdd
Re_cutoff = 38.21*(L/k)^1.053; %Subsonic, Raymer Page 434 Eq 12.28
elseif M >= Mdd
Re_cutoff = 44.62*((L/k)^1.053)*M^1.16; %Transonic, Raymer Page 434 Eq 12.29
end

Cf = 0.455 / ((log10(Re_cutoff)^2.58)*(1+0.144*M^2)^0.65); %Turbulent Flow Cf, Raymer Page 433, Eq
12.27


% Form Factor and Adjustments Section 12.5.4 Page 435
Amax = 0.819; %m^2, wing, tail strut and pylon
xc = 0.3; %chordwise location at max thickness
tc = 0.12; %thickness to chord ratio
FF_wingtail = (1 + ((0.6/xc)*(tc)) + 100*((tc)^4))*(1.34*(M^0.18)); %Form Factor Raymer Page 435 Eq
12.30
f = L/sqrt((4/pi)*Amax); %Raymer Page 436 Eq 12.33
FF_fuselage = 1 + (60/(f^3)) + (f/400); %Form Factor Raymer Page 435 Eq 12.31

Swet_fuselage = 17.84; %m^2, Wetted area (Derived from Solidworks Model)
Swet_wingtail = 6.18 + 5.26 + 4.1; %m^2, wing + elevator + tail wetted area (Derived from Solidworks
Model)
Sref = 3.6; %m^2, Planform area of wing

%Interference Factors Raymer Page 437 Section 12.5.5
Q_fuselage = 1.0; %Interference Factor
Q_wingtail = 1.03;%Interference Factor

Cd_canopy = 0.15*0.137/Sref; %Sharp edged windshield w/ 0.137m^2 frontal area, Raymer Page 442
Table 12.6
Cd_VTO = 0.3*.051/Sref; %bullet w/ 0.051m^2 frontal area, Raymer Page 442 Table 12.6


%Full throttle, VTO Boosters
if t < 8
   m = 2293 - 20*t - 6.94*t; %kg, Initial Mass with 20 kg/s for VTO, 6.94 kg/s for HWK
   F = 2900*9.81; %Newtons, 2900 kg of total thrust
   %Sum Drag Components, Raymer Page 430 Eq 12.24
   Cd = (Cf*FF_fuselage*Q_fuselage*Swet_fuselage/Sref) + ...
        (Cf*FF_wingtail*Q_wingtail*Swet_wingtail/Sref) + ...
        Cd_canopy + ...
```

```
        4*Cd_VTO; %<- 4 VTO boosters

%Full Throttle, No VTO Boosters
elseif t >= 8 & altitude < 7000
   m = 1833 - (8*6.94) - 6.94*(t-8); %1810 kg weight - burnt fuel - burning fuel
   F = 1700*9.81; %Newtons, HWK109-509 Rocket produces 1700kg
   %Sum drag components but no boosters
   Cd = (Cf*FF_fuselage*Q_fuselage*Swet_fuselage/Sref) + ...
        (Cf*FF_wingtail*Q_wingtail*Swet_wingtail/Sref) + ...
        Cd_canopy;
%Full Throttle, No VTO Boosters, Blunt Nose
elseif t >= 8 & altitude > 7000 %Estimating 7000m is when he ejects the nosecap
   m = 1833 - (8*6.94) - 6.94*(t-8); %1810 kg weight - burnt fuel - burning fuel
   F = 1700*9.81; %Newtons
   Cd = (2.608)*(Cf*FF_fuselage*Q_fuselage*Swet_fuselage/Sref) + ... % 2.608 is the ratio of Cd for
smooth and flatnose fuselage
        (Cf*FF_wingtail*Q_wingtail*Swet_wingtail/Sref) + ...
        Cd_canopy;
end

Cd =  Cd + 0.05*Cd; %Add L&P Drag, 5% increase, Raymer Page 444 Table 12.8

end

%Obtain Cl,Cd for given Angle of Attack
function [Cl, Cd_wing] = Natter_Splines(alpha)
x_l = [0 68.18 71.51 77.23 79.62 105.83 145.87 171.61 210.89 260.26 403.9 472.23]*(90/472.23);
y_l = [0 324.09 331.24 330.29 324.09 177.29 231.15 266.9 294.07 286.92 129.49 23.05]*(1.275/331.24);

x_d = [0 64.97 76.08 84.53 179.86 446.53 504.91 530.19]*(90/530.19);
y_d = [0 4.63 11.43 32.34 189.88 635.19 670.87 675.68]*(2.35/675.68);

yy_l = spline(x_l , [4.75*(1.275/331.24)/(90/472.23) y_l -1.55*(1.275/331.24)/(90/472.23)]);
yy_d = spline(x_d ,[0 y_d 0]);
e = 0.95;
Cl = ppval(yy_l,abs(alpha));
Cl = Cl/(1+Cl/(pi*e*3.6));
Cd_wing = ppval(yy_d,abs(alpha));
end
%Obtain Transonic Drag Increase for given Mach Number
function [transonic_ratio] = Natter_transonicdrag(M,Mdd)
x_d = [0 32.19 76.09 101.01 107.53 113.47 131.26 139.82]*(1-Mdd)/139.82;
y_d = ([0 15.49 73.03 153.71 211.26 227.87 240.92 242.67]*2/242.67)+1;

yy_d = spline(x_d , [0 y_d 0]);
xx_d = linspace(0,1-Mdd,50);

if M <= Mdd
   transonic_ratio = 1;
elseif M > Mdd & M < 1
   transonic_ratio = ppval(yy_d,M-Mdd);
elseif M >= 1
   transonic_ratio = 3;
```

```
end
end
%Benjamin S Hopkins Natter Lift to Drag Ratio Determination, Chapter 5.0
%11/25/22

close all
clear all
clc

g = 9.81; %m/s^2 Gravitational Acceleration
Sref = 3.6; % m^2 Planform Area of Wing
Mdd = 0.75; %Critical Mach Number
altitude = 9700;
flowspeed = 100;

for alpha = 1:45

[Cl, Cd_wing] = Natter_Splines(real(alpha));
[Cd,rho,T,M,c] = properties(altitude, flowspeed,Mdd)
e = .98; %Raymer Page 456 Eq 12.48
K_wing= 1/(pi*e*(3.6^2/Sref));
K_tail = 1/(pi*e*(2.3^2/2.53));
Cdi = K_wing*(Cl^2) + K_tail*(2.53/Sref)*(Cl^2); %Raymer Cdi Trimmed Page 264
Cd = Cd + Cd_wing + Cdi;

figure(1)
set(gcf,'color','w');
plot(alpha,Cl/Cd,'x')
hold on
xlabel('\alpha (degrees)')
ylabel('Cl/Cd')
end

function [Cd,rho,T,M,c] = properties(altitude, flowspeed, Mdd)
% Flat plate skin friction coefficient Cf Section 12.5.3 Page 433
L = 6.02; %m characteristic length
u = flowspeed;%m/s flow speed
T_amb = 15 + 273.15;%Kelvin Ambient Ground Temperature
T = T_amb - 0.00649.*altitude; %Kelvin Temperature w/ Altitude
https://www.grc.nasa.gov/www/k-12/rocket/atmosmet.html
P = 101325*(T./288.08).^5.256; %Pressure Pascals
https://www.grc.nasa.gov/www/k-12/rocket/atmosmet.html
rho = P./(286.9.*T); %kg/m^3 denisity of air https://www.grc.nasa.gov/www/k-12/rocket/atmosmet.html
mu = 1.789E-5.*((T./T_amb).^1.5).*((T_amb + 110.4)./(T + 110.4)); %Pa*s dynamic viscosity
https://www.grc.nasa.gov/www/BGH/viscosity.html
k = 1.015E-5; %Camouflage Paint  %Raymer
c = sqrt(1.4*8.3145*T/0.0289645);%m/s Speed of Sound in Air
M = u/c; %Mach Number

Re = rho.*u.*L./mu; %Reynolds Number %Raymer

if M < Mdd
Re_cutoff = 38.21*(L/k)^1.053; %Raymer
```

```
elseif M >= Mdd
Re_cutoff = 44.62*((L/k)^1.053)*M^1.16; %Raymer Tran/Supersonic
end

Cf = 0.455 / ((log10(Re_cutoff)^2.58)*(1+0.144*M^2)^0.65);


% Form Factor and Adjustments Section 12.5.4 Page 435
Amax = 0.819; %m^2
%wing, tail strut and pylon
xc = 0.3; %chordwise location at max thickness
tc = 0.12; %thickness to chord ratio
FF_wingtail = (1 + ((0.6/xc)*(tc)) + 100*((tc)^4))*(1.34*(M^0.18));
f = L/sqrt((4/pi)*Amax);
FF_fuselage = 1 + (60/(f^3)) + (f/400);

Swet_fuselage = 17.84; %m^2 wetted area
Swet_wingtail = 6.18 + 5.26 + 4.1; %wing + elevator + tail wetted area
Sref = 3.6; %m^2 planform area of wing

Q_fuselage = 1.0; %Since there is interference between fuselage and VTO rockets (act as nacelles)
Q_wingtail = 1.03;

Cd_canopy = 0.15*0.137/Sref; %Sharp edged windshield w/ 0.137m^2 frontal area
Cd_VTO = 0.3*.051/Sref; %bullet w/ 0.051m^2 frontal area


Cd = 4.45*(Cf*FF_fuselage*Q_fuselage*Swet_fuselage/Sref) + ... % 4.452 is the ratio of Cd for smooth
and emptynose fuselage
    (Cf*FF_wingtail*Q_wingtail*Swet_wingtail/Sref) + ...
    Cd_canopy;

Cd =  Cd + 0.05*Cd; %Add L&P Drag
end


function [Cl, Cd_wing] = Natter_Splines(alpha)
x_l = [0 68.18 71.51 77.23 79.62 105.83 145.87 171.61 210.89 260.26 403.9 472.23]*(90/472.23);
y_l = [0 324.09 331.24 330.29 324.09 177.29 231.15 266.9 294.07 286.92 129.49 23.05]*(1.275/331.24);

x_d = [0 64.97 76.08 84.53 179.86 446.53 504.91 530.19]*(90/530.19);
y_d = [0 4.63 11.43 32.34 189.88 635.19 670.87 675.68]*(2.35/675.68);

yy_l = spline(x_l , [4.75*(1.275/331.24)/(90/472.23) y_l -1.55*(1.275/331.24)/(90/472.23)]);
yy_d = spline(x_d ,[0 y_d 0]);

Cl = ppval(yy_l,abs(alpha));
Cl = Cl/(1+Cl/(pi*3.6));
Cd_wing = ppval(yy_d,abs(alpha));
end
```

# Appendix B.4 – AEROTRIM Downwash Angle Code

```
%Benjamin S Hopkins, Aerotrim Analytical Downwash Angle, Chapter 6.0
%AEROTRIM- A SYMMETRIC TRIM CALCULATOR FOR SUBSONIC FLIGHT CONDITIONS
%A Mathcad programme written by M.V. Cook (CONVERTED TO MATLAB BY O.A. DOUGLAS,
%version date NOVEMBER 17 2017.
%Given the operating condition and some basic geometric and aerodynamic data for a conventional
%aircraft this programme will calculate an estimate of the symmetric trim state of the
%aircraft for a chosen airspeed range . The programme is limited to subsonic flight in the troposphere
%only. However, the programme may be developed easily for application to a wider
%range of operating conditions and aircraft configurations. Data given are best estimates for
%the Cranfield Jetstream laboratory aircraft.


%FOR THE AIRCRAFT FLIGHT CONDITION
%load('FlightConditions.mat');
clear all
clc

h= 0.39;        %cg position (%c) check

%Aircraft geometry - constants
%(insert values defined by aircraft geometry)

%WING GEOMETRY
S = 3.6;      %WingArea %check
b = 3.6;      %WingSpan %check
cw = 1;     %WingMeanChord %check
Sweep14c = 0;   %1/4 chord in degrees %check
Zw = 0;   %Z coordinate of 1/4c point above (-ve) or below (+ve) ox body axis in metres %check
Arw = b^2/S;

%Tailplaine geometry
ST = 2.3;  %tail area %check
bT = 2.3;   %TailSpan %check
ct = 1;  %TailMeanChord %check
lt = 2.49; %TailArm %check
ZT = -0.57;    %Z coordinate of 1/4c point above (-ve) or below (+ve) ox body axis in metres %check
Art = bT^2/ST;

%Engine Installation
Zt = 0; %thrust line z coordinate above (-ve) or below (+ve) ox body axis in metres %check

%Wing-body aerodynamics
%(Insert values defined by the installed wing aerodynamic design)
a = 5.225/(1+5.225/(pi*Arw));    %wing body Cl-alpha(per rad) %check
h0 = 0.25;     %wing body aero centre


%Tailplane aerodynamics
%(insert values defined by the tailplane aerodynamic design)
```

```
a1 = 5.225/(1+5.225/(pi*Art));   %tailplane CL - alpha(per rad) %check

%wing and tail plain calculations
lT = 2.49;    %Tail arm, LE to LE
VT = (ST*lT)/(S*cw);

%Downwash at tail
%Ref:-Stribling, C.B. 1984: "Basic Aerodynamics", Butterworth Ltd, 1984

syms fi
x = lT/b; z=(Zw - ZT)/b;
A = ((0.5*cos((((fi*pi)/180)^2)))/((x^2 + ((0.5*cos(((fi*pi)/180)))^2) + z^2)^0.5))* (((x +((x^2 +
((0.5*cos(((fi*pi)/180)))^2) + z^2)^0.5))/(((0.5*cos(((fi*pi)/180)))^2) + z^2)) + (x/(x^2 + z^2)))*(pi/180)
dcc = vpa(symsum(A,fi,5,85))
deda = (a/(pi^2*Arw))*dcc
K_fus = 0.02; %Raymer
Wf = 0.9; %meters Fuselage Width
L_f = 6.03; %meters Length
Cma_fus = ((K_fus * Wf^2 * L_f) / (cw*S))*57.29; %Fuselage Coefficient of Moment (Per Radian)
Raymer
hn = h0 + (VT*a1/a)*(1-deda) -  Cma_fus/a
```

# Appendix B.5 – Trimmed Elevator Deflection Code

```
%Benjamin S Hopkins, Elevator Deflection, Chapter 6.0
11/25/22

Arw = 3.6; %m
Art = 2.3; %m
e = 0.95;
m= 926; %kg  mass at 94 seconds of flight
g = -9.81 %m/s^2
U1 = 275; %m/s
Sw = 3.6; %m^2
St = 2.3; %m^2

rho = 0.428; %kg/m^3

q = 0.5*rho*U1^2; %dynamic pressure


Cla = 5.225/(1+5.225/(pi*e*Arw)); %Cl/alpha NACA 0012 Caughey Eq 2.19
Clta = 5.225/(1+5.225/(pi*e*Art));
Cltde = 1.147; %Iran Paper

X_w = 2.65; %m from nose
X_CG = 2.73;
X_t = 5.12;

A = [Cla*q*Sw + Clta*q*St,  Cltde*q*St;
   Cla*q*Sw*X_w + Clta*q*St*X_t, Cltde*q*St*X_t]

B = [m*g;
   m*g*X_CG]

de_trim = (A\-B)*57.29
```

# Appendix B.6 – Longitudinal Open Loop Analysis Code

```
%Benjamin S. Hopkins Longitudinal Dynamics Open Loop Analysis, Chapter 6.0
clear all
close all
clc

g = 9.81; %m/s^2
U1 = 275; %m/s
m= 926; %kg  mass at 104 seconds of flight
S = 3.6; %m^2
c = 1; %m
Arw = 3.6; %m
Art = 2.3; %m
Vt = 1.68; %Tail Volume From Aerotrim Calculation
Iy = 986; %Iy Moment of Inertia
lt = 2.49; %Tail Arm
xCG = 0.33; % X-CG %MAC
xNP_analy = 0.725; % X-NP %MAC
xNP_avl = 0.801;
ht=9700;   % CONVERT ALTITUDE IN FEET TO METRES
R=287.05;       %Gas constant (Nm/kgK)
lr=-0.00649;     %Lapse rate (K/m)
TEMP = 288.15 + (lr*ht);    %(K)
rho = 1.225*(TEMP/288.16)^(-((g/(lr*R))+1)); % (kg/m^3)
q = 0.5*rho*U1^2; %dynamic pressure


Cd0 = 0.103; %Cd0 at 275 m/s at 9700 m
Cda = 0.083; %Calculated slope from Cd v. Alpha NACA 0012
Cl = (m*g)/(q*S); %Cl for given parameters, level flight
Cla = 5.225/(1+5.225/(pi*Arw)); %Cl/alpha NACA 0012 Caughey Eq 2.19
Clta = 5.225/(1+5.225/(pi*Art));

n = 0.9; %stabilizer efficiency T-tail = 0.9
Cltde = 1.147; %tail Cl v de
deda = 0.329; %downwash angle change with change in alpha (Aerotrim)

Cladot =  -2*n*Vt*Clta*deda;  % Eq 4.71 Page 59
Clq = 2*n*Vt*Clta; %Eq 4.66 Page 58
Cmq = -2*n*(lt/c)*Vt*Clta; %Eq 4.65
Cma = (xCG-xNP_analy)*Cla %
Cmadot = -2*n*(lt/c)*Vt*Clta*deda; %Eq 4.73

Cd0_avl = 0.106;
Cl_avl= 0.187;
Cla_avl = 4.522;
Clq_avl = 12.95;
Cma_avl = (xCG-xNP_avl)*Cla_avl %
Cmq_avl = -23.36;
Cltde_avl =1.147;
Cma_avl = (xCG-xNP_avl)*Cla_avl %
```

```
% Define dimensional stability and control derivatives
Xu = ((q*S)/(m*U1))*(2*-Cd0); %[1/s]
Xa = ((q*S)/(m*U1))*Cda; %[m/s^2] (a is short for alpha)
Zu = ((q*S)/(m*U1))*(2*-Cl); %[1/s]
Za = ((q*S)/(m*U1))*(-Cla); %[m/s^2]
Zadot = ((q*S*c)/(2*m*U1^2))*(-Cladot); %[m/s]
Zq = ((q*S*c)/(2*m*U1))*-Clq; %[m/s]
Mu = 0; %[1/m/s]
Ma = ((q*S*c)/(Iy*U1))*Cma; %[1/s^2]
Madot = ((q*S*c^2)/(2*Iy*U1^2))*Cmadot; %[1/s] Eq 4.73 Page 59
Mq = ((q*S*c^2)/(2*Iy*U1))*Cmq; %[1/s]
Xde = 0; %[m/s^2]
Zde = -((q*2.3)/(m*U1))*Cltde; %[m/s^2]
Mde = -((q*2.3*c)/(Iy*U1))*Cma; %[1/s^2]

%Stability Derivatives AVL
Xu_avl = ((q*S)/(m*U1))*(2*-Cd0_avl); %[1/s]
Xa_avl = ((q*S)/(m*U1))*Cda; %[m/s^2] (a is short for alpha)
Zu_avl = ((q*S)/(m*U1))*(2*-Cl_avl); %[1/s]
Za_avl = ((q*S)/(m*U1))*(-Cla_avl); %[m/s^2]
Zadot_avl = ((q*S*c)/(2*m*U1^2))*(-Cladot); %[m/s]
Zq_avl = ((q*S*c)/(2*m*U1))*-Clq_avl; %[m/s]
Mu_avl = 0; %[1/m/s]
Ma_avl = ((q*S*c)/(Iy*U1))*Cma_avl; %[1/s^2]
Madot_avl = ((q*S*c^2)/(2*Iy*U1^2))*Cmadot; %[1/s] Eq 4.73 Page 59
Mq_avl = ((q*S*c^2)/(2*Iy*U1))*Cmq_avl; %[1/s]
Xde_avl = 0; %[m/s^2]
Zde_avl = -((q*2.3)/(m*U1))*Cltde; %[m/s^2]
Mde_avl = -((q*2.3*c)/(Iy*U1))*Cma_avl; %[1/s^2]

%Analytical Values
de_initial = 7.15;
de_final = 5.96;
trimmed_AOA = 2.99-2.45;
trimmed_AOA_analy =2.99-2.45;

Along = [Xu Xa 0 -g;...
 Zu/U1 Za/U1 1 0;...
 Mu+(Madot*Zu)/U1 Ma+(Madot*Za)/U1 Mq+Madot 0;...
 0 0 1 0]

Blong = [Xde;...
Zde/U1;...
Mde+(Madot*Zde)/U1;...
 0]

Clong = eye(length(Along));
Dlong = zeros(size(Clong,1),size(Blong,2));

damp(ss(Along,Blong,Clong,Dlong))

tfinal = 100;
```

```
%Start the Simulink simulation
open_system('AE246_HW1_Learjet.slx');
output_analy = sim('AE246_HW1_Learjet.slx');

%AVL Values
de_initial = 7.17;
de_final = 3.85;
trimmed_AOA =3.35-2.89;
trimmed_AOA_avl =3.35- 2.89;

Along = [Xu_avl Xa_avl 0 -g;...
    Zu_avl/U1 Za_avl/U1 1 0;...
    Mu_avl+(Madot_avl*Zu_avl)/U1 Ma_avl+(Madot_avl*Za_avl)/U1 Mq_avl+Madot_avl 0;...
    0 0 1 0]

Blong = [Xde_avl;...
Zde_avl/U1;...
Mde_avl+(Madot_avl*Zde_avl)/U1;...
 0]



Clong = eye(length(Along));
Dlong = zeros(size(Clong,1),size(Blong,2));

damp(ss(Along,Blong,Clong,Dlong))

%Start the Simulink simulation
open_system('AE246_HW1_Learjet.slx');
output_avl = sim('AE246_HW1_Learjet.slx');

%Plot simulation results
figure(1)
plot(output_analy.de.time(:,1),output_analy.de.signals.values(:,1))
hold on
plot(output_avl.de.time(:,1),output_avl.de.signals.values(:,1),'--')
legend('Analytical', 'AVL')
xlabel('t [s]');
ylabel('\Delta \deltae [deg]');
set(gca,'fontsize',12);
set(gcf,'color','w');
set(findall(gcf,'type','line'),'linewidth',3);

figure(2)
title('OL Longitudinal Responses of a Natter');
subplot(2,2,1)
plot(output_analy.u(:,1)+U1)
hold on
plot(output_avl.u(:,1)+U1)
legend('Analytical', 'AVL')
xlabel('t [s]');
ylabel('u [m/s]');
set(gca,'fontsize',12);
```

```
set(gcf,'color','w');
set(findall(gcf,'type','line'),'linewidth',2);

subplot(2,2,2)
plot(output_analy.alpha(:,1) )
hold on
plot(output_avl.alpha(:,1) )
legend('Analytical', 'AVL')
xlabel('t [s]');
ylabel('\Delta \alpha [deg]');
set(gca,'fontsize',12);
set(findall(gcf,'type','line'),'linewidth',2);

subplot(2,2,3)
plot(output_analy.q(:,1))
hold on
plot(output_avl.q(:,1))
legend('Analytical', 'AVL')
xlabel('t [s]');
ylabel('q [deg/s]');
set(gca,'fontsize',12);
set(findall(gcf,'type','line'),'linewidth',2);

subplot(2,2,4)
plot(output_analy.theta(:,1) )
hold on
plot(output_avl.theta(:,1) )
legend('Analytical', 'AVL')
xlabel('t [s]');
ylabel('\Delta \theta [deg]');
set(gca,'fontsize',12);
set(findall(gcf,'type','line'),'linewidth',2);
```

# Appendix B.7 – Natter Energy-Maneuverability Code

```
%Benjamin S Hopkins Natter Level Turning Flight, Chapter 7.0
close all
clear all
clc

%Conditions for level flight
t = 94; %seconds
altitude = 9700; %meters
velocity = 100:1:500; %m/s
Mdd = 0.75;
g = 9.81; %m/s^2
Sref = 3.6; %m^2

load_factor = zeros(1,length(velocity));
psi = zeros(1,length(velocity));
psi_stall = zeros(1,length(velocity));


for i = 1:length(velocity)    %Sustained Turn Rate
[F,m,Cd,rho,T,M,c] = properties(t,altitude,velocity(i),Mdd);
Cl = (m*g)/(rho*Sref*(velocity(i)^2)/2)

e = .95; %Oswald Efficiency Factor AR = 3.6, Raymer Page 456 Eq 12.48
K_wing= 1/(pi*e*(3.6^2/Sref)); %Raymer Page 456 Eq 12.47
K_tail = 1/(pi*e*(2.3^2/2.53)); %Raymer Page 456 Eq 12.47
Cdi = K_wing*(Cl^2) + K_tail*(2.53/Sref)*(Cl^2); %Trimmed Cdi, Raymer Page 624 Eq 16.34
Cd = Cd*Natter_transonicdrag(M,Mdd);

n = (F/(m*g))*(Cl/(Cd+Cdi))
psi(i) = 57.3*g*sqrt(n^2-1)/velocity(i);
%psi_stall(i) = 57.3*sin(acos( (m*g)/(1.28*rho*Sref*velocity(i)^2/2)))/2;
psi_stall(i) = 57.3*(1.28*rho*Sref*velocity(i)^2/2)*sin(acos(
(m*g)/(1.28*rho*Sref*velocity(i)^2/2)))/(m*velocity(i));

end

figure(1)
plot(velocity,psi,'b',velocity,psi_stall,'r');
hold on
set(gcf,'color','w');
xlabel('Velocity (m/s)')
ylabel('Turn Rate (degrees/sec)')



for n = 2:8
   psi = 57.3.*g.*sqrt(n^2-1)./velocity;
   figure(1)
   plot(velocity,psi,'k')
   ylim([0 20])
```

```
    hold on

    n_cont = linspace(2,8,20);
    R = 2250;
    v = sqrt(R.*g.*sqrt(n_cont.^2-1));
    psi_radius = 57.3.*g.*sqrt(n_cont.^2-1)./v;
    figure(1)
    plot(v,psi_radius,'b')
    hold on
end

function [F,m,Cd,rho,T,M,c] = properties(t, altitude, flowspeed,Mdd)
% Flat plate skin friction coefficient (Cf) Appoximation, Raymer Section 12.5.3 Page 433
L = 6.02; %m, Characteristic Aircraft Length
u = flowspeed;%m/s, Flowspeed
T_amb = 15 + 273.15;%Kelvin, Ambient Ground Temperature (15 Celsius)
T = T_amb - 0.00649.*altitude; %Kelvin, Temperature w/ Altitude, Reference 1
P = 101325*(T./288.08).^5.256; %Pascals, Pressure w/ Altitude, Reference 1
rho = P./(286.9.*T); %kg/m^3, Denisity of Air, Reference 1
mu = 1.789E-5.*((T./T_amb).^1.5).*((T_amb + 110.4)./(T + 110.4)); %Pa*s Dynamic viscosity, Reference
2
k = 1.015E-5; %Skin Roughness Value (Camouflage), Raymer Page 435 Table 12.5
c = sqrt(1.4*8.3145*T/0.0289645);%m/s Speed of Sound in Air, Reference 3
M = u/c; %Mach Number

%Determine Reynold's Number
if M < Mdd
Re_cutoff = 38.21*(L/k)^1.053; %Subsonic, Raymer Page 434 Eq 12.28
elseif M >= Mdd
Re_cutoff = 44.62*((L/k)^1.053)*M^1.16; %Transonic, Raymer Page 434 Eq 12.29
end

Cf = 0.455 / ((log10(Re_cutoff)^2.58)*(1+0.144*M^2)^0.65); %Turbulent Flow Cf, Raymer Page 433, Eq
12.27


% Form Factor and Adjustments Section 12.5.4 Page 435
Amax = 0.819; %m^2, wing, tail strut and pylon
xc = 0.3; %chordwise location at max thickness
tc = 0.12; %thickness to chord ratio
FF_wingtail = (1 + ((0.6/xc)*(tc)) + 100*((tc)^4))*(1.34*(M^0.18)); %Form Factor Raymer Page 435 Eq
12.30
f = L/sqrt((4/pi)*Amax); %Raymer Page 436 Eq 12.33
FF_fuselage = 1 + (60/(f^3)) + (f/400); %Form Factor Raymer Page 435 Eq 12.31

Swet_fuselage = 17.84; %m^2, Wetted area (Derived from Solidworks Model)
Swet_wingtail = 6.18 + 5.26 + 4.1; %m^2, wing + elevator + tail wetted area (Derived from Solidworks
Model)
Sref = 3.6; %m^2, Planform area of wing

%Interference Factors Raymer Page 437 Section 12.5.5
Q_fuselage = 1.0; %Interference Factor
Q_wingtail = 1.03;%Interference Factor
```

```
Cd_canopy = 0.15*0.137/Sref; %Sharp edged windshield w/ 0.137m^2 frontal area, Raymer Page 442
Table 12.6
Cd_VTO = 0.3*.051/Sref; %bullet w/ 0.051m^2 frontal area, Raymer Page 442 Table 12.6

%Full Throttle, No VTO Boosters
if t >= 8 & altitude < 7000
   m = 1810 - (8*6.94) - 6.94*(t-8); %1810 kg weight - burnt fuel - burning fuel
   F = 1700*9.81; %Newtons, HWK109-509 Rocket produces 1700kg
   %Sum drag components but no boosters
   Cd = (Cf*FF_fuselage*Q_fuselage*Swet_fuselage/Sref) + ...
        (Cf*FF_wingtail*Q_wingtail*Swet_wingtail/Sref) + ...
        Cd_canopy;

%Full Throttle, No VTO Boosters, Blunt Nose
elseif t >= 8 & altitude > 7000 %Estimating 7000m is when he ejects the nosecap
   m = 1810 - (8*6.94) - 6.94*(t-8); %1810 kg weight - burnt fuel - burning fuel
   F = 1700*9.81; %Newtons
   Cd = 4.45*(Cf*FF_fuselage*Q_fuselage*Swet_fuselage/Sref) + ... % 2.608 is the ratio of Cd for smooth
and flatnose fuselage
        (Cf*FF_wingtail*Q_wingtail*Swet_wingtail/Sref) + ...
        Cd_canopy;
end

Cd =  Cd + 0.05*Cd; %Add L&P Drag, 5% increase, Raymer Page 444 Table 12.8

end

function [transonic_ratio] = Natter_transonicdrag(M,Mdd)
x_d = [0 32.19 76.09 101.01 107.53 113.47 131.26 139.82]*(1-Mdd)/139.82;
y_d = ([0 15.49 73.03 153.71 211.26 227.87 240.92 242.67]*2/242.67)+1;
yy_d = spline(x_d , [0 y_d 0]);
xx_d = linspace(0,1-Mdd,50);

if M <= Mdd
   transonic_ratio = 1;
elseif M > Mdd & M < 1
   transonic_ratio = ppval(yy_d,M-Mdd);
elseif M >= 1
   transonic_ratio = 3;
end
end
```

# Appendix C.1 – AVL Geometry File

```
# AVL Natter Wing, Tail and Elevator Geometry File
# Note : check consistency of area unit and length units in
this file
# Note : check consistency with inertia units of the .mass
file
#
#
Natter_xflr5
0.0                                  | Mach
0     0     0.0                      | iYsym  iZsym  Zsym
  3.60000     1.00000     3.60000    | Sref   Cref   Bref
 -0.00193     0.00000     0.00000    | Xref   Yref   Zref
 0.00                                | CDp  (optional)



#========TODO: REMOVE OR MODIFY MANUALLY DUPLICATE SECTIONS
IN SURFACE DEFINITION=========
SURFACE                      | (keyword)
Main Wing
#Nchord    Cspace   [ Nspan Sspace ]
13        1.0

INDEX                        | (keyword)
6972                         | Lsurf

YDUPLICATE
0.0

SCALE
1.0  1.0  1.0

TRANSLATE
0.0  0.0  0.0

ANGLE
   0.000                          | dAinc
```

```
#____PANEL 1_______
#_______________
SECTION
|  (keyword)
   0.0000    0.0000    0.0000    1.0000   0.000   20    1
| Xle Yle Zle   Chord Ainc   [ Nspan Sspace ]

AFIL 0.0 1.0
NACA 0012.dat


#_______________
SECTION
|  (keyword)
   0.0000    1.8000    0.0000    1.0000   0.000   20    1
| Xle Yle Zle   Chord Ainc   [ Nspan Sspace ]

AFIL 0.0 1.0
NACA 0012.dat




#========TODO: REMOVE OR MODIFY MANUALLY DUPLICATE SECTIONS
IN SURFACE DEFINITION=========
SURFACE                       | (keyword)
Elevator
#Nchord    Cspace   [ Nspan Sspace ]
7        1.0

INDEX                         | (keyword)
6974                          | Lsurf

YDUPLICATE
0.0

SCALE
1.0  1.0  1.0
```

```
TRANSLATE
0.0  0.0  0.0

ANGLE
   0.000                          | dAinc


#____PANEL 1_______
#_______________
SECTION
|  (keyword)
   2.4700    0.0000    0.5700    1.0000   0.000   19    1
| Xle Yle Zle   Chord Ainc   [ Nspan Sspace ]
#Cname Cgain Xhinge HingVec XYZhvec SgnDup
CONTROL
Elevator 1.0  0.66 0.0 1.0 0.0 0.0 1.0 0.0 1.0

AFIL 0.0 1.0
NACA 0012.dat


#_______________
SECTION
|  (keyword)
   2.4700    1.1500    0.5700    1.0000   0.000   19    1
| Xle Yle Zle   Chord Ainc   [ Nspan Sspace ]
CONTROL
Elevator 1.0  0.66 0.0 1.0 0.0 0.0 1.0 0.0 1.0

AFIL 0.0 1.0
NACA 0012.dat




#========TODO: REMOVE OR MODIFY MANUALLY DUPLICATE SECTIONS
IN SURFACE DEFINITION=========
SURFACE                       | (keyword)
Fin
#Nchord    Cspace   [ Nspan Sspace ]
7        1.0
```

```
INDEX                          | (keyword)
6975                           | Lsurf

SCALE
1.0  1.0  1.0

TRANSLATE
0.0  0.0  0.0

ANGLE
   0.000                           | dAinc


#____PANEL 1_______
#_______________
SECTION
|  (keyword)
   2.4700   -0.0000    1.4000    1.1000   0.000    7    0
| Xle Yle Zle   Chord Ainc   [ Nspan Sspace ]

AFIL 0.0 1.0
NACA 0012.dat


#_______________
SECTION
|  (keyword)
   2.4700    0.0000   -0.5000    1.1000   0.000    7    0
| Xle Yle Zle   Chord Ainc   [ Nspan Sspace ]

AFIL 0.0 1.0
NACA 0012.dat
```

# Appendix C.2 – AVL Run File

```
#Natter AVL Run File
 ---------------------------------------------
 Run case  1:  stability_zerolift

 alpha        ->  CL          =  0.187069
 beta         ->  beta        =   0.00000
 pb/2V        ->  pb/2V       =   0.00000
 qc/2V        ->  qc/2V       =   0.00000
 rb/2V        ->  rb/2V       =   0.00000
 Elevator     ->  Cm pitchmom =   0.00000

 alpha     =   3.35712     deg
 beta      =   0.00000     deg
 pb/2V     =   0.00000
 qc/2V     =  0.147299E-24
 rb/2V     =   0.00000
 CL        =  0.187069
 CDo       =  0.103000
 bank      =   0.00000     deg
 elevation =   0.00000     deg
 heading   =   0.00000     deg
 Mach      =   0.00000
 velocity  =   275.000     m/s
 density   =  0.428000     kg/m^3
 grav.acc. =   9.81000     m/s^2
 turn_rad. =   0.00000     m
 load_fac. =   1.00000
 X_cg      = -0.824842E-01 Lunit
 Y_cg      =   0.00000     Lunit
 Z_cg      =   0.00000     Lunit
 mass      =   1111.00     kg
 Ixx       =   0.00000     kg-m^2
 Iyy       =   1917.03     kg-m^2
 Izz       =   1917.03     kg-m^2
 Ixy       =  -0.00000     kg-m^2
 Iyz       =  -0.00000     kg-m^2
 Izx       =  -0.00000     kg-m^2
 visc CL_a =   0.00000
```

```
visc CL_u =   0.00000
visc CM_a =   0.00000
visc CM_u =   0.00000
```